

THE UNIVERSITY OF CHICAGO

INFLAMMATION-MEDIATED LYMPHATIC COAGULATION: A NEW ROLE FOR  
NEUTROPHIL EXTRACELLULAR TRAPS

A DISSERTATION SUBMITTED TO  
THE FACULTY OF THE DIVISION OF THE PHYSICAL SCIENCES  
AND  
THE FACULTY OF THE DIVISION OF THE BIOLOGICAL SCIENCES  
AND THE PRITZKER SCHOOL OF MEDICINE  
IN CANDIDACY FOR THE DEGREE OF  
DOCTOR OF PHILOSOPHY  
GRADUATE PROGRAM IN BIOPHYSICAL SCIENCES

BY  
MARGO ELIZABETH MACDONALD

CHICAGO, ILLINOIS

JUNE 2024

Copyright © 2024 by Margo Elizabeth MacDonald  
All Rights Reserved

This work is dedicated to my family, my Chicago friends who have become family, my partner Liam, and my cat Stevie.

# TABLE OF CONTENTS

LIST OF FIGURES . . . . .	vii
LIST OF TABLES . . . . .	ix
ACKNOWLEDGMENTS . . . . .	x
ABSTRACT . . . . .	xi
1 INTRODUCTION . . . . .	1
1.1 Overview . . . . .	1
1.2 The lymphatic system . . . . .	1
1.3 Lymph node organization and the adaptive immune response . . . . .	2
1.4 Coagulation and fibrinolysis in blood are controlled by tightly-regulated signalling cascades . . . . .	7
1.5 Endothelial control of coagulation and fibrinolysis . . . . .	8
1.6 Concentrations of coagulatory and fibrinolytic factors differ in blood versus lymph . . . . .	9
1.7 Neutrophil extracellular traps (NETs) . . . . .	10
1.8 Neutrophil-lymphatic interactions . . . . .	13
1.9 NETs and coagulation in blood vessels . . . . .	15
1.10 NETs and immunothrombosis in COVID-19 . . . . .	16
1.11 Endothelial cell mechanosensing in inflammation . . . . .	18
2 LYMPHATIC COAGULATION AND NEUTROPHIL EXTRACELLULAR TRAPS IN LUNG-DRAINING LYMPH NODES OF COVID-19 DECEDENTS . . . . .	21
2.1 Preface . . . . .	21
2.2 Introduction . . . . .	22
2.3 Methods . . . . .	24
2.3.1 Human tissue procurement . . . . .	24
2.3.2 Quantification of lymphatic clotting, neutrophils, and NETs . . . . .	24
2.3.3 Lymph node scoring . . . . .	25
2.3.4 Animals . . . . .	26
2.3.5 <i>In vivo</i> labeling of fibrin . . . . .	26
2.3.6 Thrombomodulin and NETosis blocking <i>in vivo</i> . . . . .	26
2.3.7 LEC culture and qPCR . . . . .	27
2.3.8 LEC cytokine treatment and immunostaining . . . . .	28
2.3.9 ELISA . . . . .	28
2.3.10 Immunofluorescence staining and imaging . . . . .	29
2.3.11 H&E Staining and Imaging . . . . .	30
2.3.12 Statistics and reproducibility . . . . .	30
2.4 Results . . . . .	31

2.4.1	Intralymphatic fibrin clots are prevalent in lungs and LDLNs of COVID-19 decedents . . . . .	31
2.4.2	Lymphatic clotting correlates with abnormal or missing GCs in LDLNs	36
2.4.3	Lymphatic clotting correlates with intralymphatic NETs and down-regulated thrombomodulin in the LDLNs of COVID-19 decedents . .	37
2.4.4	Higher neutrophil counts in patient lungs correlate with intralymphatic NETosis and lymphatic clotting in LDLNs . . . . .	40
2.4.5	Lymphatic coagulation is correlated with downregulated lymphatic thrombomodulin expression in COVID-19 decedent LDLNs . . . . .	40
2.4.6	<i>In vitro</i> , LECs secrete CXCL8, upregulate ICAM-1, and downregulate thrombomodulin in response to TNF $\alpha$ . . . . .	44
2.4.7	High NET levels in patient serum correlate with lower levels of anti-RBD antibody titers . . . . .	45
2.4.8	In mice, locally injected TNF $\alpha$ drives NET-dependent lymphatic clotting	46
2.5	Discussion . . . . .	48
3	MECHANISMS BY WHICH TNF $\alpha$ PROMOTES NET-INDUCED LYMPHATIC COAGULATION . . . . .	54
3.1	Preface . . . . .	54
3.2	Introduction . . . . .	54
3.3	Methods . . . . .	56
3.3.1	Platelet-free plasma isolation and <i>in vitro</i> coagulation assay . . . . .	56
3.3.2	Confocal reflectance imaging . . . . .	57
3.3.3	Neutrophil and NET isolation . . . . .	57
3.3.4	2D Neutrophil-LEC co-cultures . . . . .	57
3.3.5	Transmigration and NETosis assay . . . . .	58
3.3.6	Coagulatory and fibrinolytic factor ELISA and immunostaining . . .	58
3.3.7	Statistics and reproducibility . . . . .	59
3.4	Results . . . . .	59
3.4.1	Under steady state conditions, LECs slow coagulation of platelet-depleted plasma compared to BECs . . . . .	59
3.4.2	Anti-coagulatory properties of LECs are driven by secreted factors and are downregulated in response to TNF $\alpha$ . . . . .	62
3.4.3	LECs pre-treated with TNF $\alpha$ drive clotting by priming neutrophils towards NETosis . . . . .	64
3.4.4	TNF $\alpha$ promotes neutrophil transmigration across LEC monolayers . .	65
3.4.5	TNF $\alpha$ -treated LECs promote NETosis and increased neutrophil motility after transmigration. . . . .	67
3.4.6	CCR7 binding promotes both neutrophil transmigration and NETosis.	69
3.4.7	CXCR1/2 expression by neutrophils is necessary for NETosis, but not transmigration. . . . .	71
3.5	Discussion . . . . .	72

4	INVESTIGATING THE ROLE OF FHL2 IN REGULATING ENDOTHELIAL CELL INFLAMMATORY RESPONSE . . . . .	75
4.1	Preface . . . . .	75
4.2	Introduction . . . . .	75
4.3	Methods . . . . .	78
4.3.1	Inducible FHL2 under- and over-expressing cell lines . . . . .	78
4.3.2	TeloHAEC cytokine treatment and immunofluorescence staining . . . . .	78
4.3.3	ELISA . . . . .	79
4.4	Results . . . . .	79
4.4.1	TNF $\alpha$ treatment leads to an upregulation in CXCL8 and IL-6 production in teloHAECs in static cultures . . . . .	79
4.4.2	FHL2 up- or down-regulation does not impact TNF $\alpha$ -induced IL-6 secretion in the absence of flow . . . . .	80
4.4.3	FHL2 upregulation increases CXCL8 secretion in response to TNF $\alpha$ in the absence of flow . . . . .	81
4.4.4	ROCK inhibition likely leads to decreased CXCL8 secretion in response to TNF $\alpha$ . . . . .	82
4.4.5	TNF $\alpha$ regulates cell shape and size in endothelial cells, but without flow, changes in FHL2 do not significantly impact these processes, junctional organization, or ICAM-1 expression . . . . .	83
4.4.6	Media from disturbed flow experiments did not provide reliable cytokine measurements . . . . .	83
4.5	Discussion . . . . .	85
5	CONCLUSIONS AND FUTURE DIRECTIONS . . . . .	87
5.1	Summary . . . . .	87
5.2	Discussion . . . . .	87
5.2.1	Neutrophils as regulators of both the innate and adaptive immune responses . . . . .	89
5.2.2	Lymphatic endothelial cells as immunomodulators . . . . .	90
5.2.3	Physiological and pathological functions of lymphatic coagulation . . . . .	91
5.2.4	Endothelial cell mechanosensing and inflammation . . . . .	92
5.3	Future Directions . . . . .	93
5.3.1	<i>In vivo</i> studies of lymphatic clotting . . . . .	93
5.3.2	Lymphatic coagulation in cancer . . . . .	93
5.3.3	Lymphatic coagulation in lipedema . . . . .	94
5.3.4	Lymphatic coagulation in bacterial infections and viral infections other than COVID-19 . . . . .	95
5.3.5	Binding of pro- and anti-coagulant molecules on LECs vs. BECs . . . . .	96
5.3.6	Impact of NET-induced coagulation on lymph flow . . . . .	96
5.3.7	Endothelial cell mechanosensing and inflammation . . . . .	96
	BIBLIOGRAPHY . . . . .	98

## LIST OF FIGURES

1.1	Functions of the lymphatic system . . . . .	3
1.2	Lymph node organization . . . . .	4
1.3	Lymphatic vessels transport interstitial fluid, viral antigens, and immune cells from tissues to the lymph nodes. . . . .	5
1.4	Coagulation and fibrinolysis cascades . . . . .	6
1.5	Endothelial control of coagulation and fibrinolysis . . . . .	9
1.6	Coagulatory properties of lymph vs blood . . . . .	11
1.7	NETs contribute to the formation and stabilization of thrombi . . . . .	17
2.1	Fibrin clots in lymphatic vessels in lungs of COVID-19 decedents. . . . .	32
2.2	Lymphatic clotting is widespread in LDLNs of COVID-19 decedents. . . . .	35
2.3	Clot location in COVID-19 and H1N1 lung-draining lymph nodes . . . . .	36
2.4	Abnormal GC architecture in LDLNs of COVID-19 decedents correlates with lymphatic clotting in the LDLN . . . . .	38
2.5	LDLN germinal center scoring rubric for H&E and IF staining. . . . .	39
2.6	Lymph clotting in LDLNs correlates with intralymphatic NETs in the LDLN and neutrophil load in the lungs of COVID-19 decedents. . . . .	41
2.7	Rubric for intralymphatic NET scoring. . . . .	42
2.8	Neutrophil and NET counts in the lungs and LDLNs of COVID-19 do not differ significantly from those in the LDLNs of control decedents. . . . .	42
2.9	Thrombomodulin expression by lymphatic endothelium is decreased in clotted vs. un- clotted lymphatic vessels in COVID-19 decedents. . . . .	43
2.10	<i>In vitro</i> , lymphatic endothelial cells secrete neutrophil chemoattractants, upregulate ICAM-1, and downregulate thrombomodulin in response to TNF $\alpha$ . . . . .	44
2.11	In serum from patients hospitalized with COVID-19, levels of NET markers did not correlate with disease severity or D-dimer levels but did correlate with lower anti-RBD antibody titers. . . . .	47
2.12	Serum MPO-NDA levels do not correlate with disease severity, but patients with low NET levels tend to have milder disease. . . . .	48
2.13	Local injection of TNF $\alpha$ or inactivated thrombin induces NET-dependent intralymphatic fibrin coagulation in mouse skin. . . . .	49
3.1	Depletion of platelets slows but does not prevent coagulation, and platelet-free plasma (PFP) coagulates faster when cultured with BECs than LECs . . . . .	61
3.2	PRP and PFP coagulation can be visualized using confocal reflectance imaging. . . . .	62
3.3	Pre-treatment of LECs or BECs with TNF $\alpha$ promotes coagulation of PFP. . . . .	63
3.4	LECs pre-treated with TNF $\alpha$ drive clotting by priming neutrophils towards NETosis. . . . .	66
3.5	TNF $\alpha$ alone does not stimulate NETosis. . . . .	67
3.6	Pre-treatment of LECs with TNF $\alpha$ promotes neutrophil transmigration and NETosis. . . . .	68

3.7	NETosis is regulated by CCR7 and CXCR1/2 binding, and neutrophil transmigration is decreased when CCR7 is blocked. . . . .	70
3.8	$\alpha$ CCR7 isotype control . . . . .	71
4.1	IL-6 expression in teloHAECs treated with TNF $\alpha$ . . . . .	80
4.2	CXCL8 expression in teloHAECs treated with TNF $\alpha$ . . . . .	81
4.3	CXCL8 expression by teloHAECs with ROCK inhibition . . . . .	82
4.4	ICAM-1 and VE-cadherin in teloHAECs treated with TNF $\alpha$ . . . . .	84
5.1	NETs & lymphatic coagulation in COVID-19 . . . . .	88
5.2	Schematic of lymphatic-neutrophil interactions in the context of coagulation . .	89



## LIST OF TABLES

2.1	qPCR primers . . . . .	27
2.2	COVID-19 Decedent Clinical Information . . . . .	33
2.3	Non-COVID-19 Decedent Clinical Information . . . . .	34
2.4	COVID-19 patient serum information . . . . .	45

## ACKNOWLEDGMENTS

I am thankful to the Human Tissue Resource Center (RRID:SCR-019199), funded by UChicago's Comprehensive Cancer Center support grant (P30CA014599), for their assistance with tissue preparation. Whole-slide imaging was performed at the University of Chicago Integrated Light Microscopy Core (RRID:SCR-019197) by Vytas Bindokas. I would also like to thank the Regional Organ Bank of Illinois for providing the control lung tissue and Kathy Reilly, Leon Jones, and Imani Wilson at the Clinical Research Center at the Institute for Translational Medicine for their help with phlebotomy training and whole blood collection for this study. In addition, I would like to thank Chaney Giampaolo and Gavin Swartz for their contributions to image analysis in chapter 2. This work was financially supported by grants from UChicago (UChicago Big Ideas Generator COVID-19 Response Fund, UChicago Women's Board) and the National Institutes of Health (grants 1F31CA257763-01 and 5T32EB009412-12), as well as funds kindly donated by Bruce Herzfelder. I would also like to thank the members of both the Swartz and Gardel groups, who have all provided valuable feedback and support throughout my PhD, as well as the members of my thesis committee.

## ABSTRACT

This work explores how endothelial cells respond to and regulate immune responses, specifically focusing on lymphatic endothelial cells and how their interactions with neutrophils can promote intralymphatic coagulation. In this work, I introduce lymphatic coagulation in the lungs and lung-draining lymph nodes as a clinical manifestation of COVID-19 and identify a correlation between lymphatic coagulation and the presence of neutrophil extracellular traps (NETs) within lymphatic vessels. Both intralymphatic NETosis and lymphatic coagulation also correlate with dysregulated germinal centers in these patients, and in a separate cohort of hospitalized COVID-19 patients, serum NET levels inversely correlated with antiviral antibody titers, suggesting that lymphatic clotting may impair the formation or maintenance of germinal centers necessary for robust antiviral antibody responses. Additionally, in mice degrading NETs with DNase 1 prevented TNF $\alpha$ -induced coagulation in lymphatic vessels, indicating that the correlation observed in COVID-19 decedents was indicative of a mechanistic role. After establishing that NETs do induce clotting in lymphatic vessels, I next investigated the role that lymphatic endothelial cells themselves may play in regulating both lymphatic coagulation and NETosis and compared this to that of blood endothelial cells. Using platelet-free plasma as a model of lymph, I observed that lymphatic endothelial cells exhibited a higher clotting threshold compared to blood endothelial cells, which is at least partially regulated by higher secretion of tissue plasminogen activator, and that this threshold is reduced by TNF $\alpha$  pre-treatment. TNF $\alpha$  also stimulated lymphatic endothelial cells to promote neutrophil recruitment and NETosis, which are regulated by CXCL8 and CCR7 in this context. These findings provide mechanistic insights into lymphatic clotting, offering potential avenues for therapeutic interventions in associated conditions. Lastly, this work investigates the role of a mechanosensitive LIM-domain protein, FHL2, in regulating endothelial cell inflammatory response.

# CHAPTER 1

## INTRODUCTION

### 1.1 Overview

In this dissertation, I identify a novel function of neutrophil extracellular traps (NETs) in driving coagulation within the lymphatic system, as well as mechanisms by which lymphatic endothelial cells promote NETosis. Chapter 2 describes lymphatic coagulation in the lung-draining lymph nodes of COVID-19 decedents and its correlation with both intralymphatic NET formation and an impaired adaptive immune response marked by dysregulated germinal center formation in the lung-draining lymph nodes and lower antiviral antibody titers in patients with higher serum NET levels. Chapter 3 delves into the differences in clotting behavior between lymphatic and blood endothelial cells and the mechanisms by which lymphatic endothelial cells promote clotting by recruiting neutrophils and inducing NETosis in response to  $\text{TNF}\alpha$ . Chapter 4 focuses on aortic endothelial cells and investigates how a mechanosensitive LIM-domain protein, FHL2, may regulate their inflammatory response. Overall, this work establishes lymphatic coagulation and NETs as important players in both the innate and adaptive immune responses in COVID-19 and opens the door for their study in other disease contexts.

### 1.2 The lymphatic system

The lymphatic system maintains tissue fluid homeostasis and traffics immune cells and antigen to the lymph node where the adaptive immune response is initiated (Fig.s 1.1-2). Lymphatic vessels take up fluid and immune cells from the interstitium and transport them to the lymph node, where they are processed (Fig.s 1.2-3). From there, fluid is transported to the thoracic duct through efferent lymphatic vessels, where it is returned to the venous system (Fig. 1.2). The lymphatic system also has a number of tissue-specific functions, including

cerebrospinal fluid (CSF) drainage, immune tolerance, fat absorption and more[106] (Fig. 1.1). Unsurprisingly, in addition to being involved in responding to infection and inflammation, the lymphatic system is involved in a number of diseases and their malfunction can lead to a number of different pathologies. Notably, in cancer, lymph nodes are a frequent site of metastasis and lymphangiogenesis is associated with both increased metastasis and improved immunotherapy response[26, 101].

Much of the interstitial fluid that lymphatics drain leaks out of blood vessels, and as a result contains antigens, inflammatory cytokines, immune cells and coagulatory and fibrinolytic factors present in blood, although lymph notably lacks platelets (Fig.s 1.3-4). While the lymph nodes are known to be centers of immune education, containing germinal centers important for antibody production (Fig. 1.2), lymphatic endothelial cells themselves are also immunomodulators that can regulate immune cell recruitment and activation through cytokine and chemokine secretion, as well as MHC-1 expression[3, 47, 83, 89, 92, 104, 109].

### **1.3 Lymph node organization and the adaptive immune response**

Transport of immune cells and viral antigens to the LN is a key step in the adaptive immune response, and blockages in lymphatic vessels may therefore impair downstream aspects of adaptive immunity including germinal center formation and antibody production. Healthy lymph nodes contain distinct B and T cell zones, as well as primary and secondary follicles. Primary lymphoid follicles are primarily made up of B cells, and secondary follicles, or germinal centers, are made up of distinct regions of B cells, T cells and follicular dendritic cells[103] (Fig. 1.2). Germinal centers are specialized structures in the lymph node follicles where memory B cells and long-lived antibody producing plasma cells are produced with help from antigen presentation by follicular dendritic cells and T follicular helper (Tfh) cells[103]. If this process does not occur properly, a robust antibody response to viral infections will

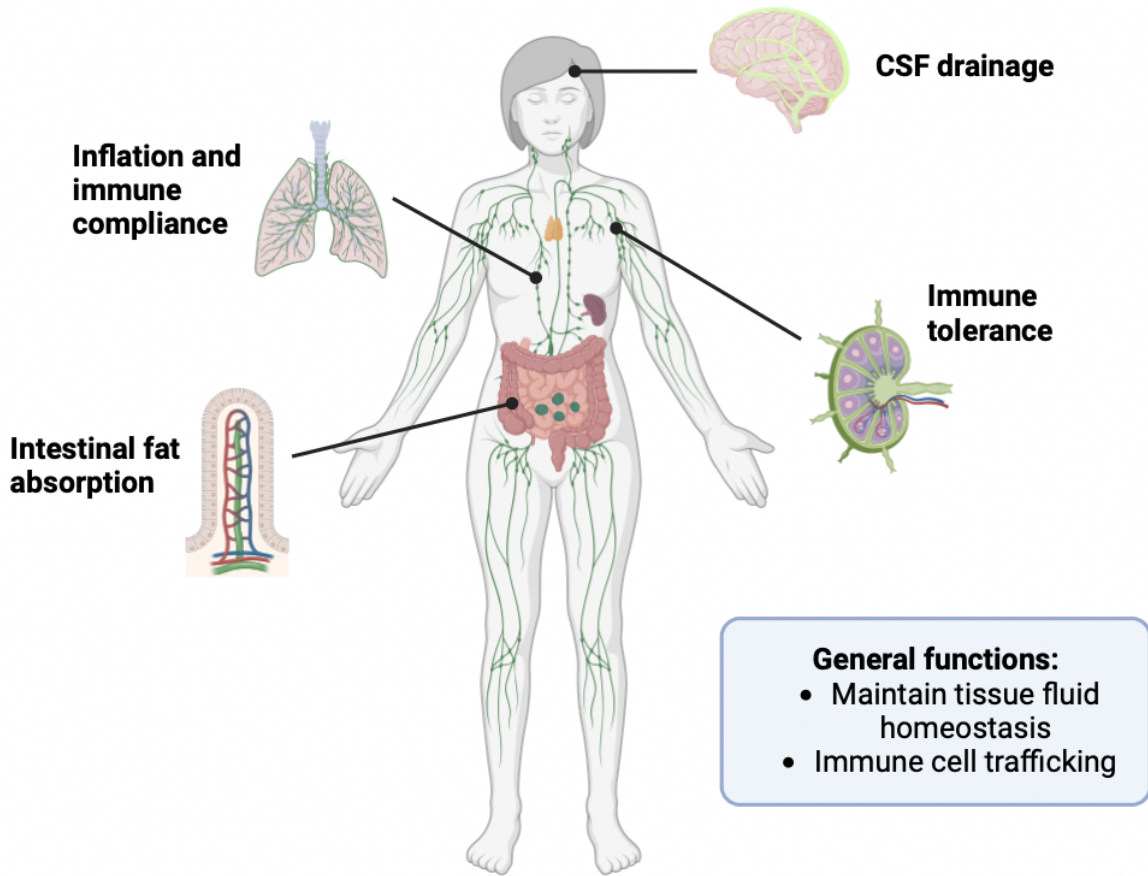


Figure 1.1: **Functions of the lymphatic system** Adapted from [106]. Tissue-specific and general functions of the lymphatic system. General functions of the lymphatic system include maintaining tissue fluid homeostasis and immune cell trafficking, but lymphatics and lymph nodes also play important functions in tissues including the lungs, brain, intestines, and more. Created using Biorender.com

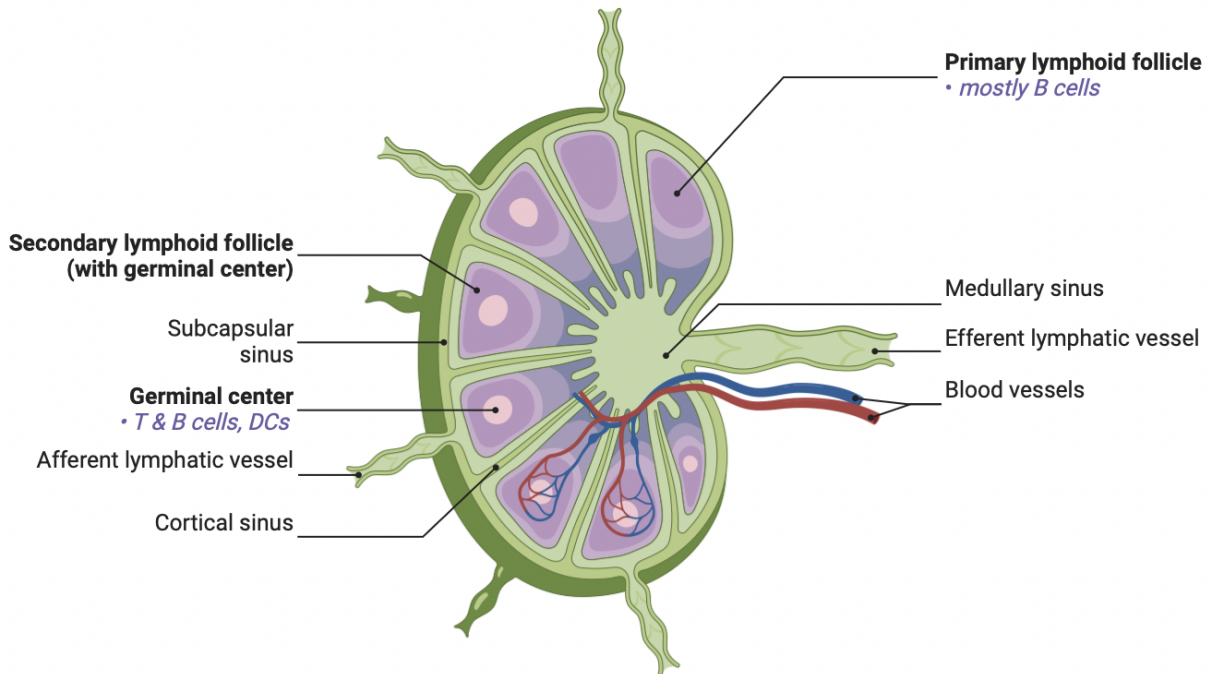


Figure 1.2: **Lymph node organization.** Created using Biorender.com.

not be possible.

A subset of patients with severe COVID-19 have been reported to exhibit an impaired adaptive immune response, marked by regressed germinal centers and extrafollicular B-cell activation[49, 98, 120], and it is possible that impaired transport through lymphatic vessels due to coagulation may be one factor, likely among many, contributing to this phenomenon. COVID-19 well-described as a coagulopathy, with some of the most widely reported clinical correlates of COVID-19 disease severity including venous and arterial thromboses, microvascular occlusions, disseminated intravascular coagulation, and bleeding disorders[93, 111]. Many patients hospitalized with COVID-19 also exhibit blood coagulation test abnormalities[33, 128]. Lymphatic coagulation has not yet been described in COVID-19, but if immune cells and viral antigens are not able to reach the lymph node due to coagulation-induced blockage of lymphatic vessels, they will not be presented to B cells in germinal centers, and antibody-producing plasma cells will not be produced. Additionally, immune

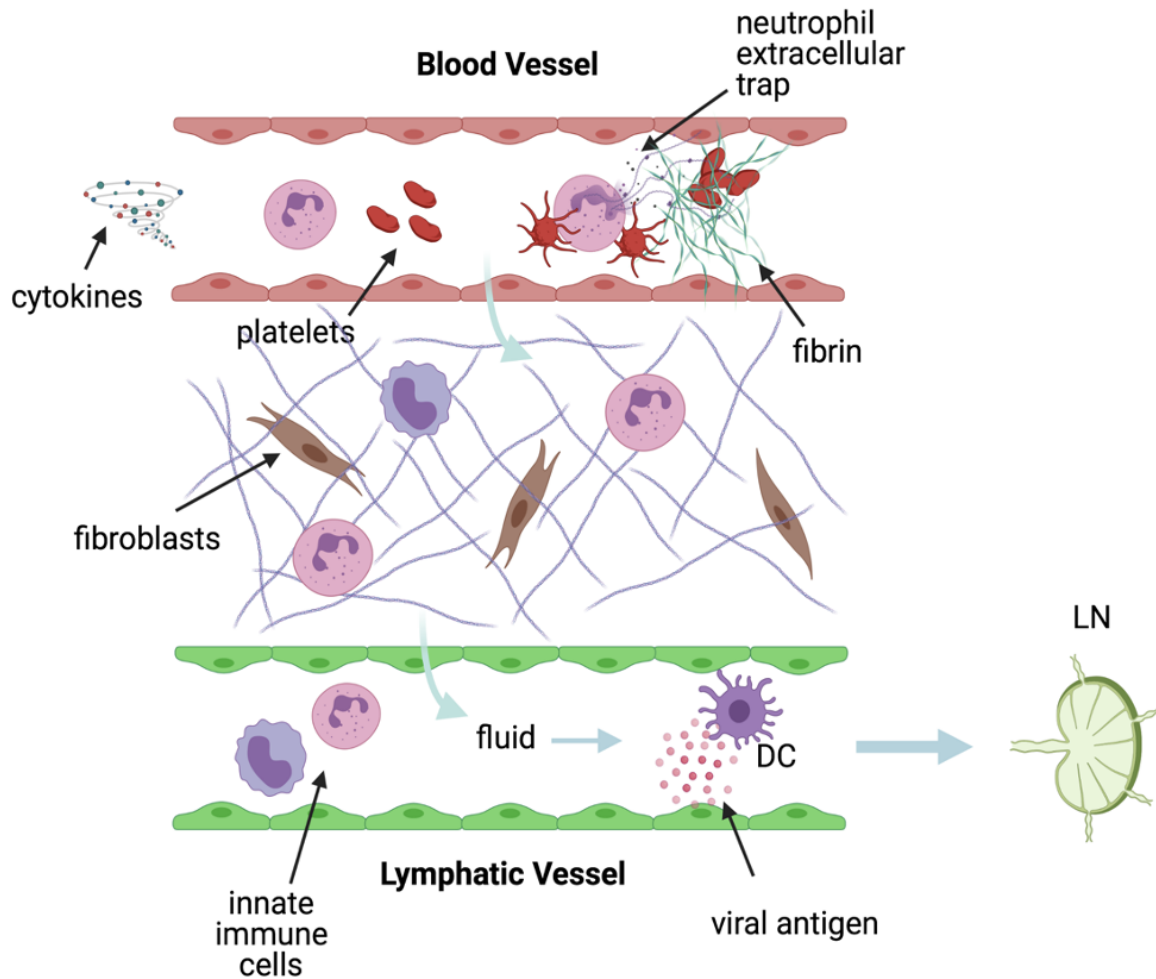
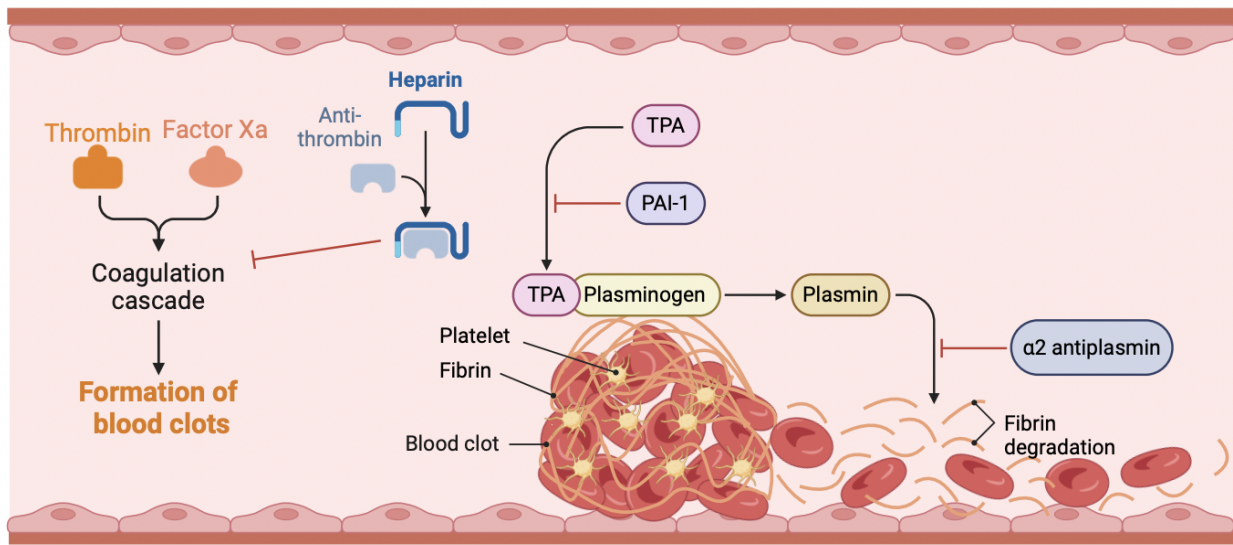


Figure 1.3: Lymphatic vessels transport interstitial fluid, viral antigens, and immune cells from tissues to the lymph nodes. Created using Biorender.com

signalling molecules necessary for germinal center maintenance would not reach the relevant resident cells in the lymph node, leading to an overall dampened antiviral antibody response to infection.





- TPA Tissue plasminogen activator
- PAI-1 Plasminogen activator inhibitor 1

Figure 1.4: **Coagulation and fibrinolysis cascades.** Binding of thrombin and factor Xa initiates the coagulation cascade in blood vessels when activated thrombin catalyzes the polymerization of fibrinogen monomers to fibrin. This can be inhibited by anti-thrombin and heparin complexes, or upstream by activated protein C through its inhibition of factors VIII and V. Tissue plasminogen activator (TPA) catalyzes the formation of plasmin from plasminogen, which then degrades fibrin back to fibrinogen, releasing platelets and red blood cells that are trapped in the thrombus. TPA is inhibited by plasminogen activator inhibitor 1 (PAI-1), and plasmin is inhibited by  $\alpha_2$  antiplasmin. Created using Biorender.com

## 1.4 Coagulation and fibrinolysis in blood are controlled by tightly-regulated signalling cascades

Blood coagulation is an important and tightly-regulated process that is necessary for the maintenance of hemostasis, or the prevention and cessation of bleeding. However, if this process is dysregulated, there are major pathological consequences, including deep vein thrombosis, stroke, and heart attacks. In blood vessels, coagulation is initiated by the recruitment, activation, and subsequent aggregation of cell fragments derived from the bone marrow called platelets[87]. Platelets adhere to the site of injury in vessels, binding to von Willebrand factor (VWF), which serves as a tether, and then can become activated in response to a wide array of stimuli[87, 124]. Once activated, platelets aggregate and form a plug to stop bleeding, which is then stabilized by fibrin - the other main player in the coagulation cascade.

The polymerization of fibrin is also key in driving clotting and maintaining hemostasis, and like platelet activation, is regulated by a number of different pro- and anti-coagulatory factors. Thrombin cleaves fibrinogen into fibrin, which can then polymerize and stabilize platelet plugs to form clots[7, 87, 95, 124]. Upstream of this, Factor X, when activated (Factor Xa), converts prothrombin to its active form, thrombin[7, 95, 124]. Factors VIII and V also make up part of the prothrombinase complex that is responsible for converting prothrombin to thrombin, by activating factor X[7]. Anti-thrombin, when activated by heparin, can inhibit this process, and activated protein C can inhibit the upstream activation of Factor X by degrading factors VIII and V[7, 95] (Fig. 1.4). Thrombin is also rendered inactive when bound to thrombomodulin, which like VWF, is expressed by endothelial cells.

Fibrinolysis is the process by which fibrin networks in blood clots are broken down in order to degrade the clot, and is also an important part of maintaining hemostasis. Tissue

plasminogen activator (TPA) converts plasminogen to plasmin, which can then break down fibrin into fibrin degradation products, including D-dimer, which is used as a clinical measure of clotting. This releases platelets and other components of the clot, leading to its dissolution[14] (Fig. 1.4). TPA is inhibited by plasminogen activator inhibitor 1 (PAI-1), and plasmin is inhibited by  $\alpha$ 2 antiplasmin[14] (Fig. 1.4).

## 1.5 Endothelial control of coagulation and fibrinolysis

While much of the coagulation cascade is mediated by factors in the blood such as platelets and coagulation factors synthesized in the liver, endothelial cells themselves can also regulate coagulation, through promoting or inhibiting either clotting or fibrinolysis. First, endothelial cells can either inhibit or promote platelet activation and binding, through secreting inhibitors such as nitric oxide and prostacyclin or expressing von Willebrand factor, which serves as a tether and activator[79](Fig. 1.5). Endothelial cells can also promote the coagulation cascade through expressing tissue factor (TF), which activates factor VII and is also expressed by other cells and present in neutrophil extracellular traps (NETs)[79]. Endothelial cells also play an important role in preventing coagulation through the secretion of tissue factor pathway inhibitor (TFPI) and the expression of a number of surface factors, including thrombomodulin, endothelial protein C receptor (EPCR), and heparin-like molecules[79](Fig. 1.5). Thrombomodulin binds thrombin and renders it inactive, and heparin-like molecules are able to bind and activate anti-thrombin. When bound to thrombomodulin, EPCR recruits protein C, which inhibits factors VIII and V.

In addition to expressing molecules that regulate platelet recruitment and activation and the coagulation cascade, they also secrete molecules important for the degradation of clots. Endothelial cells secrete both tissue plasminogen activator (TPA) and its inhibitor, plasminogen activator inhibitor 1 (PAI-1)[79](Fig. 1.5). TPA is necessary for the conversion of

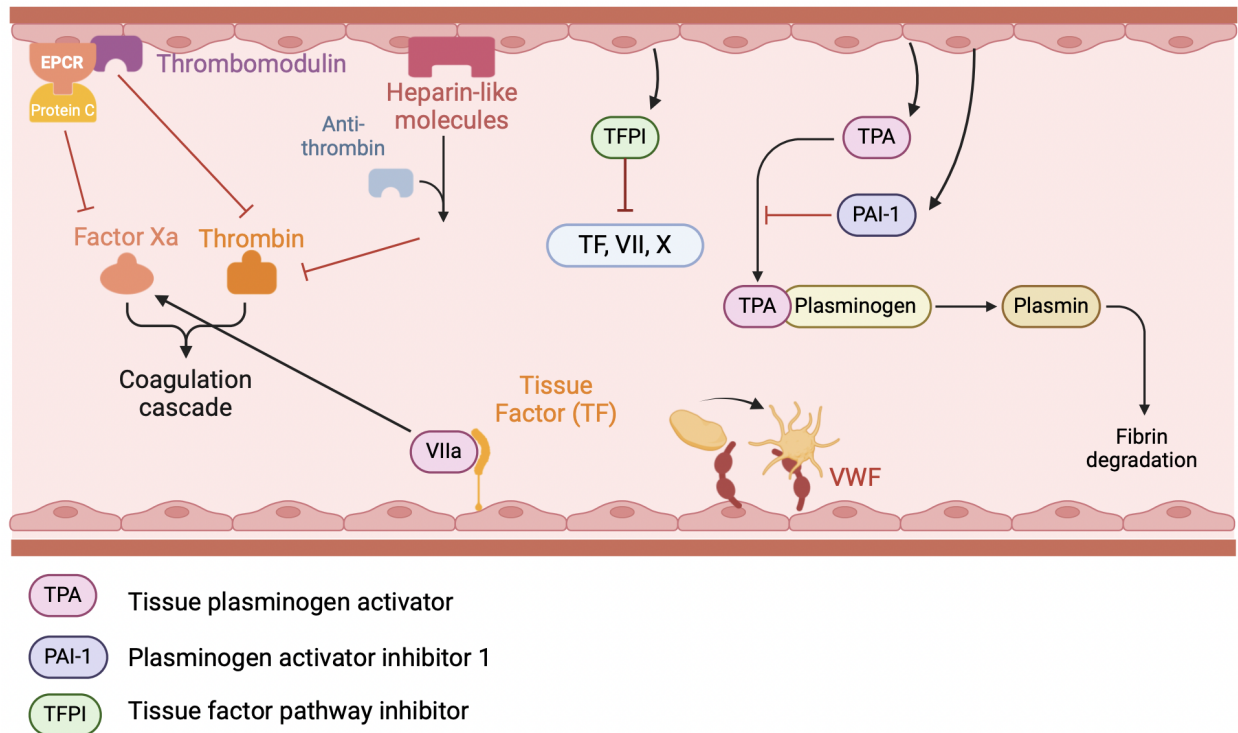


Figure 1.5: **Endothelial control of coagulation and fibrinolysis.** Endothelial cells express molecules that promote (tissue factor (TF), von willebrand factor (VWF)) or inhibit (thrombomodulin, endothelial protein C receptor (ECPR), tissue factor pathway inhibitor (TFPI)). They also express factors that regulate fibrinolysis, including tissue plasminogen activator (TPA) and plasminogen activator inhibitor 1 (PAI-1). Created using Biorender.com

plasminogen to plasmin which then degrades fibrin in clots.

## 1.6 Concentrations of coagulatory and fibrinolytic factors differ in blood versus lymph

Because lymphatic vessels drain fluid and uptake immune cells from the interstitial space, and platelets degranulate and are cleared by macrophages if they do exit blood vessels, lymph does not contain platelets (Fig. 1.3). However, despite lymph's lack of platelets, fibrin clots have been observed in lymphatic vessels and isolated lymph is able to clot, albeit slower than isolated plasma[62]. Lymphatic clots have been reported in lymphedema, lymphatic filariasis, lymphangiectasis, emphysema and cancer, and as a part of this dissertation I observed

fibrin clots in the lymphatic vessels of COVID-19 decedents[62, 71, 107]. While lymphatic clots have been observed in various lymphatic-related diseases, the mechanisms by which they form and their consequences are not well understood.

One potential reason that lymph coagulates slower than plasma *in vitro* could be that concentrations of coagulation factors in lymph are only 20-40% of what they are in plasma[17, 62, 74]. Lymph also contains higher levels of fibrinolytic factors that break down clots[17, 62, 74, 127] (Fig. 1.4). Coagulation factors VIII and V are downregulated in lymph compared to blood, while antithrombin and fibrinolytic factors such as tissue plasminogen activator (TPA) are upregulated[17, 62, 74] (Fig.s 1.4-6). While the concentrations of various clotting factors and fibrinolytic factors have been measured in lymph, some of these factors, notably thrombomodulin, TPA, PAI-1, and tissue factor pathway inhibitor (TFPI), are expressed or produced by endothelial cells, and the differences in their expression between blood and lymphatic endothelial cells have not been studied in depth, both at steady state and in response to inflammation. Work previously done in the Swartz lab showed that lymphatic vessels in mice did not strongly express von Willebrand factor (VWF)[71], which is not particularly surprising given lymph's lack of platelets, but does indicate that blood and lymphatic endothelial cells likely regulate clotting through different mechanisms that are specific to the unique microenvironmental cues presented in each type of vasculature.

## 1.7 Neutrophil extracellular traps (NETs)

While searching for candidates that may be initiating coagulation in lymphatics in the absence of platelets, neutrophil extracellular traps (NETs) were promising because they are known to initiate clotting in blood vessels both through activating platelets and through activating factors involved in the fibrin polymerization cascade[115]. Neutrophils are short-lived (6-12 hours) innate immune cells originating from myeloid precursors in the bone marrow

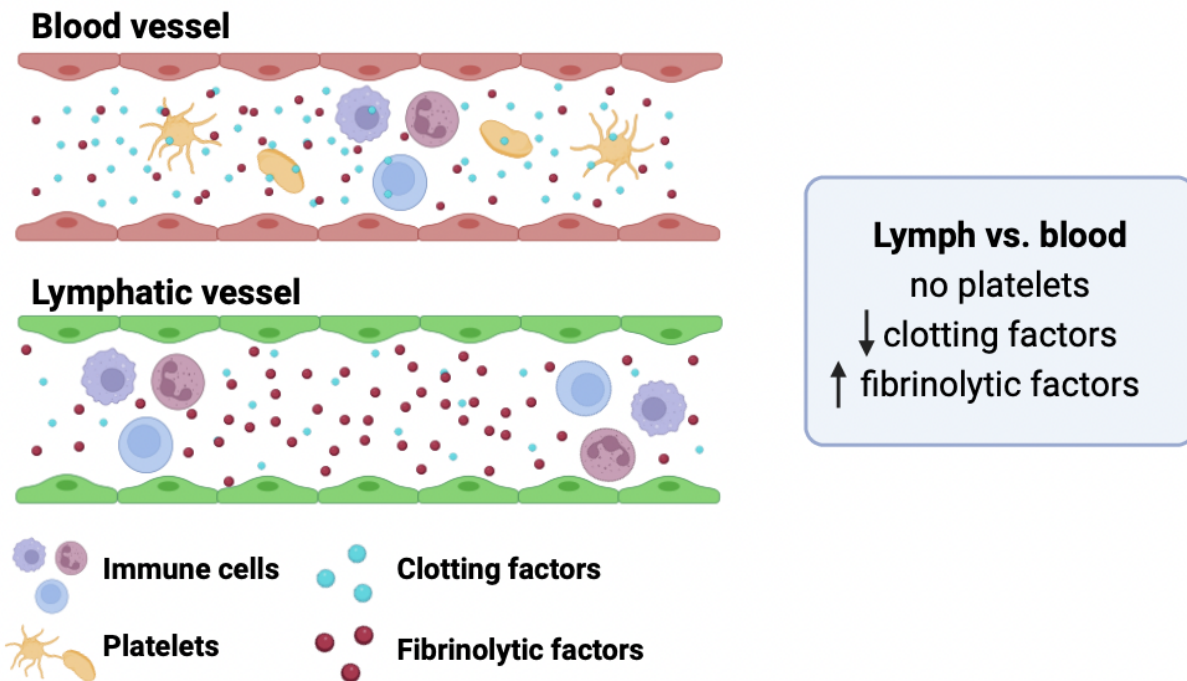


Figure 1.6: Coagulatory properties of lymph vs blood Adapted from [62]. While blood and lymph both contain immune cells, unlike blood, lymph does not contain platelets. Lymph contains higher concentrations of fibrinolytic factors and lower concentrations of clotting factors compared to blood. Created using Biorender.com.

that phagocytose pathogens as a part of the immune system's first line of defense, and are the first cells to migrate to secondary lymphoid organs carrying bacterial particles that can then be presented to T and B cells as a part of the adaptive immune response[41]. As a part of the innate immune response, they form neutrophil extracellular traps when pathogens are too large for them to phagocytose[9, 84]. NETs are large, web-like structures that burst from a dying neutrophil that are composed of cytosolic and granular proteins such as neutrophil elastase (NE), myeloperoxidase (MPO) and tissue factor (TF), that are assembled on a scaffold of decondensed chromatin[9, 84]. These mesh networks have potent antimicrobial properties and can trap, neutralize, and kill bacteria, fungi, viruses, and parasites[9, 84].

NETs form in response to a number of different stimuli, including a variety of microorganisms, as well as endogenous stimuli such as damage-associated molecular patterns, immune complexes, and cytokines[84]. They can be stimulated *in vitro* using the molecule phorbol 12-myristate 13-acetate (PMA), which activates protein kinase C (PKC) and triggers the production of reactive oxygen species (ROS) and eventually stimulates the enzyme PAD4[84], and I use this or ionomycin, an ionophore that binds calcium ions, as positive controls to stimulate NETosis in this work. Interestingly, NETs also form in response to cytokines secreted by tumor cells[61, 84, 85, 123] and are associated with metastasis and cancer-associated immunothrombosis.

When NETs form, neutrophils first arrest their actin dynamics and depolarize, and then the nuclear envelope disassembles as the chromatin decondenses. The enzyme PAD4 citrullinates histones in order to help the chromatin decondense, and then the chromatin mixes with the cytoplasmic and granular components of the neutrophil, before the cell eventually swells and ruptures, releasing the mix of chromatin and granular proteins into extracellular space[84, 113]. While these NETs play an important role in stopping the spread of pathogens

as a part of the innate immune response, they can also contribute to a number of diseases if they are over-produced or not cleared properly, including cancer, autoimmune diseases such as lupus, or coagulatory diseases[84].

## 1.8 Neutrophil-lymphatic interactions

One reason NETs are a promising candidate for clot initiation in lymphatic vessels is that it is known that neutrophils rapidly traffic through the lymphatic system in response to inflammation, and that certain subsets of lymphatic endothelial cells in the lymph node preferentially recruit neutrophils through chemoattractant secretion and expression of neutrophil adhesion molecules[4, 89, 104, 109]. It was only relatively recently discovered that neutrophils do in fact traffic from the periphery to the draining lymph nodes, both through afferent lymphatic vessels and high endothelial venules, and that CCR7 (the receptor for chemoattractants CCL19 and CCL21) expression on neutrophils is required for this in mice[4]. The rapid entry of neutrophils into the afferent lymphatic vessels through endothelial junctional retraction, and their subsequent trafficking to the lymph node, have also been shown to be dependent on  $\text{TNF}\alpha$ [3, 41, 89, 96, 104]. This, combined with the fact that both neutrophils and NETs can alter T cell activation[4, 89], implies that neutrophils, while classically associated solely with the innate immune response, may play an important role in regulating the adaptive immune response as well, and that this role may be facilitated by interactions with lymphatic endothelial cells.

Not only do lymphatic endothelial cells secrete CCL21 to recruit immune cells including neutrophils[92, 104], but in subsets of human lymph node lymphatic endothelial cells in the subcapsular sinus and the medullary sinus, these cells secrete higher levels of neutrophil chemoattractants CXCL1-5 and express higher levels of CD209, a molecule important for neutrophil adhesion[109]. This is at steady state, but in response to inflammation mediated



by  $\text{TNF}\alpha$ , lymphatic endothelial cells also secrete CXCL8, primarily from their luminal side[89], which is a potent neutrophil chemoattractant and inducer of NETosis, and express higher levels of neutrophil adhesion molecules ICAM-1 and VCAM-1[112, 123]. The role of CXCL8 and ICAM-1 has been studied in the context of neutrophil recruitment to lymphatic vessels and lymph nodes, but despite the fact that these are both known to be important in regulating NETosis, their relationship in regulating intralymphatic NETosis has not yet been investigated.

While lymphatic endothelial cells can regulate neutrophil recruitment and activation, neutrophils can also influence immune responses in the lymphatic system and lymph node. The lymphatic system can be hijacked by pathogens, or even cancer cells, in order to spread systemically if infection is not contained within the draining lymph node. CCR7-dependent neutrophil trafficking to the skin-draining lymph nodes has been shown to regulate cutaneous inflammation and resolution of *Staphylococcus aureus* infection[83]. Additionally, some subsets of neutrophils have recently been shown to patrol even naïve lymph nodes and increase CD4+ T cell and natural killer (NK) T cell activation in the lymph node, suggesting that their patrolling for infection is not limited to simply blood circulation, and that they play more of a role than previously understood in regulating the adaptive immune response[41, 68]. Exactly what this role is remains controversial, because neutrophils have also been shown to limit the local humoral response in the lymph node in response to *Staphylococcus aureus* infection[48].

*Staphylococcus aureus* infection in particular is known to rapidly disseminate throughout the lymphatic system, and the prevention of this spread is dependent on the recruitment of neutrophils to the lymph node[6]. Interestingly, while these neutrophils are recruited rapidly through high endothelial venules[6], their recruitment is largely mediated through lymph-

derived cytokines including CXCL1 and CXCL2, as lymph is transported to lymph nodes within a matter of minutes from the site of infection[121]. This indicates that while control of infection within the lymph node and lymphatic system as a whole is dependent on neutrophil behavior, the lymphatic system is actively regulating the neutrophil immune response, which will be a common theme throughout this dissertation. Additionally, *Staphylococcus aureus* is known to induce NETosis, and while I did not have time to explore the relationship between lymphatic coagulation and control of the acute spread of infection throughout the lymphatic system in this work, it could be of significant interest for future work, since it is likely that NET-induced lymphatic coagulation plays a role in the innate immune response as well as the adaptive immune response. This role could be positive, potentially through blocking the transport of pathogens through the lymphatic system, or negative, blocking the transport of lymph-derived cytokines important for immune cell recruitment and activation, and further work will need to be done to distinguish what effects, if any, lymphatic coagulation may have in this context.

## 1.9 NETs and coagulation in blood vessels

While the role of lymphatic endothelial cells in regulating NETosis has not been investigated, other groups have shown that blood endothelial cells are able to induce NETosis in response to inflammation[30, 38, 115].  $\text{TNF}\alpha$ -stimulated blood endothelial cells attract neutrophils and can induce NETosis, partially through CXCL8 secretion and increased expression of adhesion molecules including ICAM-1 and VCAM-1, and these NETs can then initiate clot formation at least partially through inducing endothelial cell damage[38]. Endothelial cell damage was one of the earliest proposed mechanisms for lymphatic coagulation[62, 81], so this, along with the pro-coagulatory properties of the NETs themselves, which are detailed below, was part of what piqued my interest in the role they may be playing in lymphatic coagulation.

One of the major ways in which NETs contribute to pathogenesis in a wide range of diseases is through promoting coagulation. In addition to damaging endothelial cells, NETs can also trap and activate platelets, and have been shown to be structurally intertwined with fibrin clots[31, 84, 115]. They are also sources of tissue factor[102] (Fig. 1.7), which activates factor X, and can impair protein C activation, which is important in preventing coagulation by inactivating factors VIII and V. This means they could potentially be promoting clotting independently of platelets.

NETs' strong negative charge enhances activation of factor XII, and their DNA backbone, as well as NET-associated histones and neutrophil elastase (NE), also stabilize clots and inhibit fibrinolytic activity[115] (Fig. 1.7). NE in particular may play conflicting roles, as it has been shown both to increase fibrinolysis through inactivating the plasmin inhibitor  $\alpha 2$  antiplasmin (Fig. 1.6) and have been shown to cleave von Willebrand factor (VWF) to release platelets, but has also been shown to cleave anticoagulant molecules including tissue factor pathway inhibitor (TFPI), thrombomodulin and antithrombin[115]. Histones in NETs, on the other hand, stimulate endothelial cells to release von Willebrand factor, which tethers and activates platelets[115]. NET-associated coagulation is implicated in many diseases, ranging from stroke and deep vein thrombosis to sepsis, cancer, and COVID-19[33, 84, 115]. Because of this wide range of pro-coagulatory effects attributed to NETs, I hypothesized that they may serve as an initiator for fibrin clot formation in lymph despite the absence of platelets.

## **1.10 NETs and immunothrombosis in COVID-19**

Coagulopathies are among the most widely reported clinical correlates of COVID-19 disease severity and include venous and arterial thromboses, microvascular occlusions, disseminated

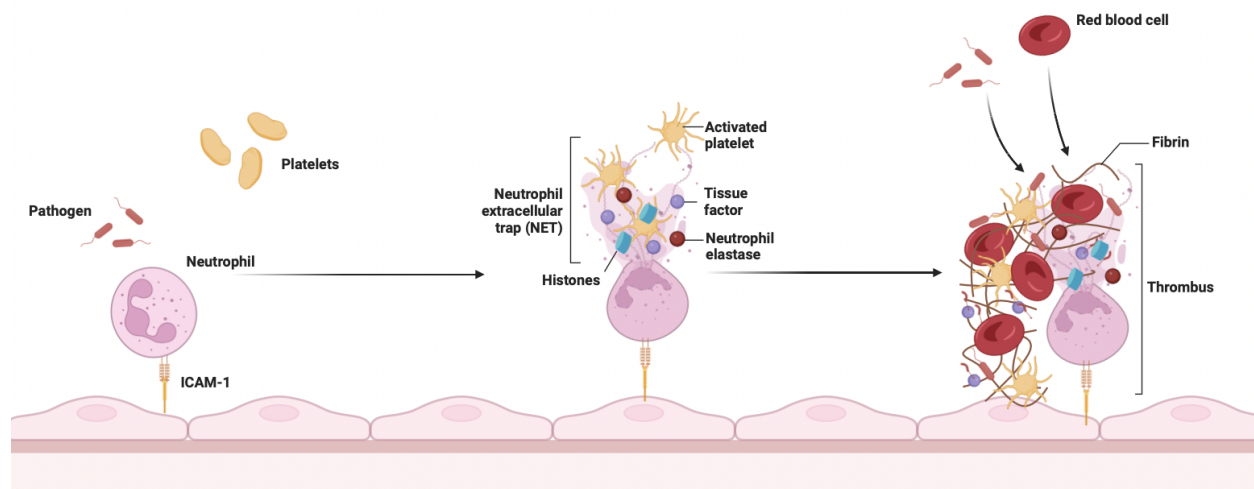


Figure 1.7: **NETs contribute to the formation and stabilization of thrombi.** NETs contain extracellular DNA, histones, tissue factor (TF), and neutrophil-elastase (NE), which contribute to the formation and stabilization of thrombi via platelet activation, impaired protein C activation, and increased thrombin production. Created using Biorender.com

intravascular coagulation, and bleeding disorders[93, 111]. Many patients hospitalized with COVID-19 exhibit blood coagulation test abnormalities[33, 128], and in addition to these standard indicators of coagulation, elevated serum levels of neutrophil extracellular trap (NET) markers have also been reported in hospitalized COVID-19 patients[33, 116, 130], and both NET levels and elevated circulating neutrophil-to-lymphocyte ratios were among the first reported predictors of disease severity[64, 130]. Additionally,  $TNF\alpha$  is upregulated and correlated with disease severity in COVID-19[19]. While  $TNF\alpha$  is known to induce clotting in blood vessels[124], it also stimulates lymphatic endothelial cells to modulate their expression of chemokines, adhesion molecules, and clotting factors that could drive immunothrombosis in lymphatics[58, 62, 65].

Immunothrombosis refers to the formation of thrombi initiated and supported by immune cells, with the intent of facilitating the recognition of pathogens and damaged cells, as well as inhibiting pathogen proliferation, and NET-associated immunothrombosis has been ob-

served in blood vessels in COVID-19 autopsy sections[33], and this was a large part of my motivation to search for NETs and immunothromboses in the lymphatic vessels of COVID-19 decedents in this work. While immunothrombosis is an important part of the innate immune response, like NETs, it can also become pathological when not properly regulated, leading to microthrombi formation in the alveolar capillaries, venous thromboembolism, and even arterial thrombotic events such as ischemic stroke, myocardial infarction, and systemic arterial embolism in the context of COVID-19[33, 115, 128].

### **1.11 Endothelial cell mechanosensing in inflammation**

Endothelial cells (ECs) of both blood and lymphatic vessels experience various mechanical cues, including blood and lymph flow, vascular stretching, or extrinsically from the extracellular matrix, that drive overall vascular homeostasis[15]. In healthy blood vessels, ECs form strong cell-cell and cell-matrix adhesions, and align with blood flow to maintain vessel morphology[15]. However, in case of disrupted flow, endothelial cells sense changes in mechanical stresses and undergo drastic remodeling. Despite early evidence showing that endothelial cells sense and respond to shear stress through cytoskeletal and cell-cell junction rearrangements, the precise mechanisms of force adaptation by endothelial cells during normal and disrupted flow remain unclear[39].

While a significant amount of work has been done studying how endothelial cells sense various mechanical cues, how these cues regulate their inflammatory response and immune interactions is comparatively under-studied. Many mechanosensitive transcription factors in the vascular endothelium, including hypoxia-inducible factor 1-alpha ( $\text{HIF-1}\alpha$ ), nuclear factor kappa-light-chain-enhancer of activated B cells ( $\text{NF-}\kappa\text{B}$ ), and Yes-associated protein (YAP)/transcriptional coactivator with a PDZ-binding domain (TAZ), have established functions in regulating inflammation, as well as vascular permeabilization, which is important

in regulating immune cell transmigration in and out of vessels[25]. While many of these mechanosensitive proteins are also known to regulate various inflammatory responses in other contexts, the mechanisms by which they do so in response to specific mechanical cues are not always well-understood.

Disturbed flow is one mechanical cue endothelial cells are regularly exposed to that is known to strongly induce vascular inflammation, but the mechanisms by which this occurs are not fully understood[16, 110]. Disturbed flow leads to increased expression of endothelial adhesion molecules ICAM-1, VCAM-1, and E-selectin[16, 110], as well as increased secretion of cytokines and chemokines such as IL-1, IL-6, CXCL8 and CCL5[76, 105]. Because changes in ICAM-1, CXCL8 and IL-6 are known to regulate neutrophil adhesion, recruitment, and NETosis[1, 122, 123], I focused on these three specifically. Secretion of these factors in response to inflammatory cytokines such as  $\text{TNF}\alpha$  is also regulated by cytoskeleton-associated factors such as Rho-kinase[100], suggesting that in addition to regulating immune responses of endothelial cells, different biomechanical microenvironments may also regulate their response to other inflammatory cues present in infection or other disease states. Because of this, different endothelial cell mechanotypes could either exacerbate or potentiate ongoing inflammatory processes. In this work, we discuss how a LIM-domain protein, FHL2, may be regulating these responses, and how the hyper-contractile phenotype induced by FHL2 overexpression may alter the response of endothelial cells to inflammatory stimuli such as  $\text{TNF}\alpha$ .

Proteomic screens of mechanotransduction pathways have revealed many proteins containing one or more LIM (Lin-11, Isl1, MEC-3) domain[2, 29, 50, 118]. The LIM domain is a 60 amino acid sequence that forms a double zinc finger protein-protein or protein-DNA binding interface[2]. 41 LIM proteins were found to be enriched at cell adhesions and/or the actomyosin cytoskeleton[2], and a screen of LIM domain proteins found that several

are recruited to actin stress fibers upon laser ablation, including the LIM-domain protein FHL2[119]. Unpublished work from the Gardel lab has established that FHL2 expression increases in response to shear stress from disrupted flow, both *in vitro* and in mouse arteries. Additionally, FHL2 localizes to stress fibers in hypercontractile tissues and endothelial monolayers exposed to disturbed flow. It also localizes to membrane ruffles or protrusions when contractility is decreased by Rho-associated protein kinase (ROCK) inhibition with Y-27, and shuttles to the nucleus with a lack of contractility[77]. While ongoing work is being done that has shown that FHL2 expression tunes actomyosin contractility and junctional strength in endothelial cells and that FHL2-stress fiber binding is necessary for junction disruption, my work focuses on how FHL2 over- or under-expression may influence endothelial cell inflammatory response to  $\text{TNF}\alpha$  or disturbed flow.

# CHAPTER 2

## LYMPHATIC COAGULATION AND NEUTROPHIL EXTRACELLULAR TRAPS IN LUNG-DRAINING LYMPH NODES OF COVID-19 DECEDENTS

### 2.1 Preface

This chapter includes work published in Blood Advances in 2022 [71]. Members from the Swartz lab and the UChicago Medical Center contributed to this work. Sandeep Gurbuxani, Phillip McMullen, Aliya Husain, Heather Smith, Jeffrey Mueller and Anne Sperling planned and carried out autopsy tissue collection and pathological analysis (tables 2.2 and 2.3), and Sandeep Gurbuxani and Emma Stewart assisted in germinal center characterization (fig.s 2.4 and 2.5). Anne Sperling's group provided control tissue and serum samples, and Sherin Rouhani, Jovian Yu, Jonathan Trujillo, Athalia Pyzer, and Thomas Gajewski planned and carried out the collection of patient serum samples and clinical data shown in figures 2.11 and 2.12. Rachel Weathered, Calixto Mateos Salles and Emma Stewart assisted with immunofluorescence staining in figures 2.2, 2.4, 2.5, and 2.6, and Rachel Weathered also assisted with image analysis in figures 2.6 and 2.8, as well as ELISAs done on patient serum in figure 2.11. Rachel Weathered, Calixto Mateos Salles, Chaney Giampaolo and Gavin Swartz assisted with image processing. Witek Kilarski developed the mouse model of lymphatic coagulation and collected the data in panels A-C of fig. 2.13, and Anish Mukherjee assisted me in conducting the experiments done in panels D-F. Alexandra Magold conducted PCR experiments included in fig. 2.10, and Melody Swartz assisted in determining scoring criteria and cut-offs for patient data in figure 2.11.



## 2.2 Introduction

Severe acute respiratory syndrome coronavirus 2 (SARS-CoV-2) infection has caused more than 6 million deaths worldwide from respiratory failure, septic shock, multi-organ failure, or other consequences of severe pulmonary infection[21]. Coagulopathies are among the most widely reported clinical correlates of disease severity and include venous and arterial thromboses, microvascular occlusions, disseminated intravascular coagulation, and bleeding disorders[93, 111]. Many patients hospitalized with COVID-19 exhibit blood coagulation test abnormalities, including elevated D-dimer levels, thrombocytopenia, and prolonged prothrombin time[33, 128]. In addition to these standard indicators of coagulation, elevated serum levels of neutrophil extracellular trap (NET) markers have also been reported in patients hospitalized with COVID-19[33, 116, 130], and both NET levels and elevated circulating neutrophil-to-lymphocyte ratios were among the first reported predictors of disease severity[64, 130]. Intravascular NETs form when neutrophils adhere to and become activated by injured endothelium, expelling their DNA into large nets that trap platelets to initiate clot formation and inhibit fibrinolysis, activate factor XII, and induce DNA-mediated thrombin generation to further promote coagulation[33, 115, 130]. Immunothromboses containing NETs have been observed in blood vessels in COVID-19 autopsy sections[73].

Fibrin clots can also occur in lymphatic vessels and have been reported in lymphedema, lymphatic filariasis, lymphangiectasia, and cancer[62], although experimental studies are scarce. In general, lymph coagulates slower than blood, consistent with the lack of platelets, lower levels of factors VIII and V, and higher levels of fibrinolytic factors[62]. However, neutrophils can enter inflamed lymphatic vessels and migrate to the draining lymph nodes (LNs)[3, 13, 35, 41, 89, 96, 104, 109], with their entry and migration facilitated by lymphatic endothelial cells (LECs) that upregulate adhesion molecules and secrete neutrophil chemoattractants such as CXCL8 when inflamed[3, 89, 109]. LECs may also activate neutrophils to

form NETs because CXCL8 is a potent driver of NETosis[34, 80].

Considering that NETs contain extracellular DNA, histones, and tissue factor[115] that may initiate coagulation in the absence of platelets, we hypothesized that lymphatic clotting is a clinical feature of severe COVID-19 disease and is promoted by lymphatic-associated NETosis. If so, this may have particular significance because a subset of patients with severe COVID-19 have been reported to exhibit an impaired adaptive immune response, marked by regressed germinal centers (GCs) and extrafollicular B-cell activation[49, 98, 120]. Transport of immune cells and viral antigens to the LN is a key step in the adaptive immune response, and blockages in lymphatic vessels may therefore impair downstream aspects of adaptive immunity including GC formation and antibody production.

Here, we examined the relationship between NETs, lymphatic vessels, and fibrin coagulation in severe COVID-19 using autopsy sections of lung and lung-draining lymph node (LDLN). We found widespread fibrin lymphatic clotting that correlated with both intra-lymphatic NETs and abnormal GC architecture in LDLNs. LECs in clotted vessels also exhibited downregulated thrombomodulin, which was also downregulated in LECs *in vitro* by tumor necrosis factor  $\alpha$  (TNF $\alpha$ ). In a separate cohort of patients with COVID-19, we found an inverse correlation between MPO-DNA, a NETosis marker, and antiviral antibody titers; furthermore, patients who failed to generate antibodies were more likely to have high MPO-DNA. In the ear skin of mice, we could demonstrate that lymphatic clotting could be induced by local injection of TNF $\alpha$  in a NET-dependent manner. Together, these findings suggest that COVID-19-associated coagulation is not limited solely to blood vasculature but extends to the lymphatic vasculature, where it may be driven by NETs rather than platelet activation. Because lymphatic vessels are responsible for the transport of antigen and immune cells to the LN and GCs are a key part of the humoral immune response, lymphatic

clotting and intralymphatic NETosis may have important consequences relating to antiviral antibody production in patients with severe COVID-19 or other viral infections.

## 2.3 Methods

### 2.3.1 *Human tissue procurement*

Postmortem tissues from lungs and LDLNs were obtained from patients at the University of Chicago Medical Center: 16 patients who died from SARS-CoV-2 infection and 9 control patients who died before the pandemic, including 3 who died of H1N1 (Tables 2.1 and 2.2). Patient demographics were representative of the patient population at the University of Chicago Medical Center. All policies were reviewed and approved by UChicago’s infection control, and autopsy procedures followed College of American Pathologists and Centers for Disease Control and Prevention guidelines. The study was conducted in accordance with the Declaration of Helsinki. Because of metastatic cancer involvement, LDLNs from 3 patients with COVID-19 and 1 control were excluded from analysis. Non-COVID-19 lung controls were obtained from the Gift of Hope Regional Organ Bank of Illinois. All tissues were formalin fixed and paraffin embedded before sectioning. Serum samples from patients hospitalized with COVID-19 were obtained from the UChicago COVID-19 biobank study (IRB 20-0520) as described earlier(cite31). Daily SpO<sub>2</sub>-to-FiO<sub>2</sub> ratios were calculated by averaging all clinical measurements available per patient per day. The lowest daily SpO<sub>2</sub>-to-FiO<sub>2</sub> ratio during a patient’s initial hospitalization was used to assign disease severity.

### 2.3.2 *Quantification of lymphatic clotting, neutrophils, and NETs*

To quantify neutrophil and NET density in patient lungs and LDLNs, sections were imaged and analyzed after thresholding using the Fiji particle analyzer plug-in. Intralymphatic fibrin and NETs were quantified manually in whole-slide tiled images (20x); each vessel was

assigned a clotting score (0 = no fibrin, 1 = fibrin along the luminal surface only, 2 = partially clotted [ $< 10\%$ ], 3 = partially clotted [ $> 10\%$ ], and 4 = fully clotted) and a NET score (0 = no NETs, 1 = NETs along the lumen only, and 2 = NETs integrated into clot). Scores for all vessels in each LDLN were averaged to give fibrin clotting and NET scores for each patient.

### 2.3.3 *Lymph node scoring*

Quality of GC structures and overall LN architecture were assessed from slides stained with hematoxylin and eosin (H&E) or immunostained for CD3, CD20, CD83, and GL7. GCs were analyzed by follicle size, ratio of tingible body macrophages (TBMs) vs medium and large body cells within the follicle, degree of hyalinization, overall LN architecture integrity, and distribution of activated T and B cells. LNs were assigned an H&E score (0 = primary follicles only as in a naïve setting, 1 = robust GCs, 2 = weak GCs, 3 = lack of GCs in infection setting, 4 = regressed GCs, and 5 = no apparent follicles). LNs were also assigned a lymphocyte distribution score (0 = small follicles only with distinct zones, 1 = large follicles with distinct zones, 2 = mixed follicle size and slight loss of integrity, 3 = small follicles only in infection setting, 4 = mixed follicle size and moderate loss of integrity, and 5 = diffuse B-cell zone and complete loss of integrity). Finally, LNs were assigned a GC activation score (0 = predominantly primary follicles, activation markers absent from follicle, and naïve setting; 1 = predominantly reactive GCs, activation markers present within follicle, and either naïve or infection setting; 2 = follicular activation with minor abnormalities in follicle structure and little or no extrafollicular activation; 3 = predominantly small primary follicles in infection setting and lack of GC response determined by decreased activation markers; 4 = moderate abnormalities in follicle activation pattern (including extensive cell drop-off) and can include strong follicle activation with extrafollicular activation; and 5 = extensive extrafollicular B-cell activation and poor overall follicle formation or activation). Scores for each patient were

summed to create an overall GC abnormality score.

#### 2.3.4 *Animals*

All procedures were approved by the University of Chicago (ACUP 72414). C57BL/6 mice (Jackson Laboratories) between 6 and 10 weeks of age were used. Intravital immunofluorescence imaging was performed as described previously[37].

#### 2.3.5 *In vivo labeling of fibrin*

Fibrinogen in phosphate-buffered saline (40 mL of 10 mg/mL [F8630-1G; Sigma-Aldrich]) was reacted with 1.6 mL of 4 mg/mL fluorescein isothiocyanate (FITC) or Alexa Fluor 647 (ThermoFisher Scientific) for 1 hour. Fibrinogen was dialyzed 4x in 4 L of phosphate-buffered saline. Labeled fibrinogen (100  $\mu$ L; IV) was injected into mouse tail veins 15 to 30 minutes after treatment expected to induce intralymphatic coagulation (thrombin or cytokine injection).

#### 2.3.6 *Thrombomodulin and NETosis blocking in vivo*

Thrombin inactivation was achieved by reacting of thrombin (50  $\mu$ L of 1 U/ $\mu$ L) with 1-mM p-amidinophenylmethylsulfonyl fluoride (Millipore Corp) for 2 hours. Inactive thrombin (0.5  $\mu$ L) was injected intradermally, alone or with 10 ng/ $\mu$ L TNF $\alpha$  or 10  $\mu$ g/ $\mu$ L interleukin-1 $\beta$  (IL-1 $\beta$ ) (both from Peprotech) into the dorsal ear dermis. To degrade NETs, mice were injected intraperitoneally with 500 IU DNase I (Sigma-Aldrich) in 0.5 mL Iscove's Modified Dulbecco's Medium (IMDM) immediately after intradermal injections of TNF $\alpha$ .

qPCR Primers			
Primer	Sequence	Primer	Sequence
Hu_Gapdh_F	ACATCATCCCTGCCTCTACTGG	Hu_Gapdh_R	AGTGGGTGTCGCTGTTGAAGTC
Hu_TM_F	AGAGCCAAGTGCAGTACCA	Hu_TM_R	GGAGATGCCTATGAGCAAGC
hu_GAPDH_Fw	CCA TGG AGA AGG CTG GGG	hu_GAPDH_Rv	CCA AGT TGT CAT GGA TGA CC
hu_CXCL8_Fw	AGA TCT GAA GTG TGA TGA CTC AGG	hu_CXCL8_Rv	GAA GCT TGT GTG CTC TGC TGT CTC
ms_TM_FW	CCTGGCTCCTATGAGTGTATCT	ms_TM_RV	CTTCCTTGGTGTCTTCCCTAAC
ms_CXCL3_FW	GCACCCAGACAGAAGTCATAG	ms_CXCL3_Rev	ACTTGCCGCTCTTCAGTATC
ms_CXCL2_FW	TAAGCACCGAGGAGAGTAGAA	ms_CXCL2_Rev	GTCCAAGGGTTACTCACAACA
ms_CXCL1_FW	GTGTCTAGTTGGTAGGGCATAAT	ms_CXCL1_Rev	CAGTCCTTTGAACGTCTCTGT
ms_CCL5_FW	CCAGAGAAGAAGTGGGTTCAAG	ms_CCL5_Rev	AGCAATGACAGGGAAGCTATAC
ms_CCL3_FW	GAAGATTCCACGCCAATTCATC	ms_CCL3_Rev	GATCTGCCGTTTCTCTTAGTC
ms_CCL2_FW	CTCGGACTGTGATGCCTTA	ms_CCL2_Rev	TGGATCCACACCTTGCATTTA

Table 2.1: qPCR primers

### 2.3.7 LEC culture and qPCR

Murine immortalized LECs (iLECs) were grown in 6-well plates in 1ml of full medium and total RNA was isolated using TriZol reagent (15-596-018; ThermoFisher Scientific). RNA was quantified and purity-ascertained via nanodrop spectrophotometric readings. Equal amounts of total RNA were reverse-transcribed using Reverse Transcriptase (A5004; Promega). Transcription product was used for real-time PCR with PowerUP SYBR Green Master Mix system (A25776; Applied Biosystems) on a CFX384 Touch Real-Time PCR Detection System (BioRad). Thresholding was performed manually to ensure readings were within linear amplification phase, and annealing temperatures were based on primer composition. Oligos were custom-made by IdtDNA (IDT, Table 2.1). Raw data was analyzed as  $2^{-\Delta\Delta C(T)}$  over control against a housekeeping gene (GAPDH) as a modification of Livak, et al., 2001[67].

### *2.3.8 LEC cytokine treatment and immunostaining*

Human iLECs (HiLECs) were cultured in 96-well plates in 100 $\mu$ l of full medium and treated with IL-6 (200-06; Peprotech, 10ng/ml or 50ng/ml), IFN $\gamma$  (300-02; Peprotech, 10ng/ml, 50ng/ml or 100ng/ml) or TNF $\alpha$  (300-01A; PeprTech, 10ng/ml, 50ng/ml or 100ng/ml) for 24h. Cells were fixed using 4% PFA/4% in PBS and stained as described below (without antigen retrieval).

### *2.3.9 ELISA*

For CXCL8 ELISA, HiLECs were cultured in 6-well plates in 1ml of full medium and treated with IL-6 (10ng/ml or 60ng/ml), IFN $\gamma$  (100ng/ml or 200ng/ml), or TNF $\alpha$  (50ng/ml or 100ng/ml) for 24h. Medium was collected at 30min, 60min, 90min, 180min, and 24h. CXCL8 secretion was measured using an IL-8/CXCL8 DuoSet ELISA kit (DY208; R&D Systems). All procedures utilizing human samples were performed under BSL2 conditions. For titration of anti-RBD antibodies, ELISA plates were coated with purified recombinant RBD (100nM) in PBS for 12-16h at 4°C. Plates were then blocked with BSA (2%) in PBS for 2h at RT and washed with PBS-Tween 0.05% (PBST). Human plasma was diluted 1:100 in PBST+BSA (0.5%), and then serially diluted by 10. Samples were added to plates and incubated for 2h at RT. Plates were washed again and incubated with (HRP)-conjugated anti-human IgG for 1h at RT in the dark. Plates were washed, revealed using 3,3',5,5'-Tetramethylbenzidine (TMB) for 30min in the dark, and the reaction was stopped using 1M H<sub>2</sub>SO<sub>4</sub>. Absorbances at 450nm were read using an Epoch plate reader (BioTek) and corrected with the absorbance at 570nm. Titers represent the highest dilution at which antibodies were detected, in log<sub>10</sub>. Anti-RBD titers are reported in log<sub>10</sub>. Controls were samples were collected from healthy donors prior to the pandemic.

Levels of MPO-DNA in human serum (diluted 10x in PBS with 0.5% BSA) were assessed

by ELISA as previously described[1] (MPO antibody:475915; Sigma-Aldrich), and results were normalized to the “NET-standard” of pooled supernatants of PMA-stimulated human neutrophils. To obtain these standards, we isolated neutrophils from the blood of healthy volunteers (IRB20-1097) collected into EDTA-coated BD vacutainer tubes by standard phlebotomy. Neutrophils were isolated using the EasySep<sup>TM</sup> Direct Human Neutrophil Isolation Kit (19666; STEMCELL Technologies) and treated with 600nM PMA to induce NETosis. Supernatants were collected after 4h and stored at -20C. **Analysis:** Patients who only had samples from <7 days after symptom onset were excluded because anti-RBD titers had likely not stabilized yet. For antibody titers that were increasing over time, values were averaged for each patient once levels stabilized. For patients where antibody levels decreased by  $\geq 2$  titers, the average was taken from the peak titer until the last timepoint. MPO-DNA values were taken from the same timepoints used for the anti-RBD titers and averaged for each patient.

### *2.3.10 Immunofluorescence staining and imaging*

All tissues were formalin-fixed, paraffin-embedded and cut into 5 $\mu$ m sections for immunofluorescence staining. After deparaffinization and rehydration, sections were heated at 50C for 40min in citrate buffer (pH 6). Sections were permeabilized in 10% DMSO in diH2O and in TBS 0.1% Tween20 (TWN510; BioShop). Samples were incubated with blocking buffer (TBS with 10% donkey serum, d9663-10ML; Sigma-Aldrich) for 30min RT. Primary antibodies were incubated in TBS with 5% donkey serum overnight at 4C. Primary antibodies used: mouse anti-podoplanin (D2-40, BioLegend), goat anti-mouse LYVE-1 (polyclonal, R&D Systems) rabbit anti-H3cit(polyclonal, Abcam), goat anti-myeloperoxidase (polyclonal, R&D Systems), sheep anti-fibrinogen (polyclonal, Invitrogen), rabbit anti-thrombomodulin(EPR4051, Abcam), rabbit anti-CD3 (polyclonal, DAKO), rat anti-GL7 (GL7, Invitrogen), rabbit anti-CD83(polyclonal, Sigma-Aldrich), and mouse anti-CD20 (L26, Invitrogen). After washing



with TBS-T and TBS, secondary antibodies were incubated in TBS with 5% donkey serum for 1h at RT in the dark. All secondary antibodies were from Invitrogen and used at 1:500. Samples were mounted with 10 $\mu$ l ProLong Antifade reagent (P36961; ThermoFisher Scientific) on glass slides and stored at RT in the dark. All samples were analyzed by fluorescence microscopy using standard filter sets. Immunofluorescence images were acquired using an Olympus IX83 spinning-disc confocal fluorescence microscope and whole-slide tiled images of patient LDLNs were acquired by the UChicago Integrated Light Microscopy Core using a Leica SP8 laser-scanning confocal microscope (Leica Microsystems Inc.). Representative z-stack images (10x or 20x magnification) and mean-z-projections were processed and analyzed using ImageJ and GraphPad Prism.

### *2.3.11 H&E Staining and Imaging*

Tiled images of whole-LN sections stained with H&E were obtained using a Leica DMi8 microscope (Leica Microsystems Inc.) at 5X magnification. Settings were as follows: 3-4ms exposure, 25% saturation, and automatic white-field adjustment. Tiles were overlapped by 10% and the Smooth Merge function was performed in Leica Application Suite X (version 3.4.2.18368). Images were exported as TIFs or PNGs for analysis. Representative images of LN sections were obtained at 20X magnification using a Leica DMi8 microscope in brightfield with 15-20ms of exposure, 25% saturation, and automatic white-field adjustment. In tiled images, sections were overlapped by 10% and Smooth Merge was performed as above. Images were exported as TIFs or PNGs for analysis.

### *2.3.12 Statistics and reproducibility*

All statistical analyses and linear regressions were performed using GraphPad Prism. One-way analysis of variance (ANOVA) with Tukey multiple comparisons post-test was used to determine P values for multiple groups, unless otherwise noted. For comparison between 2

groups, Mann-Whitney U tests and Student t tests were used as noted in Figures 2.4, 2.5, and 2.6.

## 2.4 Results

### *2.4.1 Intralymphatic fibrin clots are prevalent in lungs and LDLNs of COVID-19 decedents*

Because pulmonary coagulation is a key clinical feature of severe COVID-19[93, 111, 128], we first determined whether lymphatic vessels in patient lungs also contained fibrin clots by immunostaining lung tissue sections from 16 COVID-19 decedents (Table 2.1) and 8 controls (Table 2.2). As expected, we found abundant evidence of intravascular and interstitial coagulation, and interestingly, many intact lymphatic vessels also contained fibrin clots (Figure 2.1).

However, the lung lymphatic vessels were frequently severely damaged and interstitial fibrin widespread, precluding meaningful quantification. Surprisingly, when analyzing the LDLNs, we found more extensive lymphatic clotting within intact lymphatic vessels (Figures 2.2A-B), particularly in the subcapsular sinus (Figure 2.3).

In contrast, fibrin-containing lymphatics were rare in LDLNs of patients who died of causes unrelated to viral infection (Figure 2.2C). However, in 3 patients who died of severe H1N1 influenza, lymphatic clotting in the LDLN was similar to that observed in the COVID-19 decedents (Figure 2.2D). We then analyzed every lymphatic vessel in each tile-scanned LDLN image, assigning each vessel a fibrin score based on the extent of blockage (Figure 2.2E). The LDLNs of COVID-19 decedents had higher fractions of lymphatic vessels that were mostly or fully clotted (fibrin score of 3-4) compared with those of controls (Figure 2.2F), whereas both COVID-19 and H1N1 LDLNs had substantially higher fibrin scores than controls (Figure 2.2G). This suggests that lymphatic clotting in LDLNs may be a common

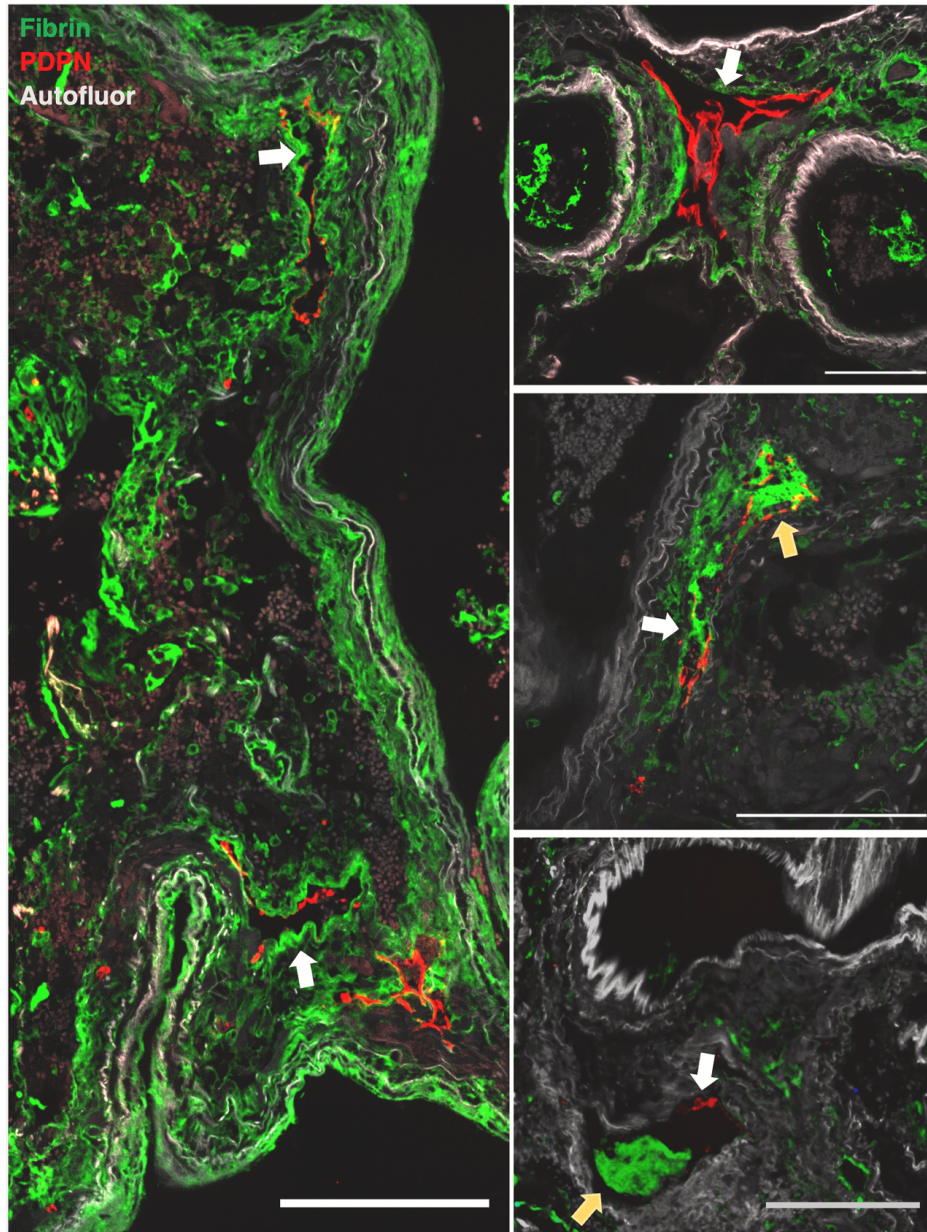


Figure 2.1: Fibrin clots in lymphatic vessels in lungs of COVID-19 decedents. Representative immunofluorescence images of lung sections showing fibrin (green) and podoplanin+ LECs (red) with 488 autofluorescence (gray) to show tissue structure. Yellow arrows indicate clotted lymphatic vessels, and white arrows indicate damaged lymphatic endothelium. Scale bars, 100  $\mu\text{m}$

Pt. ID	Age (y)	Sex	Race/Ethnicity	Respiratory Symptoms	Illness Length (days)	Ventilator	Tocilizumab	Relevant Comorbidities
1	30s	M	AA	Y	9	Y	Y	HTN, DM, morbid obesity, smoker
2	50s	F	H/L	Y	12	Y	N	congenital heart defect, COPD, smoker
3	80s	F	AA	Y	15	Y	N	Remote smoker
4	60s	F	AA	Y	4	N	N	Prior stroke, HTN, DM
5	80s	F	AA	N	17	N	N	DM, breast cancer, remote smoker
6	80s	M	AA	Y	2	N	N	Prior stroke, HTN
7	40s	M	AA	Y	23	Y	Y	DM, morbid obesity, HTN
8	70s	F	AA	Y	15	N	Y	CLL, anal carcinoma, HTN, DM
9	80s	F	C	Unknown	0	N	N	COPD, DM2, HTN, colon cancer (2001), remote smoker
10	70s	F	AA	Y	4	Y	N	HTN, remote smoker
11	50s	M	AA	Y	12	Y	N	Obesity
12	60s	F	C	N	2	Y	N	Advanced cervical cancer, COPD, smoker
13	50s	F	H/L	N	41	Y	Y	Uncontrolled DM
14	70s	M	AA	Y	7	Y	N	HTN, CAD, PAD, COPD, smoker
15	50s	M	H/L	Y	57	Y	Y	HTN, DM
16	60s	F	AA	Y	4	Y	N	Breast, salivary gland cancer, HTN

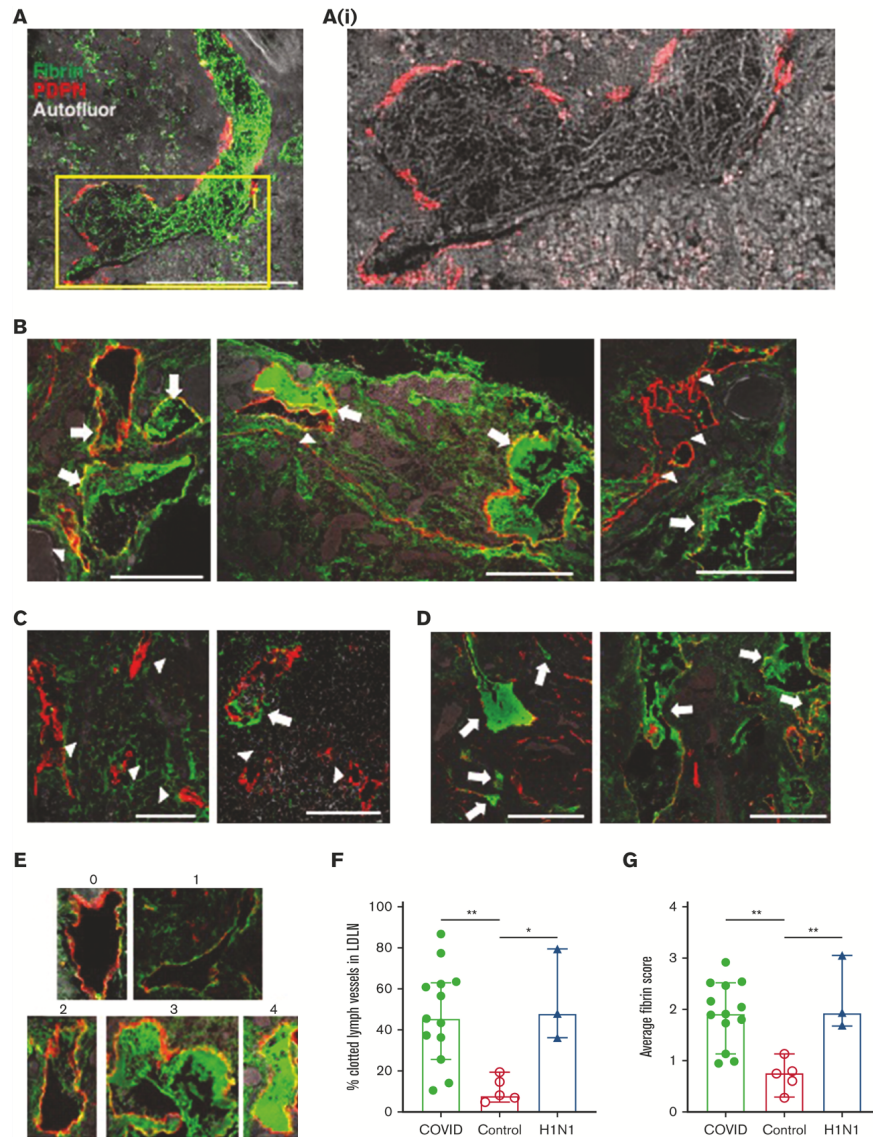
Abbreviations: AA = African American, C = Caucasian, CAD = coronary artery disease, CLL = chronic lymphocytic leukemia, COPD = chronic obstructive pulmonary disease, DM = diabetes mellitus, DM2 = diabetes mellitus type 2, H/L = Hispanic/Latinx, HTN = hypertension, PAD = peripheral artery disease

Table 2.2: COVID-19 Decedent Clinical Information

Pt. ID	Tissue	Age (y)	Sex	Race/Ethnicity	Cause of Death	Comorbidities
H1N1-1	LN	40s	F	Unknown	H1N1	No relevant medical history
H1N1-2	LN	40s	M	Unknown	H1N1	Surgery and CRT for GBM. fever, resp. failure, influenza and superimposed staph PNA, renal failure, disseminated HSV
H1N1-3	LN	30s	F	Unknown	H1N1	CAD/MI, fevers/rigors. Treated with Abx+tamiflu
Ctrl-1	LN	40s	F	Unknown	Still's Disease	Adult Still's Disease
Ctrl-2	LN	70s	M	Unknown	Cancer	Squamous cell carcinoma, CRT
Ctrl-3	LN	60s	M	Unknown	PNA	End-stage renal disease, kidney transplant, PNA
Ctrl-4	LN	10s	M	Unknown	Cancer	T lymphoblastic lymphoma
Ctrl-5	LN	40s	M	Unknown	Lung disease	Interstitial lung disease
Ctrl-6	Lung	60s	F	AA	Stroke	Anoxia, history of stroke, HTN, high cholesterol, gout, smoker
Ctrl-7	Lung	30s	M	C	Head trauma	MVA, smoker
Ctrl-8	Lung	40s	F	C	Stroke	Anoxia, history of HTN, migraine, smoker
Ctrl-9	Lung	60s	M	AA	Stroke	Intracranial hemorrhage
Ctrl-10	Lung	60s	F	C	Stroke	Intracranial hemorrhage, smoker
Ctrl-11	Lung	50s	M	C	Stroke	Hyperlipidemia >10 years, benign prostatic hyperplasia, A-fib, smoker
Ctrl-12	Lung	10s	M	C	Stroke	Intracranial hemorrhage
Ctrl-13	Lung	50s	F	H/L	Stroke	Intracranial hemorrhage, HTN
Ctrl-14	Lung	50s	F	C	Stroke	Intracranial hemorrhage, HTN, smoker
Ctrl-15	Lung	60s	M	C	Head Trauma	MVA, high cholesterol, IBS
Ctrl-16	Lung	60s	M	C	Stroke	Intracranial hemorrhage, HTN, smoker
Ctrl-17	Lung	70s	F	C	Head Trauma	Accident (non-MVA), high cholesterol

**Abbreviations:** AA = African American, Abx = antibiotics, A-fib = atrial fibrillation, C = Caucasian, CAD/MI = coronary artery disease/myocardial infarction, CRT = chemoradiotherapy, GBM = glioblastoma multiform, H/L = Hispanic/Latinx, HSV = Herpes simplex virus, HTN = hypertension, IBS = irritable bowel syndrome, MVA = motor vehicle accident, PNA = pneumonia, VTAC = ventricular tachycardia

Table 2.3: Non-COVID-19 Decedent Clinical Information



**Figure 2.2: Lymphatic clotting is widespread in LDLNs of COVID-19 decedents.** (A) Representative immunofluorescence image showing a large lymphatic clot in an LDLN section with fibrin (green) and podoplanin (red), with inset (Ai) highlighting the fibrillar structure of the fibrin clot in 488 autofluorescence (gray). (B-D) Representative images showing intralymphatic fibrin clots in LDLNs of (B) COVID-19 decedents, (C) control decedents without viral infections, and (D) H1N1 decedents, with arrows indicating partially or fully clotted vessels and arrowheads indicating open vessels. Scale bars in panels A-D, 100  $\mu\text{m}$ . (E) Lymphatic clotting score rubric showing examples for each score: 0, no fibrin (fully open); 1, fibrin confined to endothelium; 2, minimal intralymphatic fibrin (<20% of vessel lumen); 3, partially occluded (>20% of lumen); and 4, fully occluded. (F) Percentage of clotted lymphatic vessels (with a fibrin score of 3-4) in LDLNs from COVID-19, control, and H1N1 decedents; each dot shows the average from 3 sections of each patient. (G) Average lymphatic fibrin score in each LDLN. Bars in panels F-G represent median  $\pm$ 95% confidence interval; \*P < .05, \*\*P < .01 by one-way ANOVA with Tukey multiple comparisons post-test.

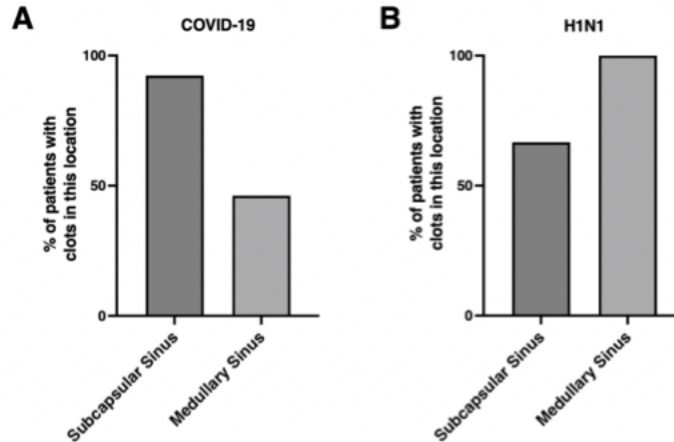


Figure 2.3: **Clot location in COVID-19 and H1N1 lung-draining lymph nodes.** Percentage of COVID-19 (A) and H1N1 (B) patient LNs that contained clots in the subcapsular and medullary sinuses.

clinical feature of severe pulmonary viral infection, where clotting in the subcapsular sinus may block lymph entry into the LN.

#### 2.4.2 *Lymphatic clotting correlates with abnormal or missing GCs in LDLNs*

It has been documented that dysregulated adaptive immune responses and impaired GC formation can occur in severe cases of COVID-19[49, 120]. Because lymphatic clotting would likely disrupt the entry and exit of fluid, antigens, and antigen-presenting cells to and from the LDLN, we asked whether the lymphatic clotting we observed in COVID-19 decedent LDLNs could be correlated to this phenomenon. To test this, we created scoring criteria: (1) H&E score for GC architecture, (2) GC activation score based on immunostaining for GL7 (B-cell activation marker) and CD83 (light-zone marker), (3) lymphocyte distribution score based on staining for B- and T-cell markers, and (4) an overall GC abnormality score reflecting the sum of (1) through (3).

Based on H&E scores, most LDLNs from COVID-19 decedents, unlike controls, showed regressed GCs and abnormal follicle architecture based on the increased presence of TBMs and

lack of a mantle zone (Figure 2.4A-B), whereas H&E scoring showed significant differences among COVID-19 and H1N1 LDLNs compared with controls (Figure 2.5A-B). When considering GC activation, COVID-19 LDLNs also exhibited increased extrafollicular activation based on GL7 staining and were more likely to show diffuse regions of B-cell activation compared with controls, whose activation patterns were contained within discrete oval-shaped follicles (Figure 2.5C-D). Overall, CD83 and GL7 staining was decreased within COVID-19 follicles, potentially indicating follicular regression or a failure to develop a strong GC reaction (Figure 2.4C). There was a significant difference in the GC activation scores between COVID-19 and control decedents and between H1N1 and control decedents (Figure 2.5C-D). Finally, we found that although the lymphocyte distribution scores were not significantly different in LDLNs between the COVID-19, H1N1, and control groups (Figure 2.5E-F), some COVID-19 LDLNs exhibited poor distinctions between B- and T-cell zones, with diffuse lymphocyte mixing not present in controls (Figure 2.4D).

### *2.4.3 Lymphatic clotting correlates with intralymphatic NETs and downregulated thrombomodulin in the LDLNs of COVID-19 decedents*

In blood vessels, NETs contribute to immunothrombosis in COVID-19 through neutrophil-platelet interactions[73]; although platelets are absent in lymph, NETs can also promote clotting in a platelet-independent manner[115]. To gain insight into possible mechanisms of lymphatic clotting, we stained LDLN sections for NETs as well as thrombomodulin, which is known to be downregulated by  $\text{TNF}\alpha$  in blood vessels to promote clotting there[73]. Interestingly, we found that in fibrin-filled lymphatic vessels, NETs were often incorporated into the fibrin clots (Figure 2.6A). On average, clotted vessels contained more NETs than open or unclotted vessels in COVID-19 LDLNs as well as in control and H1N1 LDLNs (Figure 2.6B). In addition, when vessels were scored for NETs (0 = no NETs, 1 = NETs along lymphatic lumen, and 2 = NETs incorporated into clot), the average score correlated



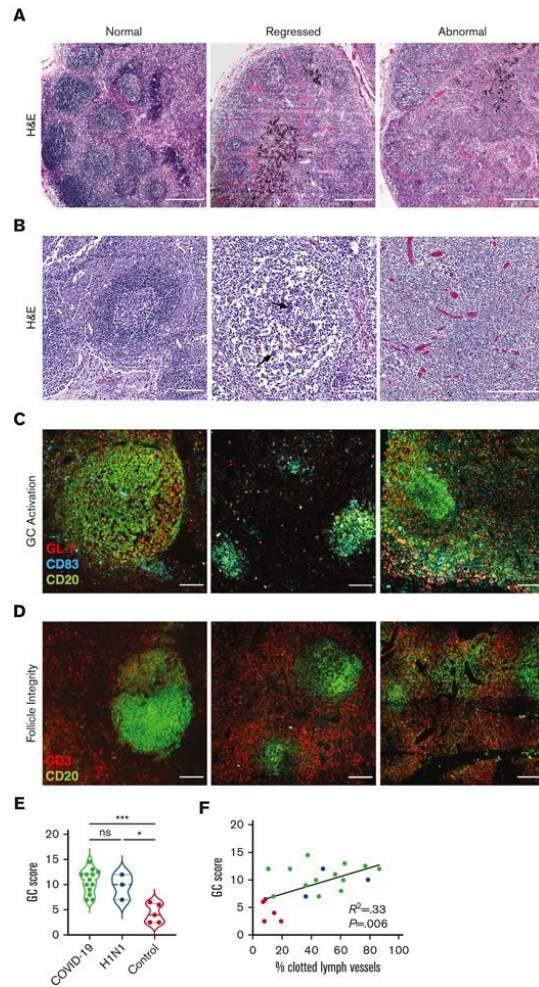


Figure 2.4: **Abnormal GC architecture in LDLNs of COVID-19 decedents correlates with lymphatic clotting in the LDLN.** (A-D) Representative images of LDLNs comparing features of normal (left), regressed (middle), and otherwise abnormal (right) GC follicles of COVID-19 & control decedents. (A) H&E-stained images where the abnormal (right) lacks secondary follicle formation altogether. (B) Zoomed-in images showing a normal secondary follicle (left), a regressed follicle lacking a mantle zone and containing TBMs (black arrows, middle), and complete lack of follicle architecture (right). (C) Representative IF images showing lymphocyte activation in control (left) and COVID-19 (middle & right) LDLNs. Left panel shows strong follicle formation & activation, middle shows decreased follicle size & density, and right shows abnormal follicle structure & extensive extrafollicular activation. (D) Representative IF images of T-cell & B-cell zone integrity in COVID-19 LDLNs. Left panel shows dense B cells and distinct T-cell & B-cell separation, middle shows decreased follicle size and density, and right shows decreased cellularity and poor T-cell & B-cell zone integrity. (E) Average GC abnormality scores for COVID-19, H1N1, and control LDLNs. Dashed lines represent the median and dotted lines represent the 1<sup>st</sup> and 3<sup>rd</sup> quartiles. \*\*\* $p < .001$ , one-way ANOVA with Tukey multiple comparisons test. (F) Linear regression of GC abnormality score vs % of clotted lymphatic vessels in all LDLNs. Scale bars, 500 $\mu\text{m}$  (A) and 100 $\mu\text{m}$  (B-D). Imaging & scoring done by Emma Stewart.

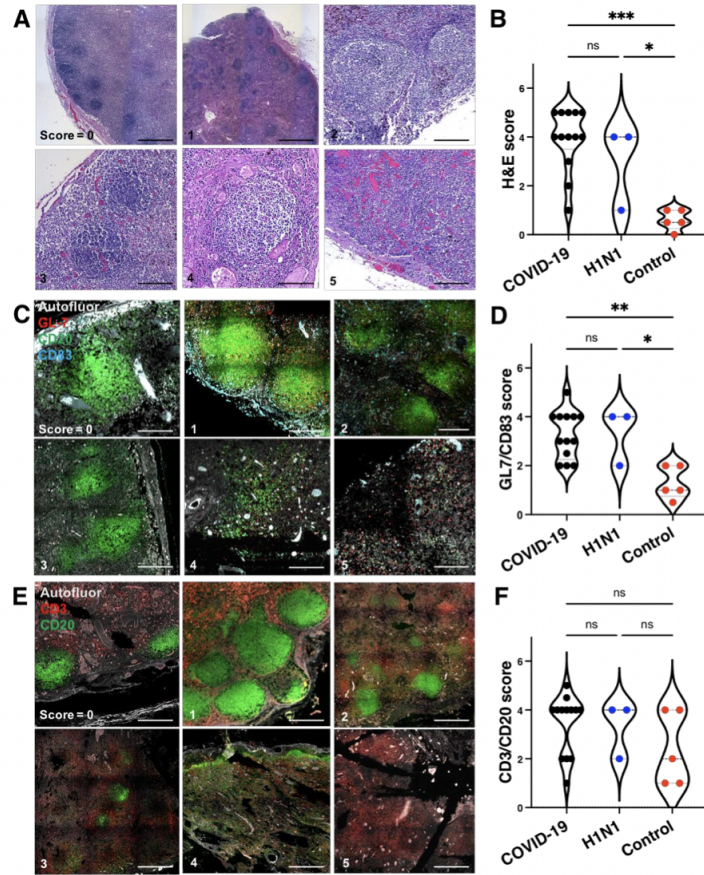


Figure 2.5: **LDLN germinal center scoring rubric for H&E and IF staining.** (A) Representative H&E images for each score. 0=Primary follicles, naïve setting, 1=robust GC formation, 2=weak GC formation, 3=lack of GC formation, infection setting, 4=regressed GCs, 5=poor architecture/no apparent follicles. (B) Comparison of H&E scores in each group. (C) Representative IF images of each GC activation score. 0=predominantly primary follicles without activation markers, naïve setting, 1=predominantly reactive GCs, activation markers present in follicle, naïve or infection setting, 2=follicular activation with minor abnormalities in follicle shape/structure, little/no extrafollicular activation, 3=small primary follicles in infection setting, lack of GC response (decreased activation markers), 4=moderate abnormalities in follicle activation pattern, structure of follicles (including extensive cell drop-off), can include strong follicular activation with extrafollicular activation, 5=extensive extrafollicular B cell activation or B cell adjacent to GL7+ T cell, and/or poor overall follicle formation & activation. (D) Comparison of GL7/CD83 scores in each group. (E) Representative IF images of each B/T cell distribution score. 0=small follicles only, distinct T/B cell zones, 1=large follicles, distinct T/B cell zones with appropriate mixing, 2=mixed follicle size, slight integrity loss, 3=small follicles only, infection setting, 4=mixed follicle size, moderate integrity loss, 5=diffuse B zone/total integrity loss. (F) Comparison of CD3/CD20 scores in each group. Dashed lines in (B,D,F) represent the median and dotted lines represent 1<sup>st</sup> & 3<sup>rd</sup> quartiles. \* $p < 0.05$ , \*\* $p < 0.01$ , \*\*\* $p < 0.001$  by one-way ANOVA with Tukey multiple comparisons test. Scale bars=100 $\mu$ m. Imaging & scoring done by ECS.

with the percentage of lymphatics containing clots as well as the GC abnormality score (Figures 2.6C-D; Figure 2.7).

#### *2.4.4 Higher neutrophil counts in patient lungs correlate with intralymphatic NETosis and lymphatic clotting in LDLNs*

Interestingly, decedents with higher neutrophil densities in the lung had higher percentages of clotted lymphatic vessels in the LDLN (Figures 2.6E-F), whereas NET counts in the lungs did not correlate with the percentage of clotted lymphatic vessels in the LDLN (Figure 2.6G). This suggests that lymphatic clots seen in the LDLN did not originate from dislodged upstream clots in the lung but rather from neutrophils trafficking out of the lung and NETosing in the LDLN lymphatics. In addition, neutrophil and NET counts were not globally increased in COVID-19 LDLNs compared with controls (Figure 2.8); hence, the correlation between lymphatic clotting and NETs appears to be specific to intralymphatic NETs rather than overall NETs in the LDLN.

#### *2.4.5 Lymphatic coagulation is correlated with downregulated lymphatic thrombomodulin expression in COVID-19 decedent LDLNs*

We next stained LDLN sections for fibrin, podoplanin, and thrombomodulin (Figure 2.9A-B). Interestingly, within each tissue, clotted vessels had decreased thrombomodulin expression compared with open vessels (supplemental Figure 2.9C). This trend was observed within every patient except 1 (supplemental Figure 2.9C) and suggests that inflammation-induced downregulation of lymphatic thrombomodulin may contribute to lymphatic clotting.

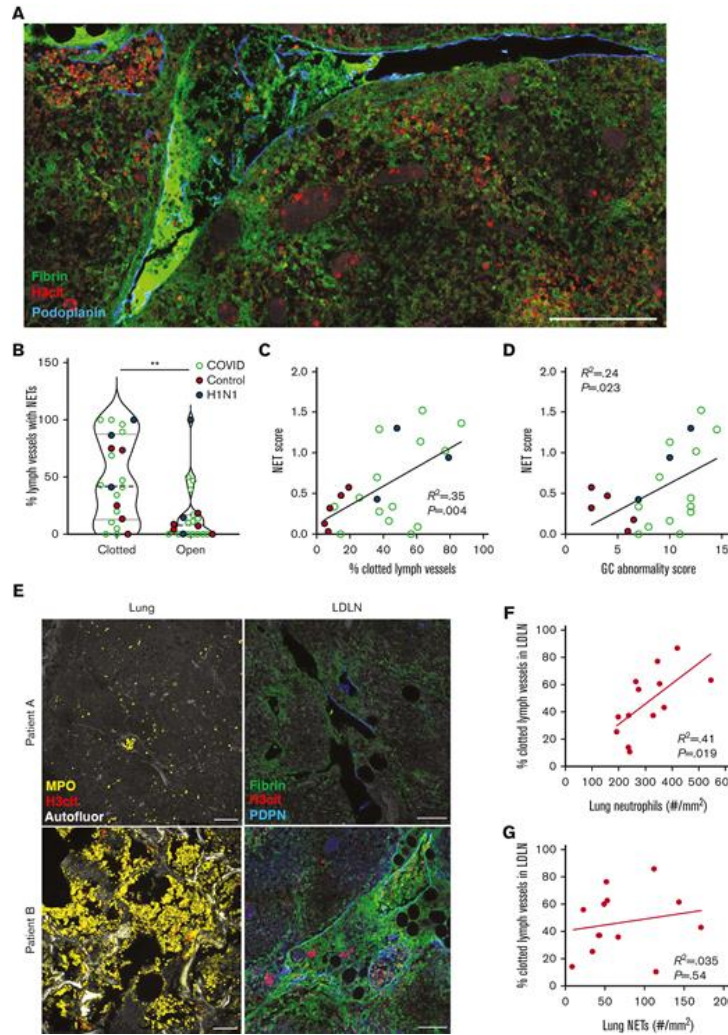


Figure 2.6: **Lymph clotting in LDLNs correlates with intralymphatic NETs in the LDLN and neutrophil load in the lungs of COVID-19 decedents.** (A) Representative IF image of COVID-19 LDLNs showing NETs(H3cit) integrated into fibrin clots within a large lymphatic vessel(podoplanin) near the subcapsular sinus. (B) % clotted or open lymphatic vessels that contain NETs in LDLNs from control(red), COVID-19(black), and H1N1(blue) decedents. Dashed line = median and dotted lines = 1<sup>st</sup> and 3<sup>rd</sup> quartiles. \*\*p<.01 by two-tailed paired Student t-test. (C-D) Correlation of average NET score with % of clotted lymphatic vessels (C) & GC abnormality score (D). (E) Representative IF images from lung(left) and matching LDLN(right) from 2 different COVID-19 patients showing relationship between lung neutrophil density and lymphatic clotting & intralymphatic NETs in the LDLN. In patient A(top), a low density of neutrophils and NETs(MPO, yellow; H3cit, red) in the lung(left) corresponds to an LDLN(right) with mostly open lymphatic vessels; in patient B(bottom), high lung neutrophils counts correspond to extensive intralymphatic fibrin clots and high intralymphatic NET levels in the LDLN. (E-F) Lung neutrophil density correlates with lymphatic clotting in the LDLN of COVID-19 decedents. Linear regression of (F) % of clotted LDLN lymphatic vessels (fibrin score 3-4) vs lung neutrophil density and (G) % of clotted LDLN lymphatic vessels vs lung NETs density. Scale bars=100 $\mu$ m (A,E).

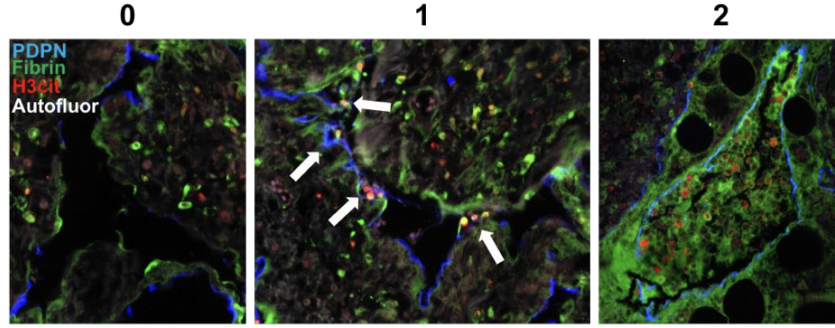


Figure 2.7: **Rubric for intralymphatic NET scoring.** Representative immunofluorescence images of podoplanin (blue), fibrin (green), and H3cit (red) staining for each score. 0 = no NETs in lymphatic vessel, 1 = NETs only along lumen of lymphatic vessel, 2 = NETs integrated into fibrin clot.

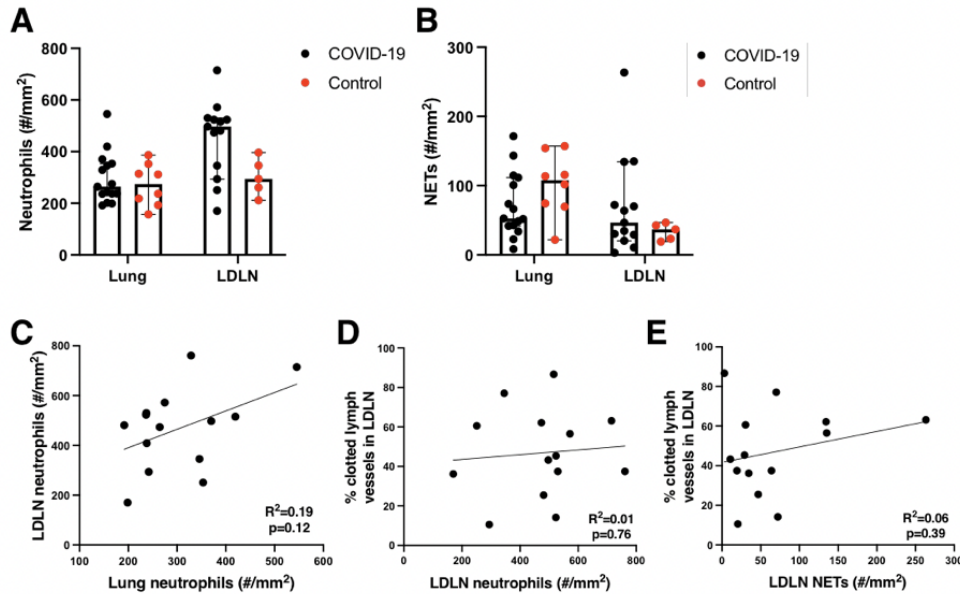


Figure 2.8: **Neutrophil and NET counts in the lungs and LDLNs of COVID-19 do not differ significantly from those in the LDLNs of control decedents.** (A) Average neutrophil counts ( $\#/mm^2$ ) in the lungs and LDLNs of COVID-19 and control decedents. (B) Average NET counts ( $\#/mm^2$ ) in the lungs and LDLNs of COVID-19 and control decedents. (C) Linear regression of LDLN neutrophils ( $\#/mm^2$ ) vs. lung neutrophils ( $\#/mm^2$ ).  $R^2=0.19$ ,  $p=0.12$  (ns). (D) Linear regression of % clotted lymphatic vessels in the LDLN vs. LDLN neutrophils ( $\#/mm^2$ ).  $R^2=0.01$ ,  $p=0.76$  (ns). (E) Linear regression of % clotted lymphatic vessels in the LDLN vs. LDLN NETs ( $\#/mm^2$ ).  $R^2=0.06$ ,  $p=0.39$  (ns). In (A,B), error bars represent median and 95% confidence interval. One-way ANOVA test with Tukey's multiple comparisons used to calculate p values, but no significant differences were observed. Neutrophil count analysis done with Rachel Weathered.

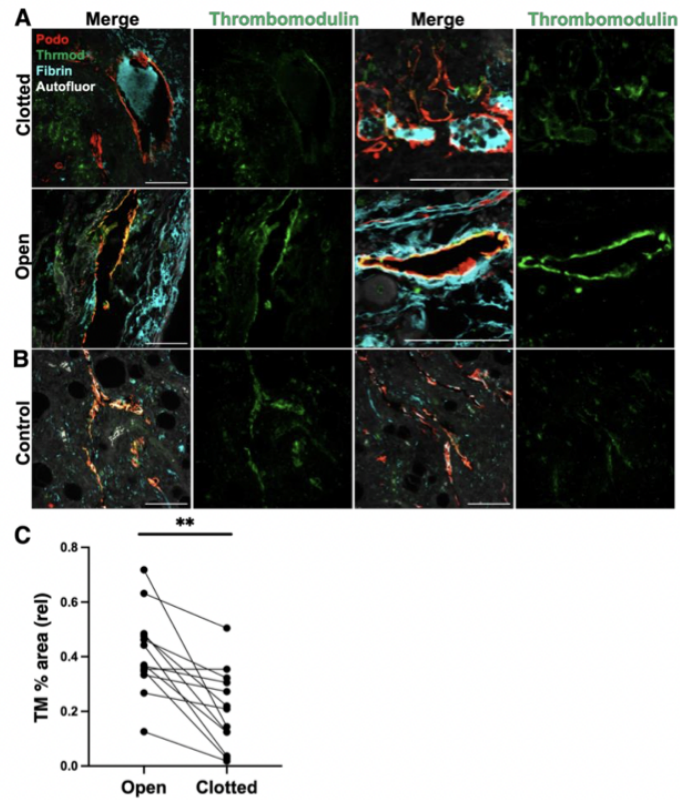


Figure 2.9: **Thrombomodulin expression by lymphatic endothelium is decreased in clotted vs. un-clotted lymphatic vessels in COVID-19 decedents.** (A,B) Representative immunofluorescence images of thrombomodulin (green), fibrin (cyan), and podoplanin (red) staining in LDLN sections from COVID-19 (A) and control (B) autopsies. Scale bars = 100  $\mu\text{m}$ . (C) Average thrombomodulin (TM) expression as measured by % area normalized to podoplanin in clotted and open lymphatic vessels for each COVID-19 patient. \* $p < 0.05$ , \*\* $p < 0.01$  by Mann-Whitney U test.

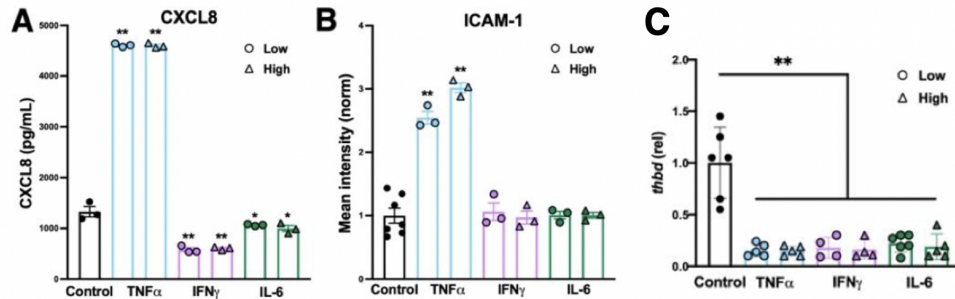


Figure 2.10: *In vitro*, lymphatic endothelial cells secrete neutrophil chemoattractants, upregulate ICAM-1, and downregulate thrombomodulin in response to  $\text{TNF}\alpha$ . (A) CXCL8 secretion (pg/ml) after 24h treatment with low and high doses of  $\text{TNF}\alpha$  (50 and 100 ng/ml),  $\text{IFN}\gamma$  (100 and 200 ng/ml), and IL-6 (10 and 50 ng/ml). (B) Normalized mean intensity of ICAM-1 staining in LECs after 24h treatment with low (all: 10 ng/ml) or high ( $\text{TNF}\alpha$ ,  $\text{IFN}\gamma$ : 100 ng/ml, IL-6: 50 ng/ml) doses of  $\text{TNF}\alpha$ ,  $\text{IFN}\gamma$ , or IL-6. Error bars represent mean  $\pm$  stdev. In (A,B), \* $p < 0.05$ , \*\* $p < 0.01$  by one-way ANOVA test with Tukey multiple comparisons test. (D) Relative thrombomodulin (thbd) mRNA expression in murine iLECs after 24h treatment with low  $\text{TNF}\alpha$ : 5 ng/ml, IL-6: 20 ng/ml,  $\text{IFN}\gamma$ : 10 ng/ml) or high (all: 50 ng/ml) doses of  $\text{TNF}\alpha$ , IL-6, and  $\text{IFN}\gamma$ . Error bars represent median and 95% confidence interval. \* $p < 0.05$ , \*\* $p < 0.01$  by one-way ANOVA test with Tukey multiple comparisons test. PCR in (C) done by Alexandra Magold.

#### 2.4.6 *In vitro*, LECs secrete CXCL8, upregulate ICAM-1, and downregulate thrombomodulin in response to $\text{TNF}\alpha$

Because the increased presence of NETs was specific to clotted vessels, we asked whether inflamed LECs may be recruiting neutrophils and inducing NETosis. In culture, LECs responded to  $\text{TNF}\alpha$  treatment by increasing their secretion of CXCL8 and expression of ICAM-1 (Figure 2.10A-B); these were not affected by IL-6 or  $\text{IFN}\gamma$ .  $\text{TNF}\alpha$  also led to increased transcription of neutrophil chemoattractants. Interestingly, thrombomodulin messenger RNA also decreased after treatment with  $\text{TNF}\alpha$  as well as IL-6, granulocyte-macrophage colony-stimulating factor, and  $\text{IFN}\gamma$  (Figure 2.10C). Together, these results suggest that LECs directly respond to inflammatory cytokines associated with COVID-19, especially  $\text{TNF}\alpha$ , in ways that promote neutrophil attraction, NETosis, and fibrin formation.

<i>Sex</i>	<i>Percent of Cohort</i>	<i>Average Age (years)</i>
<i>Female</i>	<b>51.85%</b>	<b>60.96</b>
<i>Male</i>	<b>48.15%</b>	<b>63.38</b>

Table 2.4: COVID-19 patient serum information

*2.4.7 High NET levels in patient serum correlate with lower levels of anti-RBD antibody titers*

In a separate patient cohort, serum was collected at various time points from patients with SARS-CoV-2 infection, and control serum was obtained from nonhypertensive donors before the pandemic (Table 2.4). Patients with COVID-19 with comorbidities such as active cancer, organ transplant, or immunosuppression that would affect NET levels or the anti-SARS-CoV-2 antibody response were excluded, as well as patients who had received convalescent plasma.

Using enzyme-linked immunosorbent assay, we measured levels of the NET marker, MPO-DNA, and immunoglobulin G antibody titers against the receptor-binding domain (RBD) of the COVID-19 spike protein. Consistent with other studies, serum from patients with COVID-19 contained higher levels of MPO-DNA than controls (Figure 2.11A); interestingly, these were not correlated with levels of D-dimer, a common marker of blood thrombosis (Figure 2.11B). Next, we compared serum MPO-DNA levels with anti-RBD antibody titers and found a significant negative correlation (Figure 2.11C). In addition, when categorized by having low (2-4), moderate (4.5-5.5), or high (6-8) anti-RBD titers, the MPO-DNA levels in serum from patients with low anti-RBD titers were significantly higher than those in serum from patients with high anti-RBD titers (Figure 2.11D). All patients with low anti-RBD titers had mid to high levels of serum MPO-DNA (Figure 2.11E). When cate-



gorized by having low ( $<0.33$ ), mid ( $>0.33$  and  $<0.5$ ), or high ( $>0.5$ ) serum MPO-DNA levels, anti-RBD titers were significantly lower in the high MPO-DNA and mid-MPO-DNA groups compared with the low MPO-DNA group (Figure 2.11F). Interestingly, most patients with high levels of MPO-DNA but low levels of D-dimer had low anti-RBD antibody levels (Figures 2.11B-C). All patients with low serum MPO-DNA levels had moderate or high anti-RBD antibody titers, and patients with moderate to high serum MPO-DNA levels had higher proportions of low anti-RBD titers (Figure 2.11G). Because there was no correlation between serum MPO-DNA and D-dimer, it is possible that the relationship between MPO-DNA and anti-RBD titers is independent of blood clotting and could be due to lymphatic clotting instead. Although NET levels negatively correlated with anti-RBD titers, there was no significant correlation between NET levels and the SpO<sub>2</sub>-to-FiO<sub>2</sub> ratio, a marker of disease severity where lower SpO<sub>2</sub>-to-FiO<sub>2</sub> ratios indicate more severe disease (Figure 2.11A). Although more patients with mild disease had low NET levels, patients across all severity levels also exhibited mid to high NET levels, and consistent with earlier reports of patients with severe COVID-19,(cite6-8) most patients in our cohort had high NET levels (Figures 2.12B-C).

#### *2.4.8 In mice, locally injected TNF $\alpha$ drives NET-dependent lymphatic clotting*

Finally, we sought to determine whether lymphatic clotting could be induced in mouse skin. We injected TNF $\alpha$  locally in the mouse ear and by using fluorescently labeled fibrinogen injection (IV) to visualize fibrin clot formation, we could observe fibrin clots in lymphatic vessels (Figures 2.13A-B). These clots were mostly found in collecting vessels around junctions and valves. Addition of both TNF $\alpha$  and IL-1 $\beta$  did not increase the extent or kinetics of clotting (Figure 2.13B). Clotting in lymphatic collectors could also be induced with intradermal injections of inactivated thrombin, which competitively inhibits thrombomodulin

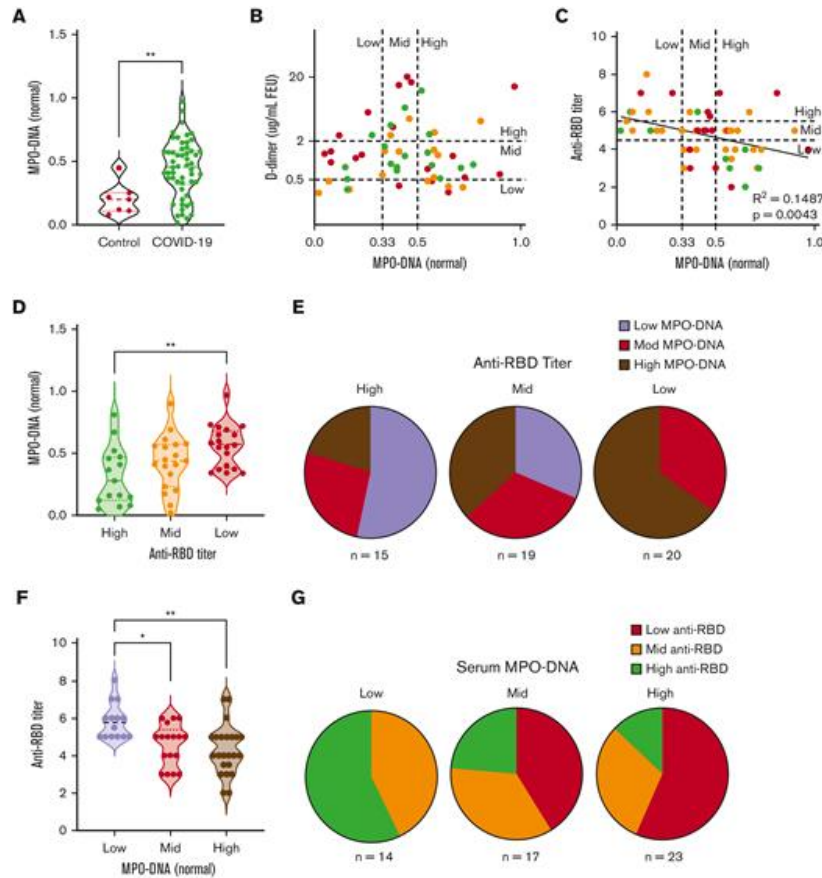


Figure 2.11: In serum from patients hospitalized with COVID-19, levels of NET markers did not correlate with disease severity or D-dimer levels but did correlate with lower anti-RBD antibody titers. (A) Serum levels of MPO-DNA from hospitalized COVID-19 and control patients, normalized to NET-standard. (B) Scatter plot of D-dimer vs MPO-DNA levels in patient serum showing no correlation ( $R^2=0.0217$ ,  $p=.29$  from linear regression analysis). Dotted horizontal lines indicate low ( $<0.5 \mu\text{g/mL}$  fibrinogen equivalent units, or FEU), mid (between  $0.5$  and  $2 \mu\text{g/mL}$  FEU), and high ( $>2 \mu\text{g/mL}$  FEU) D-dimer levels. Dotted vertical lines indicate low ( $<0.33$ ), mid ( $0.33-0.5$ ), and high ( $>0.5$ ) levels of MPO-DNA. Dot colors indicate patients with low (red), mid (orange), or high (green) anti-RBD titers. (C) Scatter plot of anti-RBD antibody titers vs MPO-DNA levels in patient serum ( $R^2=0.1487$ ,  $p=.0043$  from linear regression analysis). Dotted horizontal lines indicate low ( $<4$ ), mid ( $4.5-5.5$ ), and high ( $>6$ ) anti-RBD antibody titers, and dotted vertical lines are as in panel B. Dot colors indicate patients with high (red), mid (orange), or low (green) levels of D-dimer. (D) Average MPO-DNA levels from patients with low (2-4), mid (4.5-5.5), or high (6-8) titers of anti-RBD antibodies. (E) Proportion of patients in each anti-RBD titer group who had low, mid, or high MPO-DNA levels. (F) Average anti-RBD titers from patients with low ( $<0.33$ ), mid ( $0.33-0.5$ ), or high ( $>0.5$ ) MPO-DNA levels. (G) Proportion of patients in each MPO-DNA group who had low, mid, or high anti-RBD titers. In (A,D,F), dashed line = median and dotted lines =  $1^{st}$  and  $3^{rd}$  quartiles. In A,  $**p<.01$  by unpaired two-tailed t test and in D&F,  $*p<.05$ ,  $**p<.01$  by one-way ANOVA with Tukey multiple comparisons test. ELISA with RKW & analysis with MAS.

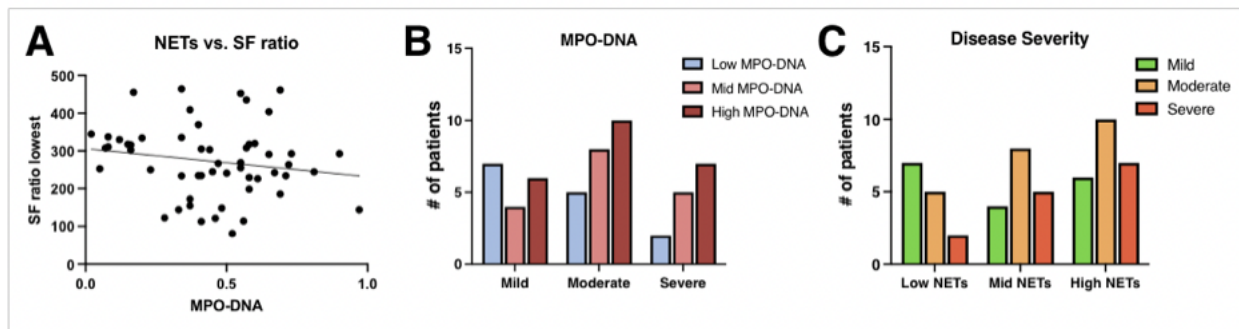


Figure 2.12: Serum MPO-NDA levels do not correlate with disease severity, but patients with low NET levels tend to have milder disease. (A) Linear regression of lowest SF (SpO<sub>2</sub> FiO<sub>2</sub>) ratio vs. serum MPO-DNA (normalized). There was no statistically significant correlation between the two groups. (B) Number of patients with mild (SF ratio > 314), moderate (SF ratio of 234-313) and severe (SF ratio < 234) disease that had low (<0.33), mid (0.33-0.5) and high (>0.5) serum MPO-DNA levels. (C) Number of patients with low, mid, and high NET levels that had mild, moderate, and severe disease.

(Figure 2.13B). Although lymphatic clots were relatively sparse, each mouse ( $n = 9$ ) exhibited some level of lymphatic occlusion, and clot formation was sufficient to prevent lymphatic drainage from lymphatics efferent to clotted collectors. NETs are involved in TNF $\alpha$ -induced lymphatic clotting, we used DNase I (injected intraperitoneally) to degrade NETs immediately after intradermal TNF $\alpha$  injection (Figure 2.13C). Whole-mount staining for LYVE-1 and H3cit, a specific marker of NETosis, revealed that many of the clots within lymphatic vessels contained NETs (Figure 2.13D). Importantly, we found substantially fewer lymphatic clots in the ears of mice that received DNase I (Figures 2.13D-E), suggesting that NETs play important roles in TNF $\alpha$ -induced lymphatic clotting.

## 2.5 Discussion

Our findings demonstrate that lymphatic coagulation, particularly in the LDLN, is a clinical feature of fatal COVID-19. Furthermore, we found that fibrin-filled lymphatic vessels were more likely to contain intralymphatic NETs and that lymphatic clotting in the LDLN correlated with abnormal or missing GCs, whereas serum NET levels negatively correlated

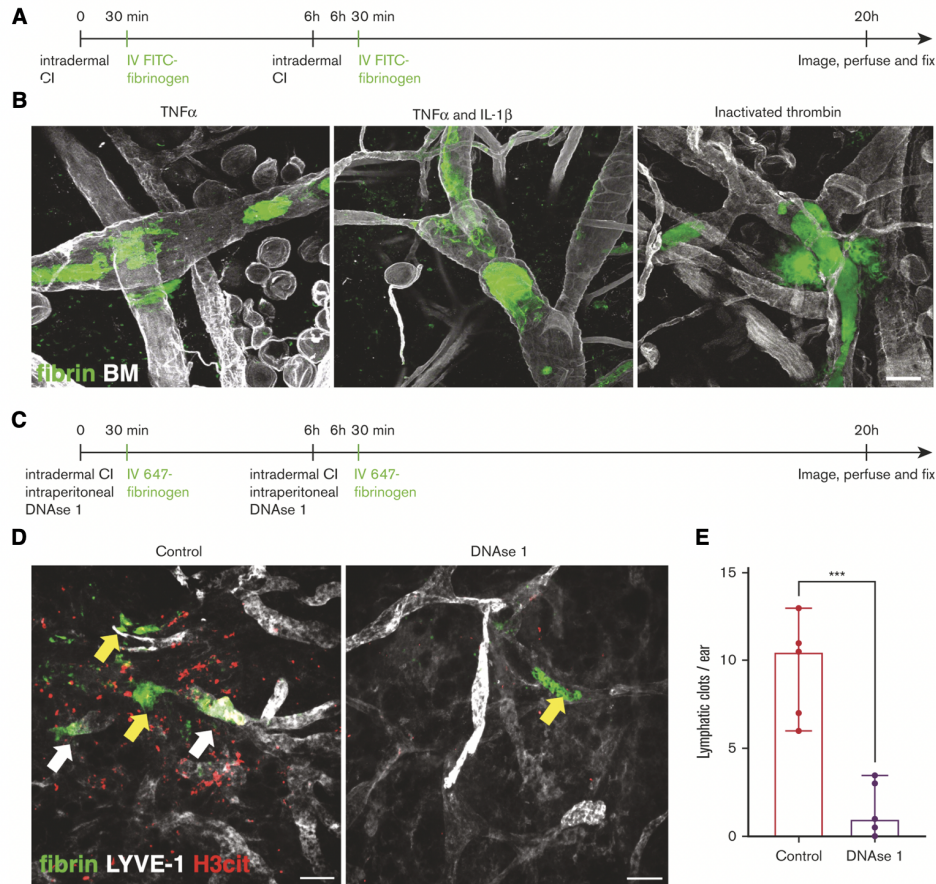


Figure 2.13: **Local injection of TNF $\alpha$  or inactivated thrombin induces NET-dependent intralymphatic fibrin coagulation in mouse skin.** (A) Schematic of experimental design: ID injection of clot initiators (CIs) TNF $\alpha$ , TNF $\alpha$  & IL-1 $\beta$ , or inactivated thrombin, on day 0 was followed by IV injection of FITC-labeled fibrinogen 30 min later. 6h after the first injection, procedure was repeated. Mice were perfused & fixed after 20h. (B) Representative whole-mount images of lymphatic collectors occluded by fibrin(green) after treatment with TNF $\alpha$  (left), TNF $\alpha$  and IL-1 $\beta$  (middle), or inactivated thrombin (right). Basement membrane (BM) is represented by collagen-IV staining. Scale bars=50 $\mu$ m. (C) Schematic of experimental design: ID injection of clot initiator (TNF $\alpha$ ) and IP injection of DNase I on day 0 was followed by IV injection of 647-labeled fibrinogen 30 min later. 6h after the first injection, the procedure was repeated, and mice were perfused and fixed after 20h. (D) Representative whole-mount images of lymphatic vessels & clots in the mouse ear in control mice(left) and mice that received DNase I injections(right). White arrows indicate lymphatic clots (left inset: clot containing NETs; right inset: clot outside of a lymphatic with no NETs), and yellow arrows indicate clots outside of lymphatics, likely in a blood vessel. Scale bar=100 $\mu$ m. (E) Average number of lymphatic clots in the left & right ear dorsal dermis for each mouse injected ID with TNF $\alpha$  (n=5) and each mouse injected with both TNF $\alpha$  and DNase I (n=5). Bars and error bars represent median and 95% confidence interval, respectively. \*\*\*p<.001 by unpaired two-tailed t test. Images in (B) from WWK.

with anti-RBD antibody titers. Elevated NETs and regressed GCs have both been reported independently in severe COVID-19[33, 49, 116, 120, 130]; however, our findings suggest a possible link between these.

Lymph coagulation was first recognized more than a century ago[46, 81, 82]; however, it has received little research attention[62]. It has been described in lymphatic-related diseases[10, 23, 42–44, 62] but otherwise, clinical evidence of pathological lymph clotting is rare. We speculate that this is because the effects of lymphatic clots are likely less detectable and less acute than those of blood clots. When isolated, lymph clots 2- to 5-times slower than corresponding plasma[46, 62, 81]. Lymph lacks platelets and contains lower concentrations of clotting factors and higher levels of fibrinolytic factors than blood[8, 27, 59, 72]). So, how are lymphatic clots initiated? Early studies used chemically induced damage to vital organs to trigger lymphatic thrombosis in LN sinuses and found that clots originated from areas of severely damaged endothelium, leading to the speculation that an intact lymphatic endothelium prevents clotting[82]. However, we observed lymphatic clotting even in intact vessels.

NETs are among many factors that help initiate blood coagulation and have been observed in the lungs and blood of patients with COVID-19[73, 116, 130].  $\text{TNF}\alpha$ -stimulated blood endothelial cells attract neutrophils and can induce NETosis to initiate clot formation[38]; therefore, we hypothesized that NETosis may also initiate lymphatic clotting. In response to inflammation or infection, neutrophils are among the first immune cells to reach the LN after encountering virus in the lung; they rapidly enter afferent lymphatics by inducing endothelial junctional retraction[89, 96] before entering the LN through the subcapsular sinus[35, 41, 96, 109]. Neutrophil recruitment to the LN is  $\text{TNF}\alpha$ -dependent[3, 41, 96, 104], and  $\text{TNF}\alpha$  is upregulated and correlated to disease severity in COVID-19[19].  $\text{TNF}\alpha$  stimulates LECs

to modulate expression of chemokines, adhesion molecules, and clotting factors[58, 62, 65]., and we found that *in vitro*, TNF $\alpha$  stimulation of LECs upregulated secretion of CXCL8 and expression of ICAM-1, both of which are necessary for recruitment of neutrophils to lymphatic vasculature[3, 104]. We further investigate how TNF $\alpha$  drives LECs to recruit neutrophils and promote NETosis in chapter 3.

In addition to recruiting neutrophils, CXCL8 also stimulates NETosis[34, 60, 80]. In blood, DNA and histones in NETs trap platelets to promote clotting,[31] but they are also sources of tissue factor[102] and impair protein C activation and may promote clotting independently of platelets. Inflamed LECs may selectively recruit neutrophils and stimulate NET formation, in turn promoting lymphatic clotting, and we examine this relationship in depth in chapter 3. In our *in vivo* studies, degrading NETs with DNase I injections almost completely eradicated lymphatic clots, indicating that NETosis is a key factor in this pathway.

Interestingly, there is evidence that LN neutrophils, in particular, can affect adaptive immune responses. Neutrophils, along with macrophages, facilitate antigen capture and presentation in the lymphatic system and carry antigen to the LN[41, 68, 104]. They can also activate or inhibit T- and B-cell immunity[41]. Promoting lymphatic clotting through NETosis and therefore impairing antigen and immune cell transport to the LN could be another way neutrophils affect adaptive immunity; our data showing that serum NET levels negatively correlate with anti-RBD antibody titers indicate that NETs likely do play a role in regulating adaptive immune responses in COVID-19. Alternatively, lymphatic clotting could play a role in the innate immune response; the primary role of neutrophils is to limit the spread of pathogens throughout the body, and neutrophil depletion can lead to systemic spread of bacterial infection through the lymphatic system[51]. We are also interested in how intralymphatic NETosis may influence metastasis and immunotherapy response in can-

cer. NETosis-induced lymphatic clotting could be another way neutrophils coordinate innate and adaptive immunity by preventing the spread of pathogens throughout the lymphatic system.

Lymphatic vessels are responsible for fluid, solute, and immune cell trafficking to the LN, and GCs require persistent antigen presentation via follicular dendritic cells[56]; therefore, it was not surprising to find strong correlations between lymphatic clotting and dysfunctional follicles or GCs in the LDLN. Abnormal GC architecture and declining neutralizing antibody titers have been described in a subset of patients with COVID-19[45, 49, 63, 69, 70, 90, 98]. Although our data only demonstrate a correlative relationship between clotted LDLN lymphatics and abnormal GC architecture and NETosis and low anti-RBD antibody titers, one might speculate that blocked lymph flow to and within the LN could impair the progression of adaptive immune responses, although many contributing mechanisms to GC dysfunction in COVID-19 likely coexist[49]. In future work, it will be important to determine whether lymphatic clotting is also present in non-LDLNs because dysregulated or missing GCs have been reported in multiple regional LNs in COVID-19[45] but these were not to us available in this study.

Our findings have both basic and translational relevance to COVID-19. Our data support a new hypothesis that NETosis is a key initiator in lymphatic clotting and highlight the need to further study the consequences of blocked lymph flow in the LN. Translationally, blood coagulopathies, NETosis, and GC dysfunction have all been independently described in COVID-19[33, 49, 116, 120, 128, 130], but our data suggest a new hypothesis that ties them together to suggest therapeutic strategies. Targeting NETs with DNase I could help restore lymph flow and normalize LN architecture. In conclusion, our data suggest that treatments designed to mitigate  $\text{TNF}\alpha$  and degrade NETs may reduce lymphatic clotting

and benefit patients with COVID-19.



# CHAPTER 3

## MECHANISMS BY WHICH TNF $\alpha$ PROMOTES NET-INDUCED LYMPHATIC COAGULATION

### 3.1 Preface

This work is included in a manuscript that we are planning to submit to Circulation Research this spring. Anish Mukherjee, and two undergraduate students I supervised in the lab, Ariana Baginski and Chaney Giampaolo, contributed to this work. Anish Mukherjee assisted with platelet-free plasma isolation and initial clotting assays in figure 3.2, Chaney Giampaolo assisted with endothelial cell culture, and Ariana Baginski analyzed a portion of the data included in figure 3.6 using Trackmate.

### 3.2 Introduction

While coagulation in blood vessels is well described and associated with many diseases, including heart disease, cancer[24, 52], and COVID-19[21, 93, 111], clotting in lymphatic vessels has been comparatively understudied. It is surprising that lymph can clot due to its lack of platelets, but fibrin clots in lymphatic vessels have been reported in lymphedema, lymphatic filariasis, lymphangiectasis, emphysema and cancer, and we recently observed fibrin clots in the lymphatic vessels of COVID-19 decedents[62, 71, 107]. These clots likely occur in other disease states which have not yet been identified, but their consequences and the mechanisms by which they occur are not well understood. Isolated lymph has been shown to coagulate slower than blood, and contains lower levels of factors VIII and V and higher levels of fibrinolytic factors[17, 62, 74, 127]. In this study, we aimed to investigate differences in blood and lymphatic coagulation, and the mechanisms by which lymphatic clotting is driven in the absence of platelets.

The lymphatic clots we observed in COVID-19 decedents frequently co-localized with neutrophil extracellular traps (NETs), and we found that intralymphatic NETs correlated with more widespread lymphatic coagulation. NETs have also been observed in immunothromboses in blood vessels in COVID-19[71, 73]. Neutrophil extracellular traps (NETs) are known to drive coagulation in blood vessels through platelet activation, activation of factor XII, and DNA-mediated thrombin generation[31, 86, 115], and also contain extracellular DNA, histones, and tissue factor[115] that may initiate coagulation in the absence of platelets. Neutrophils also enter lymphatic vessels and migrate to draining lymph nodes in response to inflammation[3, 35, 41, 89, 96, 104, 109], and in this paper we focus on how lymphatics may be recruiting neutrophils and promoting them to form NETs, and in turn if that is one of the mechanisms promoting fibrin clotting in lymphatics.

One of the major factors that drives coagulation in blood vessels is  $\text{TNF}\alpha$ [78, 88, 97], and we have recently demonstrated that in the mouse ear skin it can also promote the formation of fibrin clots within lymphatic vessels[71]. In lymphatics, this  $\text{TNF}\alpha$ -induced clotting was prevented by DNase 1 treatment to degrade NETs, and intralymphatic NETs frequently co-localized with lymphatic clots. Here, we investigate whether this is mediated by lymphatic activation of neutrophils. Lymphatic endothelial cells influence immune cell behavior through modulating their expression of adhesion molecules like ICAM-1 and VCAM-1 and their secretion of cytokines and chemokines[3, 47, 83, 89, 92, 104, 109], although most of this work has focused on dendritic cell migration through lymphatics. In chapter 2, we showed that both ICAM-1 and CXCL8 were significantly upregulated in LECs in response to  $\text{TNF}\alpha$ [71], both of which promote NETosis.

Here, we investigate whether lymphatic endothelial cells are recruiting neutrophils and driv-

ing NETosis in response to  $\text{TNF}\alpha$  and the mechanisms by which they may be doing so. CXCL8 and CCL21 have both been shown to be important for neutrophil recruitment into lymphatics, but their role in NETosis has not been studied in as much depth and is likely dose-dependent(cite9,30). In this study, we introduce a new *in vitro* method to study lymphatic clotting using platelet-free plasma to show that one of the mechanisms by which lymphatic clotting is driven is through  $\text{TNF}\alpha$ -driven recruitment and activation of neutrophils by LECs to promote intralymphatic NETosis. We also identify CXCL8 and CCR7 as key players in how LECs promote neutrophils to form intralymphatic NETs.

### 3.3 Methods

#### 3.3.1 Platelet-free plasma isolation and *in vitro* coagulation assay

Platelet-free plasma (PFP) was isolated from whole human blood drawn into BD vacutainer blood collection tubes with sodium citrate (BD 366560) as previously described[5] and stored at -20C (IRB20-1097). Lack of platelets was confirmed by staining with Rees Ecker fluid (<1% compared to PRP, Ricca Chemical Company 660016). For clotting assays, PFP was thawed on ice and mixed with PBS or isolated NETs to reach desired concentration (30% PFP unless otherwise noted) and 1  $\mu\text{m}$  beads used for visualization. Immediately before PFP mixture was added to ibidi 6-channel  $\mu$ -slides (ibidi 80606), 1:10  $\text{CaCl}_2$  was added to counteract the sodium citrate and allow coagulation to occur. If the coagulation assay was performed with neutrophil or LEC co-cultures, PFP was diluted with EGM-2 media (Lonza CC-3162) rather than PBS. Phase contrast time lapse images were taken at 20X using the Keyence microscope, and clot time was determined by tracking the average velocity of the 1  $\mu\text{m}$  beads (calculated using optic flow plugin in ImageJ), using the inflection point of the average velocity curve.

### 3.3.2 *Confocal reflectance imaging*

A Leica SP8 confocal microscope was used to take confocal reflectance images of platelet-free and platelet-rich plasma in ibidi 6-channel  $\mu$ -slides using a 40x oil objective. Samples were excited at 488 nm and the light reflected from the sample was collected over time at multiple locations in the channel. The inflection point of the average intensity over time for each channel was used as the clot time.

### 3.3.3 *Neutrophil and NET isolation*

Neutrophils were isolated from whole human blood drawn into BD vacutainer blood collection tubes (BD 366560) using the EasySep Direct Human Neutrophil Isolation Kit (STEMCELL Technologies 19666) (IRB20-1097). Neutrophils were cultured in RPMI + 5% FBS (Gibco 11875093) with 600nM PMA to induce NETosis and NETs were isolated as previously described in Najmeh, et al.(cite31). The concentration of NET samples was measured using NanoDrop spectrophotometric readings and samples were stored at -20C until use.

### 3.3.4 *2D Neutrophil-LEC co-cultures*

Human immortalized lymphatic endothelial cells (LECs) were cultured for 24h in 100 $\mu$ l EGM-2 medium (Lonza CC-3162) in 96-well plates pre-coated with 50  $\mu$ g/ml collagen 1 (Corning CB-40236) for 30 min at 37C. After letting cells attach in the incubator for 15-30 minutes, 0, 1, 5 or 50 ng/ml TNF $\alpha$  (final concentration) was added in 100 $\mu$ l EGM-2 (Pepro-Tech 300-01A). After 24h, neutrophils isolated from whole human blood as described above were added with 1 $\mu$ M SYTOX green dye (ThermoFisher Scientific S7020). For conditions with CCR7 blocking antibody (ThermoFisher Scientific 16-1971-85) or CXCR1/2 inhibitor (MedChem Express HY-119339), appropriate inhibitor was added 1h prior to addition of neutrophils. Neutrophils were imaged for 4h in the Keyence live imaging set up and NET counts were determined using particle analyzer in ImageJ, excluding dead cells by removing

any particle under  $300\mu m^2$ .

### *3.3.5 Transmigration and NETosis assay*

The bottom sides of 24-well cell culture inserts ( $3\mu m$  pore size; Sterlitech 9323012) were coated with  $50\ \mu g/ml$  collagen 1 for 30 minutes at  $37C$ .  $1 \times 10^5$  LECs were seeded on the collagen-coated side of the inserts and allowed to attach for 2h in the incubator before the inserts were flipped over into 1ml of EGM-2 media containing  $1\mu M$  SYTOX Green to visualize NETosis. Cells were then cultured with or without  $TNF\alpha$  for 24h before  $1 \times 10^4$  neutrophils were added to the top of the cell culture insert in  $100\mu l$  EGM-2 immediately before imaging. Cell culture inserts were imaged for 2-3h at the LEC-media interface using the Keyence microscope, and neutrophils were counted and tracked as they transmigrated using the TrackMate plugin on ImageJ(cite32). After live imaging, cell culture inserts were removed and plates were centrifuged at 1500rpm for 5 minutes to bring all transmigrated neutrophils to the bottom of the well, where they were then imaged and counted to get a final count. For conditions with CCR7 or CXCR1/2 blocking, appropriate inhibitor was added to the 24-well plate 1h prior to addition of neutrophils as well as to the medium the neutrophils were added in.

### *3.3.6 Coagulatory and fibrinolytic factor ELISA and immunostaining*

$5 \times 10^3$  LECs and BECs were seeded in  $100\ \mu l$  EGM-2 media in 96-well plates, and  $100\ \mu l$  of either media or  $TNF\alpha$  (final concentration of 0, 1, 5 or 50 ng/ml) was added after cells were allowed to attach for 15 min at  $37C$ . After 24h, media was collected and centrifuged at 2000rpm for 5 min to remove any cellular debris, and was stored at  $-80C$  until ELISAs were performed. Cells were fixed for 15 min at RT with 2% PFA and were store at  $4C$  until immunostaining was performed. R&D DuoSet ELISAs were used to measure anti-thrombin, tissue plasminogen activator (tPA), plasminogen activator inhibitor 1 (PAI-1),

and tissue factor pathway inhibitor (TFPI). Fixed cells were stained for tissue factor (TF), thrombomodulin, endothelial protein C receptor (EPCR) and von Willebrand Factor (vWF) as described in chapter 2. All secondary antibodies were from Invitrogen and used at 1:500.

### *3.3.7 Statistics and reproducibility*

All statistical analyses and regressions were performed using GraphPad Prism. One-way ANOVA with Tukey multiple comparisons post-test was used to determine p values for multiple groups, unless otherwise noted. For comparison between two groups, Student's t-tests were used as noted in figure legends.

## **3.4 Results**

### *3.4.1 Under steady state conditions, LECs slow coagulation of platelet-depleted plasma compared to BECs*

To mimic the lack of platelets and lower concentration of clotting factors in lymph compared to plasma[17, 62, 74, 127] using a more accessible model than lymph isolation through cannulation, we used platelet-free plasma, which can be easily isolated from whole human blood using standard phlebotomy techniques and centrifugation[5]. To ensure that this platelet-free plasma (PFP) still formed clots in vitro, we used confocal reflectance imaging to visualize clot formation of PFP and plasma that had not been depleted of platelets (platelet-rich plasma, or PRP). While both PFP and PRP formed clots (Fig. 3.2A), the PRP clotted significantly faster, with the average clot time determined by the inflection point of the intensity curve of the confocal reflectance images (Fig. 3.2B-C). This is consistent with previous studies in canine lymph demonstrating lower coagulation activity compared to plasma[17, 62, 74, 127].

Moving to a model where we would be able to co-culture this PFP with live cells, we used a

live imaging set up at 37C using a Keyence microscope and used phase contrast imaging and velocity tracking of  $1\mu\text{m}$  beads suspended in the plasma to determine clot time. The velocity of the beads in representative fields of view decrease dramatically when clotting occurs and the beads become fixed in place (Fig. 3.1A), and this occurs much earlier in PRP than PFP (Fig. 3.1A rows 1&2). The inflection point of the magnitude of the average velocity vectors over time was used to determine clot time (Fig. 3.1B), and the average clot time for PRP was significantly shorter than PFP (Fig. 3.1F). To account for the fact that lymph has been found to contain 20-40% of the clotting factors of plasma[17, 74, 127], we also tested various concentrations of PFP, ranging from 10-100% diluted in PBS, and compared their clot times (Fig. 3.1C-D). Based off this characterization, all further experiments have a final PFP concentration of 30%.

We next compared the coagulatory behavior of PFP when cultured in channels with confluent monolayers of human lymphatic or blood endothelial cells (LECs and BECs). Clotting was again characterized using the velocity vectors of beads suspended in PFP over time (Fig. 3.1A, rows 3&4), and clot time as determined by the inflection point of their magnitude over time was on average significantly lower when PFP was cultured in channels with BECs (Fig. 3.1E-F). This indicates that not only the content of lymph, but also the expression of clotting and thrombolytic factors by lymphatic endothelial cells, is important in determining clot formation in lymphatic vessels. Interestingly, PFP clotted slower when co-cultured with LECs than when cultured alone, supporting the hypothesis that lymphatics may naturally be less prone to clotting than blood vessels due to higher anticoagulant and fibrinolytic activity.

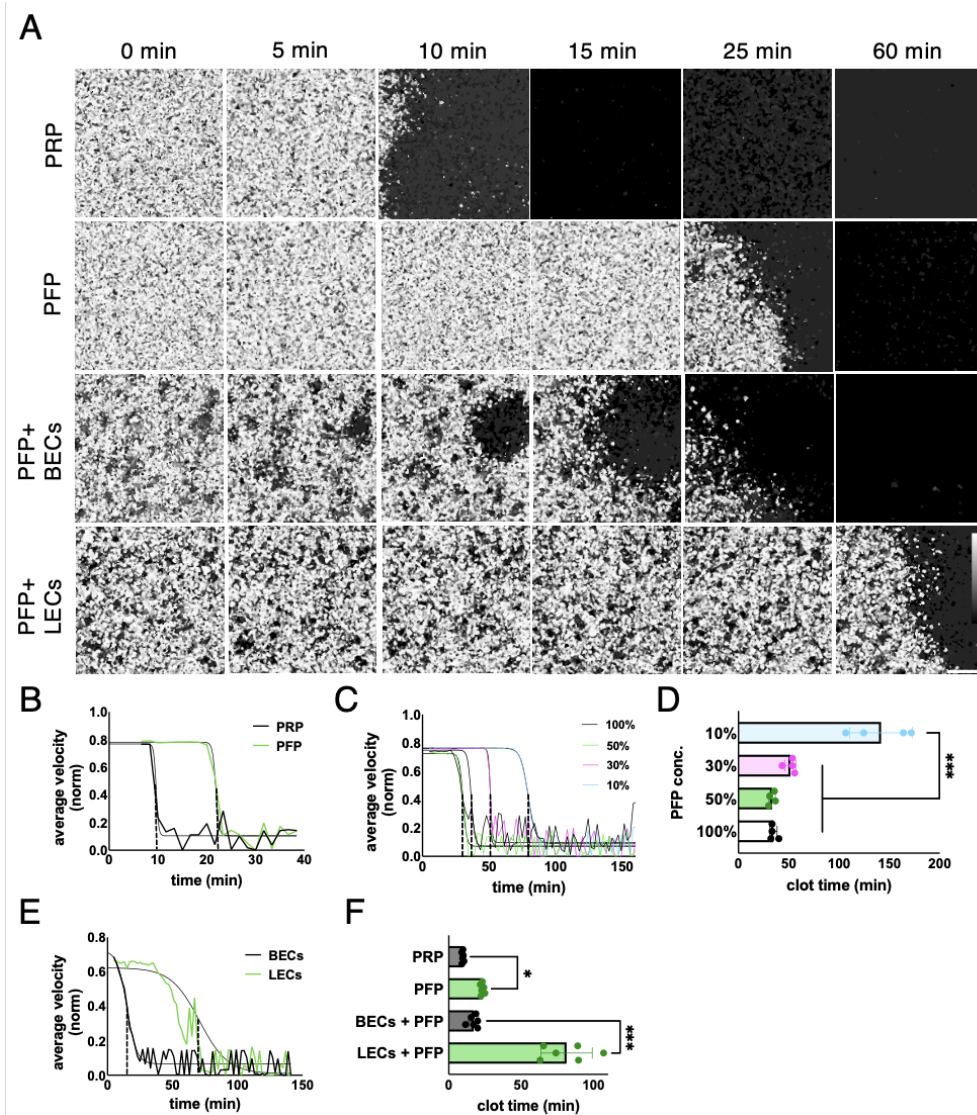


Figure 3.1: **Depletion of platelets slows but does not prevent coagulation, and platelet-free plasma (PFP) coagulates faster when cultured with BECs than LECs.** A) Representative optic flow fields for  $1\mu\text{m}$  beads in platelet-rich (PRP) and platelet-free (PFP) plasma over time without ECs (rows 1&2) and optic flow fields for PFP when cultured with LECs or BECs (rows 3&4). White = highest local speed and black = no movement. B) Representative average velocity curves for PRP and PFP over time. Dotted lines correspond to clot time defined as inflection point of sigmoidal curve fit to data. C) Representative average velocity curves for PFP diluted in PBS to final PFP concentrations ranging from 10-100%. D) Average clot times of PFP at dilutions of 10-100%. E) Representative average velocity curves for PFP when cultured with BECs or LECs. F) Average clot time of PRP and PFP when cultured with no ECs, LECs or BECs. Scale bars =  $50\mu\text{m}$  and color scale bars range from 0 to 1. Unpaired t-test was used to calculate p values in C and F, and one-way ANOVA with Tukey multiple comparisons test was used to calculate p values in G. Error bars represent mean  $\pm$  stdev. \* $p < 0.05$ , \*\* $p < 0.01$ , \*\*\* $p < 0.001$ .



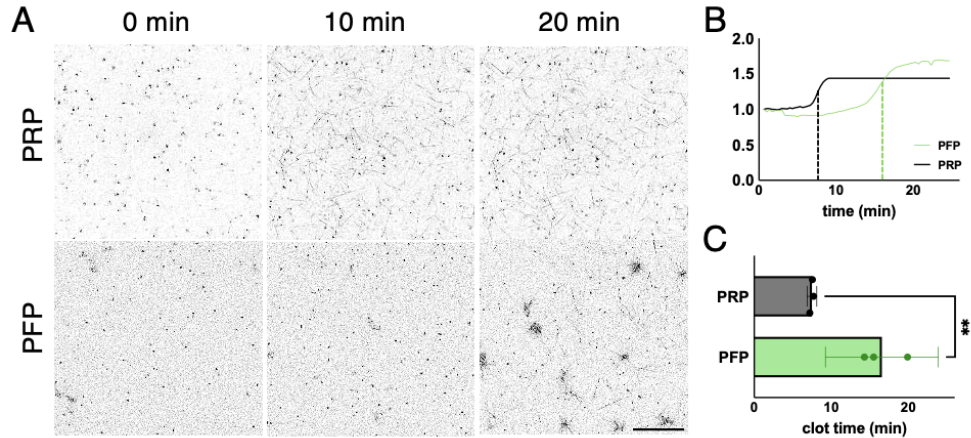


Figure 3.2: **PRP and PFP coagulation can be visualized using confocal reflectance imaging.** A) Representative confocal reflectance images of PRP and PFP over time. Scale bars =  $50\mu\text{m}$ . B) Normalized confocal reflectance intensity over time for representative PRP and PFP samples. Dotted lines indicate inflection point of sigmoidal curves. C) Average clot time for PRP and PFP. Error bars represent mean  $\pm$  stdev. Unpaired t-test used to calculate p values. \*p < 0.05, \*\*p < 0.01.

### 3.4.2 *Anti-coagulatory properties of LECs are driven by secreted factors and are downregulated in response to $\text{TNF}\alpha$ .*

To see the regulation of clotting by LECs and BECs is altered by  $\text{TNF}\alpha$ , which is known to promote clotting in blood vessels[53, 78, 97], we pre-treated LECs with 0, 1, 5 or 50 ng/ml  $\text{TNF}\alpha$  for 24h before the addition of PFP. PFP clotted significantly faster when cultured with the LECs that had been pre-treated with  $\text{TNF}\alpha$  (Fig. 3.3A), closer to the clot time previously observed with untreated BEC co-cultures. When BECs were pre-treated with  $\text{TNF}\alpha$  for 24h, there was an additional decrease in clot time similar to what was observed in LECs (Fig. 3.3B), indicating that LECs and BECs modulate their coagulatory phenotype in response to  $\text{TNF}\alpha$  in a similar manner, but that this leads to a larger fold change in clot time in LEC cultures. This is again consistent with the idea that lymphatics may have a higher threshold for clotting than blood vessels, but that inflammation may lower this threshold.

We next compared clot times of PFP in channels with LECs or BECs that had been fixed

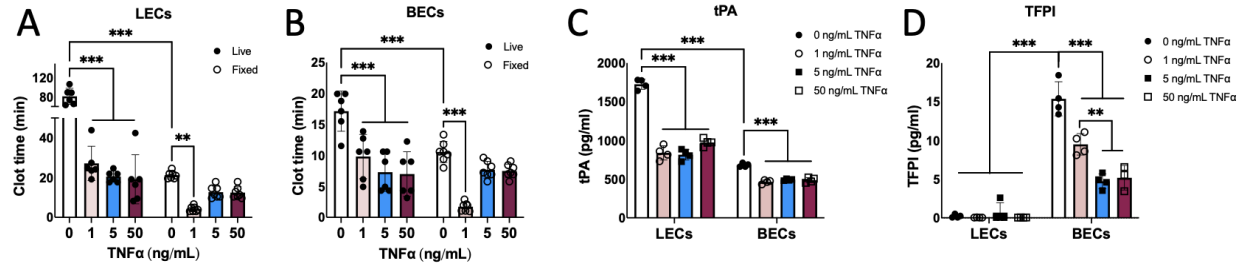


Figure 3.3: **Pre-treatment of LECs or BECs with TNF $\alpha$  promotes coagulation of PFP.** Clot time of PFP added to channels with live or fixed LECs (A) or BECs (B) pre-treated with 0, 1, 5 or 50 ng/ml TNF $\alpha$ . C) Secretion of tissue plasminogen activator (tPA) by LECs or BECs after 24h TNF $\alpha$  treatment. D) Secretion of tissue factor pathway inhibitor (TFPI) by LECs or BECs after 24h TNF $\alpha$  treatment. Two-way ANOVA with Tukey post-tests were used to calculate p-values for A-B. \*p < 0.05, \*\*p < 0.01, \*\*\*p < 0.001.

with 4% PFA after 24h pre-treatment with TNF $\alpha$  to see if this effect seemed to be driven primarily by surface factors or molecules secreted by the endothelial cells. In both LECs and BECs, we saw a decrease in clot time for fixed ECs without TNF $\alpha$  treatment, though this was more pronounced in the LECs (Fig. 3.3A-B). PFP cultured with fixed LECs and BECs clotted at very similar timescales, indicating that the anticoagulatory effect of the LECs is primarily due to secreted factors. We measured various coagulatory or fibrinolytic factors in conditioned media from the TNF $\alpha$ -treated ECs to identify molecules that may be driving these differences and found that at steady-state LECs secreted much higher levels of the fibrinolytic factor tissue plasminogen activator (tPA) than BECs, and that this was decreased in both cell types in response to TNF $\alpha$  (Fig. 3.3C). Interestingly, LECs secreted barely any tissue factor pathway inhibitor (TFPI), but in BECs secretion of this anticoagulatory factor was decreased in response to TNF $\alpha$  (Fig. 3.3D). This could be due to LEC's lack of tissue factor expression, but it is interesting that the main changes we were observed in LECs were in the fibrinolytic pathway rather than the clotting cascade.

### *3.4.3 LECs pre-treated with TNF $\alpha$ drive clotting by priming neutrophils towards NETosis*

While LECs can promote clotting in PFP through a combination of surface and secreted factors, we also established a strong correlation between NETosis and lymphatic coagulation in COVID-19 decedents in a previous study[71]. To see if NETosis has a similar or additive effect on clotting, we added neutrophils to our channel set up with LECs 4h prior to adding PFP to give them sufficient time to form NETs. When neutrophils were added to channels with LECs that had been cultured for 24h with or without TNF $\alpha$ , the decrease in clot time associated with the TNF $\alpha$  pre-treatment was exacerbated even further (Fig. 3.4A). Clot time was also decreased when 5000 pg/ml CXCL8 was added along with neutrophils (Fig. 3.4A). CXCL8 is known to promote NETosis[34, 60, 80], but does not induce pro-coagulatory phenotype in LECs, and does not decrease clot time in this setup in the absence of neutrophils (Fig. 3.4A). When channels were treated with 20 $\mu$ g/ml DNase 1, which degrades NETs, concurrently with the addition of neutrophils, additional decrease in clot time in the TNF $\alpha$ -treated LECs + neutrophil condition no longer occurred, and there was no longer a decrease in clot time with the CXCL8 + neutrophil condition (Fig. 3.4A). Given these results, it seems that LECs and NETs are both driving clotting in lymphatics, with an additive effect in cases where LECs are exposed to TNF $\alpha$  and NETs are present.

Because the addition of DNase 1 abrogated the additional decrease in clot time associated with TNF $\alpha$ -treated LEC and neutrophil co-culture compared to TNF $\alpha$  pre-treatment alone, we next investigated whether this difference could be explained by LECs activating neutrophils to promote NETosis. In co-cultures of LECs that had been pre-treated with 0, 1, 5 or 50 ng/ml TNF $\alpha$  for 24h and neutrophils, neutrophils that had been cultured with the TNF $\alpha$ -treated LECs formed the most NETs over time, with the LECs pre-treated with 50ng/ml TNF $\alpha$  forming the most NETs (Fig. 3.4B-E). TNF $\alpha$  treatment alone did not induce NETosis

in neutrophils at these doses (Fig. 3.5). When neutrophils were cultured with conditioned medium from LECs with or without  $\text{TNF}\alpha$  pre-treatment, the conditioned medium from the  $\text{TNF}\alpha$ -treated LECs promoted NETosis at higher rates than non-conditioned medium or conditioned medium from control LECs, at similar levels to the co-cultures, indicating that this effect is primarily due to factors secreted by the LECs (Fig. 3.4F-H). This is consistent with our previous work showing that these LECs secrete high levels of CXCL8 in response to  $\text{TNF}\alpha$ [71].

#### 3.4.4 *$\text{TNF}\alpha$ promotes neutrophil transmigration across LEC monolayers*

In addition to seeing how LECs could be promoting clotting in lymphatic vessels by priming neutrophils to form NETs, we were curious to see if, consistent with prior work from other groups[89],  $\text{TNF}\alpha$ -treated LECs could be driving neutrophil recruitment into lymphatic vessels prior to their activation, and if this transmigration may further prime them to form NETs. We seeded LECs on the bottom side of cell culture inserts with  $3\mu\text{m}$  pores and added neutrophils to the upper compartment after 24h of culture with or without 50 ng/ml  $\text{TNF}\alpha$ , which was the dose that promoted the most significant increase in NETosis in 2D co-cultures (Fig. 3.6A). This setup allows us to mimic neutrophil transmigration into lymphatic vessels as they will cross the basal side of the lymphatic endothelium, and SYTOX green in the bottom compartment allows us to visualize NETosis at the bottom interface of the cell culture inserts as the neutrophils transmigrate (Fig. 3.6B).

When LECs were pre-treated with  $\text{TNF}\alpha$ , the total number of neutrophils transmigrated to the bottom well was significantly higher than when LECs were cultured in control medium (Fig. 3.6C), and the rate of neutrophil transmigration over time was also significantly higher (Fig. 3.6D-E). This increase in transmigration was not seen when neutrophils were added to cell culture inserts without a LEC monolayer, indicating that it is not the  $\text{TNF}\alpha$ , but the

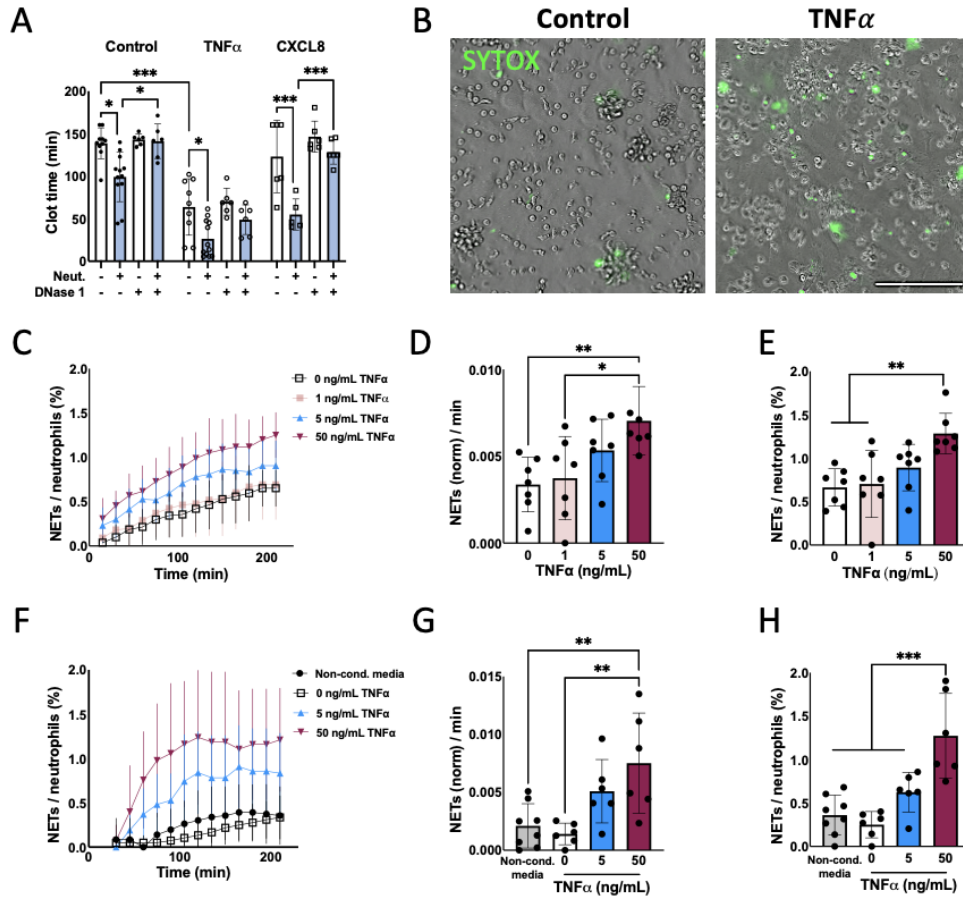


Figure 3.4: **LECs pre-treated with TNF $\alpha$  drive clotting by priming neutrophils towards NETosis.** A) Clot time of PFP added to channels containing control LECs, LECs and 5000pg/ml CXCL8, or LECs that had been pre-treated for 24h with 50ng/ml TNF $\alpha$ , with and without neutrophils and DNase 1. PFP added 4h after neutrophils to allow for NETosis to occur. B) Representative phase contrast and immunofluorescence images of neutrophil-LEC co-cultures after 4h with and without TNF $\alpha$  pre-treatment. NETs and dead cells are stained by SYTOX green and differentiated by size. Scale bar=50 $\mu$ m. B) % of neutrophils that form NETs over time when cultured with LECs pre-treated for 24h with 0, 1, 5 or 50 ng/ml TNF $\alpha$ . C) % of neutrophils that have formed NETs at endpoint of neutrophil-LEC co-cultures. D) Rate of NETosis over time for the first 100 minutes of neutrophil-LEC co-culture. E) Percent of neutrophils that form NETs over time when cultured with control medium or LEC-conditioned medium collected 24h after addition of 0, 5 or 50 ng/ml TNF $\alpha$ . F) Percent of neutrophils that formed NETs at endpoint after culture with LEC-conditioned medium or control medium. G) Rate of NETosis over time for the first 100 minutes of culture with control or conditioned medium. One-ANOVA with Tukey post-tests used to calculate p-values for C-D and F-G. \*p < 0.05, \*\*p < 0.01, \*\*\*p<0.001.

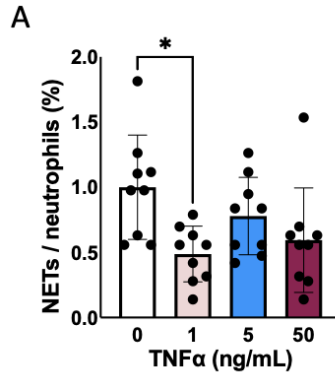
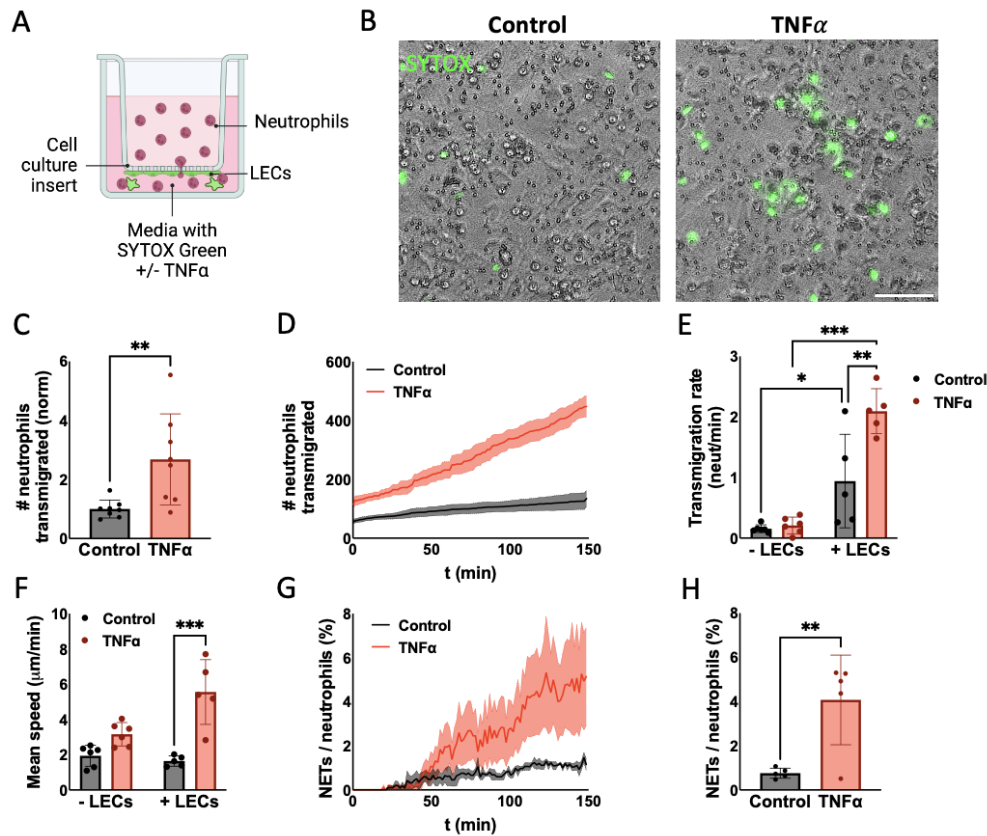


Figure 3.5: **TNF $\alpha$  alone does not stimulate NETosis.** A) Percent of neutrophils that have formed NETs at endpoint after addition of 0, 1, 5 or 50 ng/ml TNF $\alpha$  without LECs. \*p < 0.05.

LECs and the factors they are secreting that are driving the transmigration (Fig. 3.6E). In fact, transmigration rates were significantly higher in the presence of LECs with and without TNF $\alpha$ , and very few neutrophils transmigrated across the cell culture inserts when the LECs were not present (Fig. 3.6E).

#### *3.4.5 TNF $\alpha$ -treated LECs promote NETosis and increased neutrophil motility after transmigration.*

To see if LECs also contributed to neutrophil activation post-transmigration, we also measured the average speed of the neutrophils after transmigration and the rate at which they formed NETs. Neutrophils that transmigrated across an endothelium that had been pre-treated with 50 ng/ml TNF $\alpha$  for 24h had a higher average mean speed than those that transmigrated across an untrained LEC monolayer (Fig. 3.6F). The mean speed of the neutrophils was only significantly higher in the presence of LECs, even in the presence of 50 ng/ml TNF $\alpha$  (Fig. 3.6F). Additionally, the neutrophils that transmigrated across the TNF $\alpha$  pre-treated LECs formed more NETs over time compared to neutrophils that transmigrated across a control LEC monolayer, but not at significantly higher rates than what was observed in 2D co-cultures (Fig. 3.6G-H). It appears that the transmigration and the constriction of



**Figure 3.6: Pre-treatment of LECs with TNF $\alpha$  promotes neutrophil transmigration and NETosis.** A) Experimental setup: LECs are cultured on the bottom well of a 24-well cell culture insert for 24h with or without 50 ng/ml TNF $\alpha$ , then neutrophils are added to top compartment and LEC monolayer is imaged for 4h to quantify transmigration and NETosis. B) Representative phase contrast and immunofluorescence images of neutrophils, LECs and NETs(green) at cell culture insert interface at endpoint with and without TNF $\alpha$  pre-treatment. Scale bar = 25 $\mu$ m. C) Total number of neutrophils transmigrated across the lymphatic endothelium in each condition, normalized to control for each experiment. D) Number of neutrophils that have transmigrated over time. E) Transmigration rate (neut/min) with and without LECs and with and without TNF $\alpha$  pre-treatment. F) Average mean speed of the neutrophils that transmigrated across LEC monolayer or cell culture insert without LECs. G) Percent of neutrophils that formed NETs at the endothelium over time. H) Percent of neutrophils that formed NETs at endpoint. Two-way ANOVA with Tukey post-test was used to calculate p values for experiments with multiple groups and unpaired t-tests were used to calculate p values for comparisons between two groups. \*p < 0.05, \*\*p < 0.01, \*\*\*p < 0.001.

the neutrophils as they crossed the monolayer did not activate them, but rather the LECs that had already recruited them were also increasing their motility and NETosis.

### *3.4.6 CCR7 binding promotes both neutrophil transmigration and NETosis.*

LECs are known to recruit immune cells by secreting CCL21 in response to various stimuli[47, 54, 66, 83, 92], so we blocked CCR7, CCL21's receptor on neutrophils, to see if CCL21-CCR7 binding was necessary for the recruitment of neutrophils to lymphatic vessels. While the total number of neutrophils that transmigrated from the cell culture inserts to the bottom well was not affected by CCR7 blocking when the LECs were not treated with  $\text{TNF}\alpha$ , the number that transmigrated when the LECs were pre-treated with 50 ng/ml  $\text{TNF}\alpha$  was significantly decreased when CCR7 was blocked (Fig. 3.7A). The transmigration rate was also significantly lower when the neutrophils in the  $\text{TNF}\alpha$  pre-treated conditions were treated with  $\alpha\text{CCR7}$  blocking antibody, although not as low as the untreated conditions (Fig. 3.7B-C). Interestingly, CCR7 blocking also significantly reduced the average speed of the neutrophils after transmigration across the  $\text{TNF}\alpha$  pre-treated LECs, although again not to the level of the neutrophils that transmigrated across untreated LECs (Fig. 3.7D). Isotype control for CCR7 blocking did not impact neutrophil transmigration or motility (Fig. 3.8).

Surprisingly, we also observed a decrease in NETosis with CCR7 blocking, both in 2D co-cultures and the cell culture insert set-up (Fig. 3.7E-F). CCL21 has not previously been described as an inducer of NETosis, but it can upregulate the ERK1/2 pathway[54, 66], which has been shown to drive NETosis after other upstream stimuli[91]. Like we saw with the transmigration rates and neutrophil motility, this was only a partial decrease in NETosis.



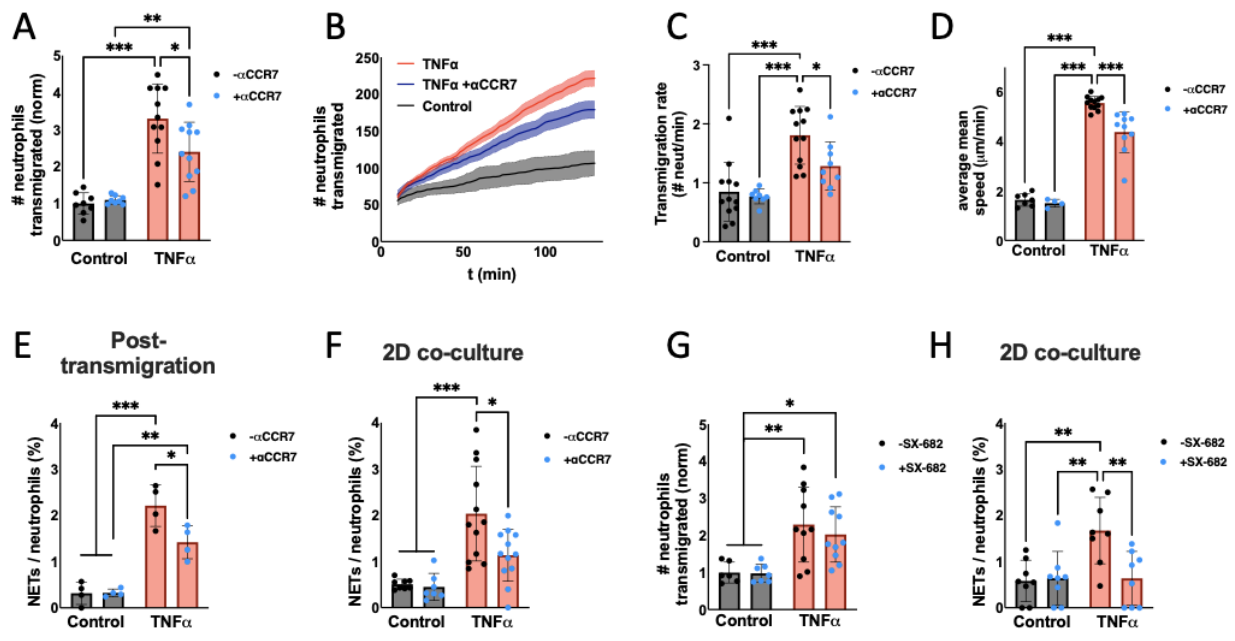


Figure 3.7: NETosis is regulated by CCR7 and CXCR1/2 binding, and neutrophil transmigration is decreased when CCR7 is blocked. A) Number of neutrophils that transmigrated to bottom well with and without TNF $\alpha$  (24h, red) and  $\alpha$ CCR7 blocking antibody (blue). Normalized to control without  $\alpha$ CCR7 for each experiment (3 independent experiments). B) Neutrophil transmigration over time across LEC monolayer pre-treated with or without TNF $\alpha$  for 24h, with and without  $\alpha$ CCR7. C) Transmigration rate (neutrophils/minute) with and without TNF $\alpha$  and  $\alpha$ CCR7. D) Average of the mean speed of each neutrophil that transmigrated across LEC monolayer with and without TNF $\alpha$  and  $\alpha$ CCR7. Average mean speed normalized to control without  $\alpha$ CCR7 blocking antibody for each experiment (3 independent experiments). E) Percent of neutrophils at endothelium that have formed NETs at endpoint of transmigration assay with and without TNF $\alpha$  and  $\alpha$ CCR7. F) Percent of neutrophils that have formed NETs at endpoint of a 2D co-culture with LECs pre-treated with TNF $\alpha$  with and without  $\alpha$ CCR7. G) Normalized number of neutrophils that transmigrated at endpoint of transmigration assay with and without TNF $\alpha$  and SX-682 CXCR1/2 inhibitor (blue). H) Percent of neutrophils that formed NETs at endpoint of a 2D co-culture with LECs with and without TNF $\alpha$  and SX-682. Two-way ANOVA with Tukey post-test was used to calculate p values for experiments with multiple groups and unpaired t-tests were used for comparisons between two groups. \*p < 0.05, \*\*p < 0.01, \*\*\*p < 0.001.

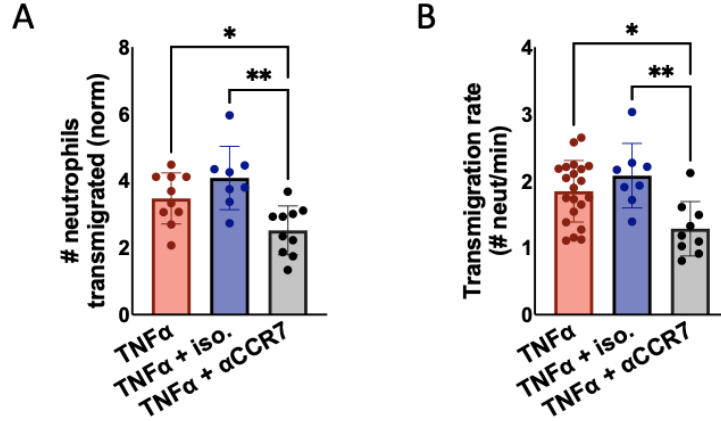


Figure 3.8: Isotype control antibody for anti-CCR7 (anti-rat igG) does not impact the number of neutrophils that transmigrates across a TNF $\alpha$ -pre-treated endothelium (normalized to control). (A) or neutrophil transmigration rate (B). \*p < 0.05, \*\*p < 0.01.

### 3.4.7 CXCR1/2 expression by neutrophils is necessary for NETosis, but not transmigration.

Because this effect only partially explains the increase in NETosis we see in the TNF $\alpha$  treated co-cultures, we next looked to CXCL8, which is both a neutrophil chemoattractant and NET inducer[34, 80, 89]. Using SX-682, a small molecule inhibitor of CXCR1 and CXCR2 - the receptors that bind CXCL8, we saw that the increased transmigration of neutrophils across TNF $\alpha$  pre-treated LECs did not depend on CXCR1/2 binding of CXCL8 in this context (Fig. 3.7G). This could be due to the fact that neutrophils' response to CXCL8 is dose-dependent, and higher levels of CXCL8 have been shown to promote NETosis, but not migration[112]. Supporting this idea, we saw that CXCR1/2 blocking led to a complete reduction of NETosis to levels consistent with control conditions (Fig. 3.7H). In this context, both CCL21 and CXCL8 play a role in promoting NETosis after transmigration, but CXCL8 is not driving transmigration.

### 3.5 Discussion

In this study, we develop a novel *in vitro* model of lymphatic clotting and use it to probe interactions between lymphatic endothelial cells and neutrophils in the context of coagulation while comparing clotting behavior of platelet-free plasma when cultured with blood vs. lymphatic endothelial cells. We also link LECs and NETosis through pathways involving CXCR1/2 and CCR7 and show that LECs can directly promote NETosis in 2D and 3D co-cultures with neutrophils and build on previous work our group has done establishing NETs as initiators of coagulation in lymph in the absence of platelets.

While lymphatic coagulation was first described over a century ago[46, 81], this phenomenon has remained relatively understudied, in large part due to the difficulty of isolating lymph, especially human lymph. In fact, much of the information on immune cell types in lymph still relies on ovine and bovine studies performed decades ago[94], and the process of cannulation required to isolate lymph has only recently been successful in smaller animal models like mice[126], with previous studies relying on larger animal models such as cows, pigs, dogs and rats[11, 74]. Studies involving human lymph have been very limited and require complicated surgical procedures and access to the thoracic duct[22, 99]. Having a model of human lymph that is easy to isolate and exhibits clotting behavior similar to that of isolated lymph from other animal models provides lymphatic researchers with the tools to study the dynamics of lymphatic coagulation in a way that has not previously been possible.

Using platelet-free plasma as a model of lymph provides a high-throughput way to study lymph clotting dynamics and could be used to investigate not only LEC influence on clotting, but the impacts of clot formation of LEC behavior and flow through lymphatic vessels, as we know they are sensitive to shear stress as well as transmural and interstitial flow[75]. It would also be straightforward to incorporate flow into this system, as the ibidi channel

slides are designed to be compatible with pump systems – this would be an important future direction because LECs likely respond differently to flow than BECs due to the significant differences in flow rates in lymph and blood *in vivo*.

Many open questions remain regarding the mechanisms and function of the decreased coagulatory behavior of LECs compared to BECs. Blood endothelial cells are known to increase their expression of tissue factor and decrease their expression of fibrinolytic factors tissue plasminogen activator (tPA) and plasminogen activator inhibitor-1 (PAI-1) in response to  $\text{TNF}\alpha$ [78, 97], and it is likely that other factors in addition to tPA and TFPI differ between LECs and BECs[114, 124]. It is also possible that molecules like anti-thrombin may also preferentially bind LECs compared to BECs, and there are many other potential relationships between LECs and factors involved in the clotting pathway that are not produced by endothelial cells.

In addition to describing a more coagulatory phenotype when LECs were treated with  $\text{TNF}\alpha$ , we also further confirmed the link between NETosis and lymphatic clotting suggested by our previous work by showing a decrease in coagulation accompanying DNase 1 treatment in neutrophil-LEC co-cultures. This *in vitro* set up allowed us to probe the dynamics of NETosis and coagulation and visualize that NET formation did occur prior to the formation of clots, in a much simpler experimental setup that did not require intravital imaging and allowed us to use primary human neutrophils. We were also able to confirm our suspicions that inflamed LECs were driving NETosis through *in vitro* co-cultures. We, along with others, have previously showed that CXCL8 and ICAM-1 are upregulated in LECs in response to  $\text{TNF}\alpha$ [47, 71], and others have shown that these molecules are important for inducing NETosis, but in this study we showed a direct link between CXCL8 binding and NETosis in neutrophil-LEC co-cultures, in addition to describing a new link between CCL21 and NE-

Tosis. NETs themselves activate blood endothelial cells to express higher levels of VCAM-1, ICAM-1 and tissue factor[28], so this could also promote a positive feedback loop to further promote clotting and NETosis if a similar process occurs in LECs. Interestingly, NETs themselves activate blood endothelial cells to express higher levels of VCAM-1, ICAM-1 and tissue factor[28], so this could also promote a positive feedback loop to further promote clotting and NETosis if a similar process occurs in LECs.

This further establishes an immunomodulatory role of LECs in the context of neutrophils and NETosis. While the role of LECs as immunomodulators has been well described in terms of their interactions with other immune cell types[32, 108, 117], little of this work has focused specifically on neutrophils and even less on NETosis. This new link has important implications for the role of lymphatics in disease, as NETs are known to promote metastasis, inflammation, and autoimmune disease in addition to coagulation[12, 18, 40, 60, 61, 84]. Of particular interest for future work is the relationship between lymphatics, NETs, and metastasis, because both NETs and lymphangiogenesis are associated with an increase in metastasis[26] and it is possible they respond in a coordinated manner in the tumor microenvironment and premetastatic niche. This work has broad translational relevance and reiterates the importance of considering the lymphatic system when identifying and developing therapeutic targets for NETosis-driven pathologies.

# CHAPTER 4

## INVESTIGATING THE ROLE OF FHL2 IN REGULATING ENDOTHELIAL CELL INFLAMMATORY RESPONSE

### 4.1 Preface

This work was done in collaboration with Shailaja Seetharaman, who is leading the project studying FHL2 in endothelial cell mechanosensing. She provided the teloHAEC cell lines that she engineered to under- or over-express FHL2 and provided VE-cadherin antibodies.

### 4.2 Introduction

Endothelial cells (ECs) of blood and lymphatic vessels experience various mechanical cues, including blood and lymph flow, vascular stretching, or extrinsically from the extracellular matrix, that drive overall vascular homeostasis[15]. In healthy arteries, ECs form strong cell-cell and cell-matrix adhesions, and align with blood flow to maintain vessel morphology[15]. However, in case of disrupted flow, ECs sense changes in mechanical stresses, and undergo drastic vascular remodeling, which in certain circumstances leads to atherosclerosis. Despite early evidence showing that ECs sense and respond to shear stress through cytoskeletal and cell-cell junction rearrangements, the precise mechanisms of force adaptation by ECs during normal and disrupted flow remain unclear[39].

While a significant amount of work has been done studying how endothelial cells sense various mechanical cues, how these mechanical cues may regulate their inflammatory response and immune interactions is comparatively under-studied. Many of the transcription factors that are mechanosensitive in the vascular endothelium, including hypoxia-inducible factor 1-alpha (HIF-1 $\alpha$ ), nuclear factor kappa-light-chain-enhancer of activated B cells (NF- $\kappa$ B),

and Yes-associated protein (YAP)/transcriptional coactivator with a PDZ-binding domain (TAZ), have established functions in regulating inflammation, as well as vascular permeabilization, is important in regulating immune cell transmigration in and out of vessels[25]. Zyxin, a focal adhesion/cytoskeleton-associated protein that is mechanosensitive, is also implicated in inflammatory responses and changes in cytokine/chemokine secretion by endothelial cells[25], and has been shown to stabilize viral RNA sensors and promote type 1 interferon responses important in the innate immune response[55]. While many of these mechanosensitive proteins are also known to regulate various inflammatory responses in other contexts, the mechanisms by which they do so in response to specific mechanical cues are not always well-understood.

Disturbed flow is one mechanical cue endothelial cells are regularly exposed to that is known to strongly induce vascular inflammation, but the mechanisms by which this occurs are not fully understood[16, 110]. Disturbed flow leads to increased expression of endothelial adhesion molecules ICAM-1, VCAM-1, and E-selectin[16, 110], as well as increased secretion of cytokines and chemokines such as IL-1, IL-6, CXCL8 and CCL5[76, 105]. Because changes in ICAM-1, CXCL8 and IL-6 are known to regulate neutrophil adhesion, recruitment, and NETosis[1, 122, 123], we focused on these three specifically. Secretion of these factors in response to inflammatory cytokines such as  $\text{TNF}\alpha$  is also regulated by cytoskeleton-associated factors such as Rho-kinase[100], suggesting that in addition to regulating immune responses of endothelial cells, different biomechanical microenvironments may also regulate their response to other inflammatory cues present in infection or other disease states. Because of this, different endothelial cell mechanotypes could either exacerbate or potentiate ongoing inflammatory processes. In this work, we discuss how a LIM-domain protein, FHL2, may be regulating these responses, and how the hyper-contractile phenotype induced by FHL2 overexpression may alter the response of endothelial cells to inflammatory stimuli such as  $\text{TNF}\alpha$ .

Proteomic screens of mechanotransduction pathways have revealed many proteins that contain one or more LIM (Lin-11, Isl1, MEC-3) domains[2, 29, 50, 118]. The LIM domain is a 60 amino acid sequence that forms a double zinc finger protein–protein or protein-DNA binding interface[2]. There are 41 LIM proteins found to be enriched at cell adhesions and/or the actomyosin cytoskeleton[2], and a screen of LIM domain proteins found that several are recruited to actin stress fibers upon laser ablation, including the LIM domain proteins zyxin and FHL2[119]. We hypothesize that mechanical forces lead to the activation and differential localization of various LIM domain proteins, triggering distinct mechanotransduction pathways that influence tissue adaptation through altering cell adhesion, migration, and inflammatory response, and in this chapter we will specifically focus on FHL2 and the inflammatory response.

Unpublished work from the Gardel lab has established that FHL2 expression increases in response to shear stress from disrupted flow, both *in vitro* and in mouse arteries. Additionally, FHL2 localizes to stress fibers in hypercontractile tissues (phenotype induced by RhoA activation by CNO3) and endothelial monolayers exposed to disturbed flow. It also localizes to membrane ruffles or protrusions when contractility is decreased by ROCK inhibition with Y-27, and shuttles to the nucleus with a lack of contractility[77]. While ongoing work is being done that has shown that FHL2 expression tunes actomyosin contractility and junctional strength in endothelial cells and that FHL2-stress fiber binding is necessary for junction disruption, this chapter focuses on how FHL2 over- or under-expression may influence endothelial cell inflammatory response to  $\text{TNF}\alpha$  or disturbed flow.



## 4.3 Methods

### 4.3.1 *Inducible FHL2 under- and over-expressing cell lines*

hTERT-immortalized human aortic endothelial cells (teloHAECs) were transfected by Shailaja Seetharaman with two different shRNAs to knockdown FHL2 expression (shFHL2-1 and shFHL2-2) or were transfected to induce FHL2 overexpression (FHL2-mEm). Shailaja maintained these cell lines and also confirmed changes in FHL2 expression levels using either western blotting or immunofluorescence staining, periodically testing for mycoplasma contamination. Both over- and under- expression of FHL2 are inducible by doxycycline treatment for 3 days (knockdown) or 1-3 days (overexpression). ShFHL2 cells were labeled with cyan fluorescent protein (CFP) and FHL2-mEm overexpressing cells were labeled with mEmerald. The immunofluorescence images and enzyme-linked immunosorbent assay (ELISA) data included in this chapter are both from cells that were not exposed to flow, and cells were cultured in endothelial growth medium (EGM-2 with singlequots kit, Lonza).

### 4.3.2 *TeloHAEC cytokine treatment and immunofluorescence staining*

After induction of FHL2 under- or overexpression with doxycycline, teloHAECs were seeded at  $5 \times 10^3$  cells in 100  $\mu$ l EGM-2 media in wells in a 96-well plate, or at  $5 \times 10^4$  in 1ml on glass coverslips in a 6-well plate for immunofluorescence staining. An equal volume of either media or 50 ng/ml TNF $\alpha$  was added to each well for 24h, after which media was collected for ELISA and cells were fixed with 2% paraformaldehyde (PFA) in PBS. Cells were not exposed to flow in these experiments. For cells treated with Y-27632 ROCK inhibitor (Y-27, STEMCELL Technologies), 25 $\mu$ M was added with TNF $\alpha$ . Cells were stained without antigen retrieval for VE-cadherin and ICAM-1 overnight at 4C as previously described. All secondary antibodies were from Invitrogen and diluted 1:500.

### 4.3.3 ELISA

R&D DuoSet ELISA kits were used to measure CXCL8 and IL-6 secretion by teloHAECs cultured in 96 well plates that were treated for 24h with 50 ng/ml TNF $\alpha$  and/or 25 $\mu$ M Y-27 ROCK inhibitor (described above) or from FHL2 over- and under-expressing teloHAECs that had been subjected to unidirectional or disturbed flow as adapted by Yun Fang's group[57] from Dai, et al.[20]. Unidirectional or disturbed flow was replicated using a flow device consisting of a computerized stepper motor UMD-17 (Arcus Technology) and a 1° tapered stainless steel cone, which was modified based on the flow system developed by Dai et al[20]. The flow devices were placed in a 37°C incubator with 5% CO<sub>2</sub>. teloHAECs were cultured in EGM-2 medium in 6-well plates, and subjected to unidirectional or disturbed flow waveforms for 24-72 hours. Media from cytokine treated cells and cells exposed to flow was collected and centrifuged at 2000rpm for 5 minutes to remove any cell debris and were stored at -80C until use. Samples were diluted 1:1 in reagent diluent (1% bovine serum albumin (BSA) in PBS). ELISA measurements were taken in duplicates for each sample, and the average of the two values was used in figures 4.1-3.

## 4.4 Results

### 4.4.1 *TNF $\alpha$ treatment leads to an upregulation in CXCL8 and IL-6 production in teloHAECs in static cultures*

Consistent with prior work[125, 129], teloHAECs significantly increased their secretion of both CXCL8 and IL-6 in response to 24h treatment with 50 ng/ml TNF $\alpha$  (Fig.s 4.1 and 4.2). This was consistent across the FHL2 under- and over-expressing cell lines, and occurred with and without the doxycycline induction of FHL2 overexpression or knockdown. There was some variation in IL-6 production in particular across experiments (Fig 4.3, pooled data from 3 independent experiments), but the trends in each experiment were the same. The

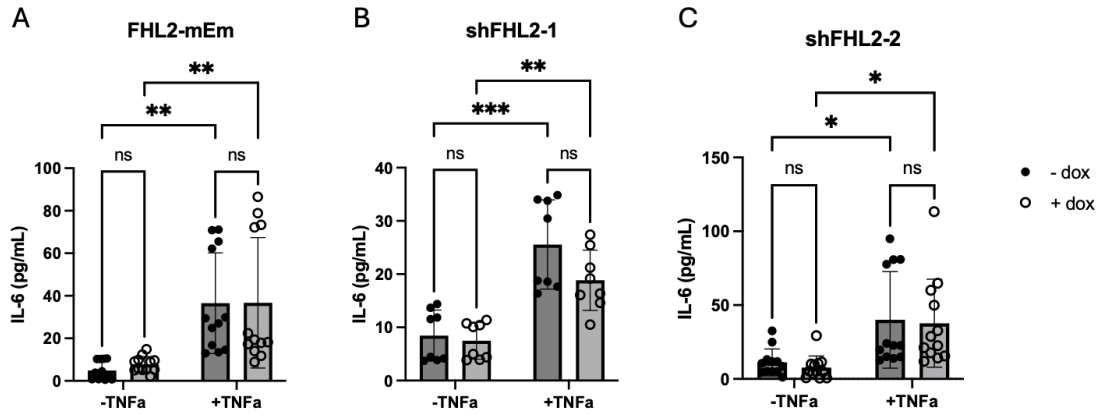


Figure 4.1: **IL-6 expression in teloHAECs treated with TNF $\alpha$ .** IL-6 secretion by teloHAECs pre-treated with doxycycline to induce FHL2 over- (A) or under- (B&C) expression after 24h cultured with or without 50 ng/ml TNF $\alpha$ . \* $p < .05$ , \*\* $p < .01$ , \*\*\* $p < .001$  by one-way ANOVA test with Tukey multiple comparisons test. Pooled data from 3 independent experiments, each point representing one well in a 96-well plate.

cells in these experiments were in static cultures not exposed to flow.

#### 4.4.2 *FHL2 up- or down-regulation does not impact TNF $\alpha$ -induced IL-6 secretion in the absence of flow*

In these static experiments, FHL2 up- or down-regulation did not significantly impact the TNF $\alpha$ -induced secretion of IL-6 by teloHAECs (Fig. 4.1). While we did see significant decreases in IL-6 secretion in response to TNF $\alpha$  when FHL2 was knocked down in individual experiments (Fig. 4.1B-C), when we pooled normalized data from multiple experiments, variability between repeats meant this was not significant overall. It is possible that in the presence of flow, or with higher n, these differences would be significant, but FHL2 may not be one of the main regulators of IL-6 secretion in the absence of flow since previous work has primarily described its role in responding to changes in flow-based mechanotypes or substrate stiffnesses, and neither of these are changed between conditions in this experiment.

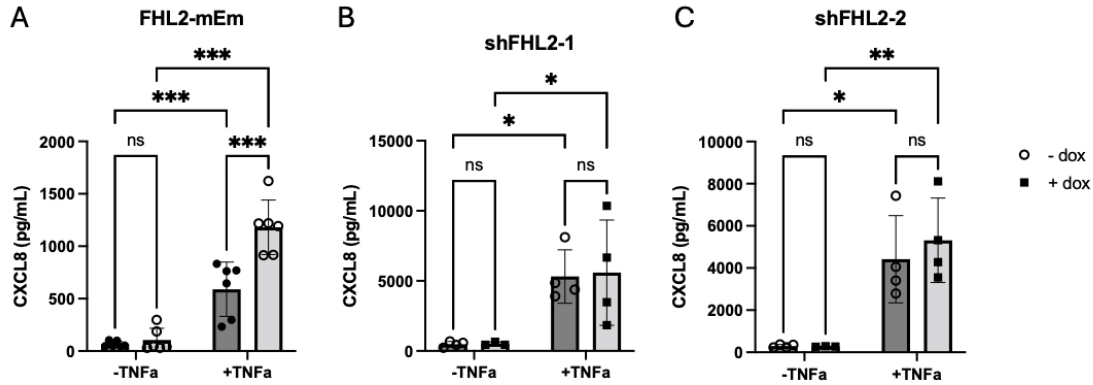


Figure 4.2: **CXCL8** expression in teloHAECs treated with  $TNF\alpha$ . CXCL8 secretion by teloHAECs pre-treated with doxycycline to induce FHL2 over- (A) or under- (B&C) expression after 24h cultured with or without 50ng/ml  $TNF\alpha$ . \* $p < .05$ , \*\* $p < .01$ , \*\*\* $p < .001$  by one-way ANOVA test with Tukey multiple comparisons test. Pooled data from 2 independent experiments, each point representing one well in a 96-well plate.

#### 4.4.3 *FHL2* upregulation increases CXCL8 secretion in response to $TNF\alpha$ in the absence of flow

Surprisingly, even in the absence of flow, we did see changes in CXCL8 secretion when FHL2 was upregulated (Fig. 4.2A), although its role in endothelial response to disturbed flow is less well-described compare to IL-6[36, 76, 105]. We did not observe decreases in CXCL8 secretion in response to FHL2 knockdown (Fig. 4.2B-C), but again FHL2 may be more relevant in regulating this in the presence of flow. Given the recent work describing important roles for neutrophils and NETs in regulating clotting, and the fact that disturbed flow is associated with a more coagulatory phenotype in blood vessels, this could provide an interesting link between the two phenomena.

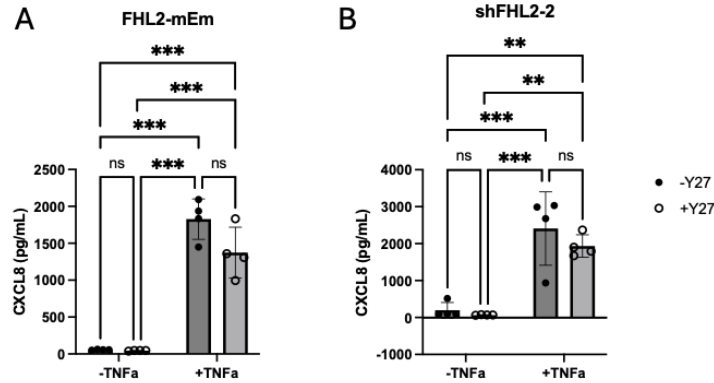


Figure 4.3: **CXCL8 expression by teloHAECs with ROCK inhibition** CXCL8 secretion by FHL2 over- (A) or under- (B) expressing teloHAECs when treated with 25  $\mu$ M Y27 ROCK inhibitor after 24h 50 ng/ml TNF $\alpha$  treatment. \*p<.05, \*\*p<.01, \*\*\*p<.001 by one-way ANOVA test with Tukey multiple comparisons test. Data from one experiment, each point representing one well in a 96-well plate.

#### 4.4.4 *ROCK inhibition likely leads to decreased CXCL8 secretion in response to TNF $\alpha$*

Rho-kinase has been shown to mediate secretion of CXCL8 by endothelial cells in response to lipophosphatidic acid (LPA)[100], so we next looked to see if ROCK inhibition was also involved in mediating its secretion in response to TNF $\alpha$ . While the differences were not significant, ROCK inhibition with 25 $\mu$ M Y-27 showed trends of decreasing CXCL8 secretion in response to 24 hour 50 ng/ml TNF $\alpha$  treatment in both FHL2 over- and under-expressing teloHAEC cell lines (Fig. 4.3, all conditions with doxycycline induction of FHL2 over- or under-expression). There were no differences observed in response to ROCK inhibition in the non-TNF $\alpha$ -treated conditions, which all secreted very low levels of CXCL8, and we did not observe any differences in response to changes in FHL2 expression (Fig. 4.3). This again suggests that a more contractile phenotype primes endothelial cells towards a more pronounced response to inflammation.

*4.4.5 TNF $\alpha$  regulates cell shape and size in endothelial cells, but without flow, changes in FHL2 do not significantly impact these processes, junctional organization, or ICAM-1 expression*

While we did see changes in endothelial cell size and shape in response to TNF $\alpha$ , these changes did not appear to be impacted by an overexpression of FHL2 (Fig. 4.4). Cells in the top panel (-dox) expressed typical levels of FHL2, while cells in the bottom panel (+dox) over-expressed FHL2. No significant changes in cell shape, size or junctional organization were observed between these groups. None of the groups in figure 4.4 were exposed to flow. In the cells that were treated with 50 ng/ml TNF $\alpha$  for 24h (right), cells appeared to be more elongated and larger, although this was not quantified. It will be important to quantify at average cell shape and aspect ratio in the presence of flow in future work. We also did not observe significant changes in ICAM-1 expression (red, Fig. 4.4), even in response to TNF $\alpha$ , which was unexpected and may indicate an issue with the staining as we would expect to see an inflammation-associated increase based off of prior work[3]. Again, these changes are likely going to be more pronounced in the presence of flow, but were not significantly impacted by changes in FHL2 in these static conditions.

*4.4.6 Media from disturbed flow experiments did not provide reliable cytokine measurements*

Unfortunately, cytokine measurements from conditioned media collected from flow experiments did not provide reliable or reproducible data, likely due to variable evaporation and cell density in different conditions. In the disturbed flow condition, cell growth was impaired, and there were likely higher levels of evaporation due to the fact that the 6-well plates needed to be open in order to accommodate the flow induction set up, which was exacerbated in disturbed flow conditions. Evaporation could increase the relative concentrations of cytokines

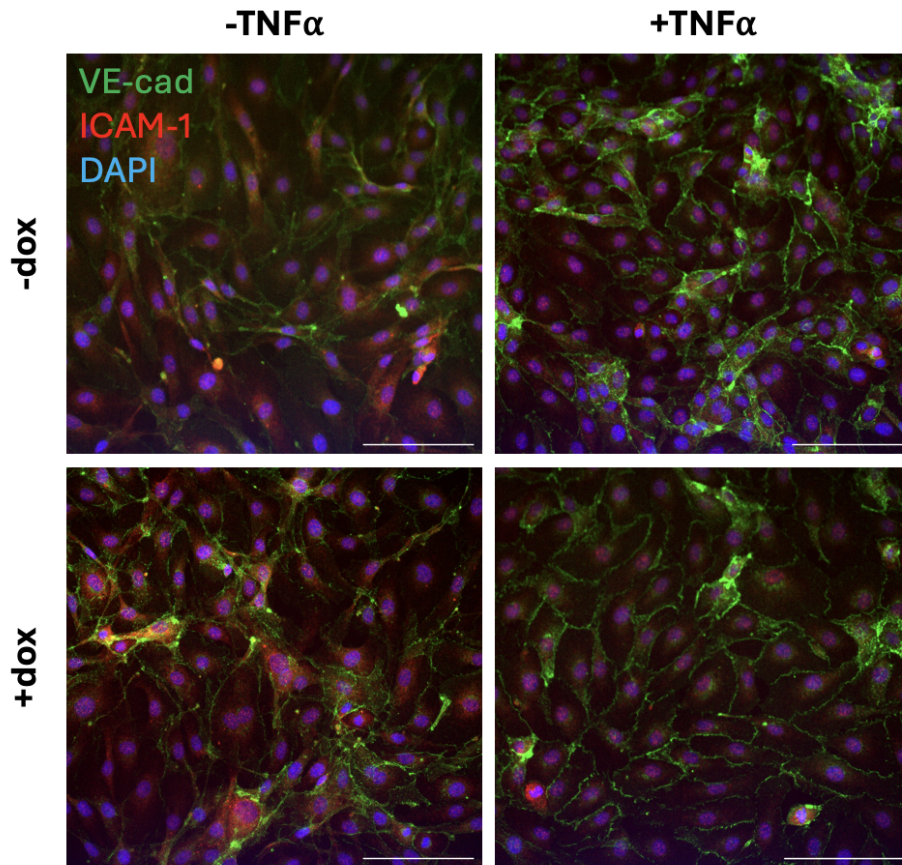


Figure 4.4: VE-cadherin (green), ICAM-1 (red) and DAPI (blue) staining of FHL2-mEm teloHAECs with or without doxycycline induction of FHL2 overexpression, with and without 24h  $\text{TNF}\alpha$  treatment. Scale bars =  $100\mu\text{m}$

in the media collected, but decreased cell growth would decrease the concentration, and the fact that these were different in the conditions we were aiming to compare made any results here impossible to interpret. In future work it will be important to either use techniques that will allow for conditioned medium collection in a more controlled manner, or focus on transcriptional data or cell surface factors that can be normalized more easily in this setup, and this work is currently ongoing in the Gardel lab.

## 4.5 Discussion

While the data in this chapter was primarily negative data, the question of whether FHL2 is involved in regulating the inflammatory response of endothelial cells remains open and warrants further investigation. It is likely that many of the negative results we were observed were due to limitations with the experimental setups used, and that changes are more likely to be observed under conditions of disturbed or unidirectional flow. In these experiments, the conditioned media from cells subjected to unidirectional and disturbed flow was not able to be used for secreted cytokine measurements, so all of the ELISA data included above is from endothelial cells in static conditions without flow. However, new methods to subject cells to different flow conditions in a more controlled manner are currently being developed in the Gardel lab and repeating these measurements with samples from those experiments will likely be more successful, although it is possible that changes in FHL2 expression do not regulate the inflammatory response of endothelial cells to  $\text{TNF}\alpha$ .

In future work, it will be important to look at endothelial cell expression of IL-6, CXCL8, ICAM-1 and other molecules known to be regulated by disturbed flow[110] in cells that have been exposed to both unidirectional and disturbed flow. The potential link between CXCL8 secretion and FHL2 is particularly interesting in the context of this work, given the similar impacts of both disturbed flow and NETs on coagulation in blood vessels[16, 110, 115].



Promoting neutrophil recruitment and NETosis may be one of the mechanisms by which endothelial cells promote coagulation in response to disturbed flow, and NETs themselves can create disturbances in blood flow due to clot formation, potentially leading to a positive feedback loop.

Additionally, it would be interesting to see if lymphatic endothelial cells also express FHL2, and if its role differs in LECs. LECs are exposed to much slower flow than blood vessels, and the roles of interstitial and transmural flow are very important in regulating lymphatic recruitment of immune cells[75]. FHL2 may play a different role in the sensing of various types of flow beyond luminal flow, and regulation of its expression could potentially influence the role of lymphatics as immunomodulators.

# CHAPTER 5

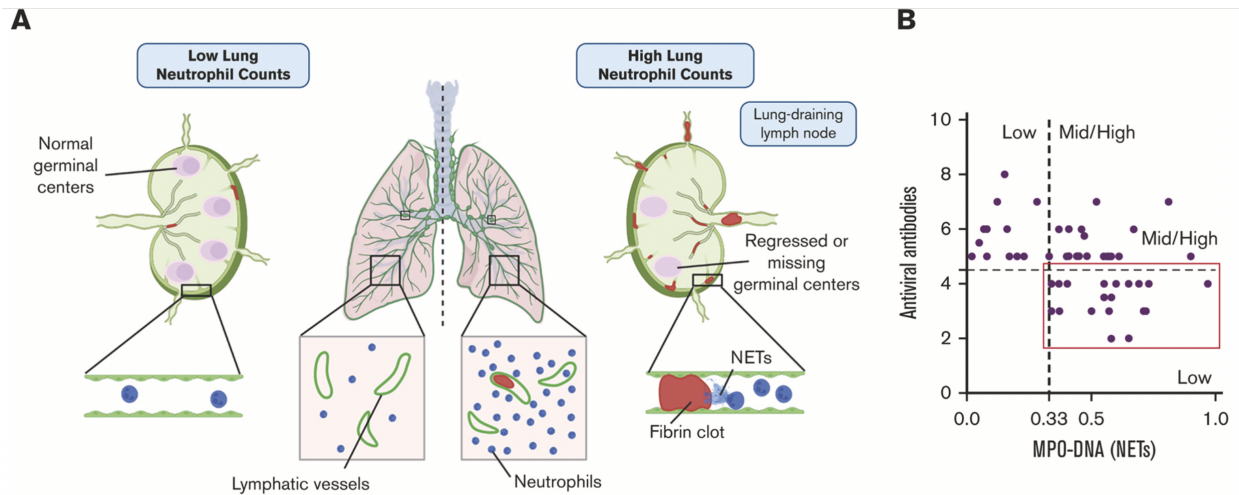
## CONCLUSIONS AND FUTURE DIRECTIONS

### 5.1 Summary

In this body of work, I establish a new role for neutrophil extracellular traps in promoting intralymphatic coagulation, and examine a number of the mechanisms by which NETs and LECs collaborate to drive this process. In chapter 2, I describe the presence of lymphatic clots in COVID-19 decedents, as well as a correlation between NETosis, lymphatic clotting and antiviral antibody levels, identifying a potential mechanism by which neutrophils are able to impact both the innate and adaptive immune response through driving lymphatic coagulation and disrupting germinal center formation and antibody production. In chapter 3, I utilize platelet-free plasma as a model of lymph in order to study clotting behavior *in vitro*, and identify key differences in blood and lymphatic coagulation, as well as mechanisms by which lymphatic endothelial cells drive intralymphatic NETosis in response to  $\text{TNF}\alpha$  in order to induce clotting. I identify CXCR1/2 and CCR7, as well as tissue plasminogen activator, as key players in this process. Lastly, in chapter 4, I investigate the role of FHL2, a mechanosensitive LIM-domain protein, in regulating the inflammatory response in endothelial cells, suggesting potential roles for endothelial cell mechanosensing in the regulation of immune responses and coagulation.

### 5.2 Discussion

While much of the discussion for this dissertation is included in the respective chapters, here I will discuss some of the overarching themes of the work. The main theme tying this work together is that both endothelial cells and neutrophils play much more active roles in various areas of immunity than has previously been believed. Neutrophils are not simply first responders limited to participating in the innate immune response, but play important



A) Lymphatic vessels in lungs and lung-draining lymph nodes of COVID-19 decedents exhibit widespread fibrin clotting which is correlated with NETosis. B) Patients with low antiviral antibody titers had all mid or high serum NET levels. Created with BioRender.

Figure 5.1: NETs & lymphatic coagulation in COVID-19

roles in regulating adaptive immunity in a number of contexts. Blood and lymphatic endothelial cells are much more than simply the walls of vessels to transport blood and immune cells, but rather potent immunomodulators that can have significant influence on both innate and adaptive immune responses. Coagulation in the lymphatic system was correlated with severe germinal center disruption and decreased antiviral antibodies in severe cases of COVID-19, and while neutrophil extracellular traps were driving this coagulation, I found in chapter 3 that it was actually the LECs that were recruiting neutrophils and priming them towards NETosis in response to inflammation. I also saw in chapter 4 that endothelial cell mechanosensing of disturbed flow influences their secretion of factors important in immune cell recruitment and activation. Together, this data reiterates the importance of immune cell-endothelial interactions, and opens up many questions to be pursued in future studies, some of which are outlined below. While this work has focused on the mechanisms by which lymphatic coagulation occurs, we have only begun to examine its consequences in the context of COVID-19, and it likely plays an important role we have yet to understand in multiple other disease contexts. I think some of the most interesting work stemming from this project

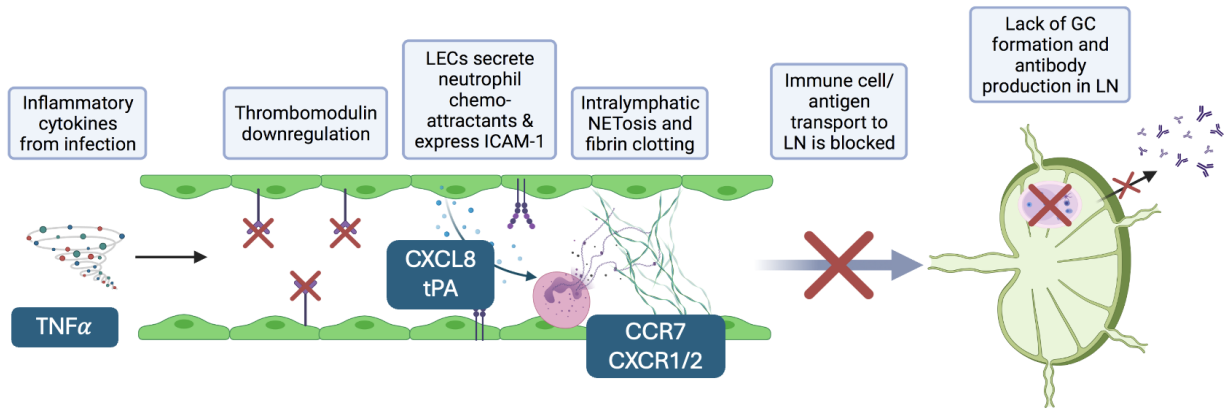


Figure 5.2: **Schematic of lymphatic-neutrophil interactions in the context of coagulation** Created using Biorender.com

will be in the areas of examining how lymphatic coagulation influences immune responses in cancer or autoimmune disease, and also how lymphatic coagulation may be a necessary component of the innate immune response in order to stop the spread of infection.

### 5.2.1 *Neutrophils as regulators of both the innate and adaptive immune responses*

There is evidence that LN neutrophils in particular can affect adaptive immune responses. Neutrophils, along with macrophages and dendritic cells, facilitate antigen capture and presentation in the lymphatic system and carry antigen to the lymph node[41, 68, 104]. They can also activate or inhibit T- and B-cell immunity[41]. Some subsets of neutrophils have recently been shown to patrol even naïve lymph nodes and increase CD4+ T cell and natural killer (NK) T cell activation in the lymph node, suggesting that their patrolling for infection is not limited to simply blood circulation, and that they play more of a role in regulating the adaptive immune response than expected[41, 68]. However, exactly what this role is remains controversial, because neutrophils have also been shown to limit the local humoral response in the lymph node in response to *Staphylococcus aureus* infection[48]. Promoting lymphatic

clotting through NETosis and therefore impairing antigen and immune cell transport to the lymph node could be another way neutrophils affect adaptive immunity; the data in chapter 2 showing that serum NET levels negatively correlate with anti-RBD antibody titers indicate that NETs likely do play a role in regulating adaptive immune responses in COVID-19.

### 5.2.2 *Lymphatic endothelial cells as immunomodulators*

Lymph nodes are known to be sites of immune activation and antigen processing, and lymphatic vessels transport immune cells and pathogenic material to the lymph node to be processed, but lymphatic endothelial cells themselves are also immunomodulators that regulate immune cell recruitment and activation through cytokine and chemokine secretion, as well as MHC-1 expression[3, 47, 83, 89, 92, 104, 109]. Much of the previous work focusing on lymphatic endothelial cells, aside from some work done by the Jackson and Liao groups, has focused on dendritic cells and monocytes[32, 108, 117], but neutrophil-lymphatic interactions have only begun to be studied in depth more recently, and LECs' role in promoting NETosis has not yet been established. This work establishes a new role for lymphatic endothelial cells in regulating NETosis, and the impact on lymphatic coagulation, which is also regulated by lymphatic endothelial cells, likely plays an important role in regulating both the innate and adaptive immune responses.

In chapter 2, I discuss how lymphatic coagulation is correlated with the presence of dysregulated germinal centers in the lung-draining lymph nodes of COVID-19 decedents and how higher serum NET levels correlated with lower antiviral antibody titers[71], but it will be important in future work to piece out the role of lymphatic coagulation in *in vivo* models of infection where its effect can be studied directly. Additionally, I didn't have the chance to examine how NET-induced lymphatic coagulation may be regulating the innate immune response by blocking the dissemination of pathogens through the lymphatic system, and I

think this is a really exciting future direction since there is likely a physiological reason that lymphatic coagulation occurs. I believe that like immunothrombosis in blood vessels, lymphatic coagulation is likely an important part of the innate immune response's local control of infection, but can become pathological when dysregulated in contexts such as COVID-19 infection.

### *5.2.3 Physiological and pathological functions of lymphatic coagulation*

In this dissertation, I identified potential pathological consequences of lymphatic coagulation in COVID-19 based off of correlations with germinal center dysregulation and impaired antibody production, but there is likely a physiological function for lymphatic clotting in healthy immune responses. Pathogens are able to hijack the lymphatic system to rapidly disseminate throughout the body, and because prevention of this, at least in some contexts, is neutrophil-dependent[6], I think it's possible that NET-induced lymphatic coagulation could be part of the mechanism preventing rapid spread of infection through the lymphatic system, or could potentially help prevent the dissemination of cancer cells through the lymphatic system, since lymph nodes are frequently the first sites of metastasis. Alternatively, lymphatic coagulation could also play a negative role in regulating the adaptive immune response in both infection and cancer, blocking the transport of lymph-derived cytokines important for immune cell recruitment and activation and preventing a strong antiviral or anti-tumor immune response, or even providing scaffolding that could be used by tumor cells to traffic through lymphatic vessels. Likely, lymphatic coagulation is a double-edged sword in immunity, playing a protective role in some contexts and a pathogenic one in others, although this will need to be studied in more detail in future work in order to be able to make any concrete conclusions.

#### 5.2.4 *Endothelial cell mechanosensing and inflammation*

While the data on this topic was primarily negative, the question of whether FHL2 is involved in regulating the inflammatory response of endothelial cells remains open and warrants further investigation. It is likely that many of the negative results we were observed may be altered under conditions of disturbed or unidirectional flow. In future work, it will be interesting to measure endothelial cell expression of IL-6, CXCL8, ICAM-1 and other molecules known to be regulated by disturbed flow[110] in cells that have been exposed to both unidirectional and disturbed flow. The potential link between CXCL8 secretion and FHL2 is particularly interesting in the context of this work, given the similar impacts of both disturbed flow and NETs on coagulation in blood vessels[16, 110, 115]. Promoting neutrophil recruitment and NETosis may be one mechanism by which endothelial cells promote coagulation in response to disturbed flow, and NETs themselves can create disturbances in blood flow due to clot formation, potentially leading to a positive feedback loop. This would create an interesting link between the first two chapters of this thesis and the work done on FHL2.

Additionally, it would be interesting to see if lymphatic endothelial cells also express FHL2, and if its role differs in LECs. LECs are exposed to much slower flow than blood vessels, and the roles of interstitial and transmural flow are very important in regulating lymphatic recruitment of immune cells[75]. FHL2 could play a different role in sensing of various types of flow beyond luminal flow, and regulation of its expression could potentially influence the role of lymphatics as immunomodulators, since their response to transmural flow in particular has been shown to regulate the transmigration of immune cells[75].

## 5.3 Future Directions

### 5.3.1 *In vivo studies of lymphatic clotting*

In future work, it will be important to study the impact of blocking lymphatic coagulation *in vivo*, particularly in a disease context. While I was able to observe correlations between lymphatic coagulation and germinal center disruption in COVID-19 decedents, and also between NETosis and antiviral antibody titers, I was not able to study the impact of lymphatic coagulation on the adaptive immune response directly due to the nature of our samples. In a mouse study, lymph nodes could be collected and serum samples could be taken over time with or without anticoagulant treatment or prevention of NETs. This would provide us with important mechanistic and kinetic insights into whether lymphatic coagulation is the main factor driving this disruption of the adaptive immune response, or if it is simply also a consequence of the underlying cause. It is likely this decrease in adaptive immune response is driven by lymphatic coagulation alongside other factors.

Additionally, methods to block coagulation specifically in lymphatic vessels would be useful in order to further investigate how the impact of clotting in lymphatic vessels differs from that in blood vessels. I have hypothesized that lymphatic coagulation is rarer and more transient than blood coagulation, and also that its effects are less acutely severe than the effects of blood clots, making them harder to detect. However, it would be useful to directly test this hypothesis and see how the changes in immune response differ when lymphatic, but not blood coagulation is prevented.

### 5.3.2 *Lymphatic coagulation in cancer*

Of particular interest for future work is the relationship between lymphatics, NETs, and cancer, because both NETs and lymphangiogenesis are associated with an increase in metas-



tasis[18, 26, 61, 123] and it is possible they respond in a coordinated manner in the tumor microenvironment and premetastatic niche. It is also possible that coagulation could either impede or promote the migration of tumor cells through lymphatic vessels, which are known to be routes of transport for tumor cells to metastasize to lymph nodes or other distant sites[26, 101]. Additionally, transport of tumor antigens and immune cells to the lymph node to mount the anti-tumor immune response may be inhibited by lymphatic coagulation, so higher levels of lymphatic coagulation may be associated with poorer immunotherapy response due to an impaired adaptive immune response similar to that we observed in COVID-19.

In addition to investigating how lymphatic coagulation may impact cancer progression and treatment response, it is also of interest to determine how cancer and cancer treatments may promote lymphatic coagulation. Radiotherapy in particular is known to induce endothelial cell damage, which has been associated with lymphatic coagulation[82], and inflammatory cytokines such as  $\text{TNF}\alpha$  are upregulated in many types of cancer. Secreted factors from tumors are also known to promote NETosis[61, 123], which we now know drives lymphatic coagulation, so it is reasonable to assume there may be an increase in lymphatic coagulation in cancer.

### 5.3.3 *Lymphatic coagulation in lipedema*

Another disease of interest when it comes to lymphatic coagulation is lipedema. It has long been hypothesized that lipedema is a lymphatic disease, but the mechanisms driving it are still not understood. However, samples of interstitial fluid, which is representative of the local lymph composition, from lipedema patients contained high levels of markers of coagulation, and immunofluorescence staining of patient tissue samples showed evidence of lymphatic clot formation in lipedema patients. Preliminary data did not show strong correlations between

lymphatic clotting scores and disease stage, but further investigation is needed to determine the role lymphatic clotting plays, if any, in this disease.

#### 5.3.4 *Lymphatic coagulation in bacterial infections and viral infections other than COVID-19*

In chapter 2, I also observed significant lymphatic coagulation in the lung-draining lymph nodes from a limited number of H1N1 decedents. This clotting was very similar to that seen in COVID-19 LDLNs, and it is likely this effect is not specific to COVID-19, but rather a general part of the immune response to severe viral respiratory infections. However, to confirm this, the presence of lymphatic clotting in more viral infections will need to be confirmed, and work will need to be done to investigate if the consequences of these clots are consistent across different types of viral infection.

Additionally, to investigate the role of NET-induced lymphatic coagulation on dissemination of bacterial infection throughout the lymphatic system, more *in vivo* studies will need to be carried out, probably using *Staphylococcus aureus* as a model because of neutrophils' established role in controlling infection in the lymph node in particular. *S. aureus* rapidly disseminates through the lymphatic system, and the prevention of this spread is dependent on the recruitment of neutrophils to the lymph node[6]. While these neutrophils are recruited rapidly through high endothelial venules[6], their recruitment is largely mediated through lymph-derived cytokines, as lymph is transported to lymph nodes within minutes from the site of infection[121]. This indicates that while control of infection within the lymph node and lymphatic system as a whole is dependent on neutrophil behavior, the lymphatic system is actively regulating the neutrophil immune response, which will be a common theme throughout this dissertation. Additionally, *S. aureus* is known to induce NETosis, providing further motivation to look for lymphatic coagulation in this context. It would be interest-

ing to see if blocking NETosis had the same effect as neutrophil depletion in regulating the spread of *S. aureus* through the lymphatic system.

### 5.3.5 *Binding of pro- and anti-coagulant molecules on LECs vs. BECs*

While I was able to measure the secretion of various coagulatory or fibrinolytic factors by LECs and BECs and could stain for relevant factors on their surfaces, it will be important in future work to study the binding of non-endothelial cell-derived factors in the clotting cascade. Anti-thrombin, for example, is synthesized in the liver and is present in blood and lymph, but is not produced by endothelial cells. It is possible that some of the decreased proclivity of LECs towards clotting is related to differential binding of factors such as anti-thrombin to LECs and BECs, and that anticoagulatory factors may bind LECs preferentially.

### 5.3.6 *Impact of NET-induced coagulation on lymph flow*

The *in vitro* model of lymphatic coagulation that was used in chapter 3 could easily be adapted to incorporate flow using an ibidi pump system, and it would be interesting in future studies to examine both the impact that NETs and NET-induced clots have on the flow of lymph and how different types of flow may influence the coagulatory and NET-inducing properties of LECs. It is likely that NETs alone, and especially NETs incorporated into clot, would prevent or decrease the flow of lymph, and that the resulting stasis could create a more coagulatory phenotype in the nearby endothelial cells, which could in turn recruit more neutrophils and drive more clotting.

### 5.3.7 *Endothelial cell mechanosensing and inflammation*

As mentioned in chapter 4, there are many remaining questions when it comes to the work begun in this thesis on the role FHL2 plays in regulating the inflammatory response of endothelial cells to disturbed flow. The most obvious next step for this work is to measure the

inflammatory molecules that are up-regulated by disturbed flow when FHL2 is up- or down-regulated under more physiological conditions incorporating disturbed and unidirectional flow since I did not see significant difference under static conditions. Additionally, it would be very interesting to look into the differences in mechanosensing between endothelial cell types, ranging from aortic endothelial cells and blood endothelial cells in other environments to lymphatic endothelial cells, since they are exposed to very different forces and may exhibit different responses to the same stimuli.

## BIBLIOGRAPHY

- [1] Zhujun An et al. “Neutrophil extracellular traps induced by IL-8 aggravate atherosclerosis via activation NF- $\kappa$ B signaling in macrophages”. In: *Cell Cycle* (2019). ISSN: 15514005. DOI: 10.1080/15384101.2019.1662678.
- [2] Caitlin A. Anderson et al. *LIM domain proteins in cell mechanobiology*. 2021. DOI: 10.1002/cm.21677.
- [3] Samantha Arokiasamy et al. “Endogenous TNF $\alpha$  orchestrates the trafficking of neutrophils into and within lymphatic vessels during acute inflammation”. In: *Scientific Reports* 7 (Mar. 2017). ISSN: 20452322. DOI: 10.1038/srep44189.
- [4] Céline Beauvillain et al. “CCR7 is involved in the migration of neutrophils to lymph nodes”. In: *Blood* 117.4 (2011). ISSN: 15280020. DOI: 10.1182/blood-2009-11-254490.
- [5] Britta Bettin et al. “Removal of platelets from blood plasma to improve the quality of extracellular vesicle research”. In: *Journal of Thrombosis and Haemostasis* 20.11 (2022). ISSN: 15387836. DOI: 10.1111/jth.15867.
- [6] Ania Bogoslawski, Eugene C. Butcher, and Paul Kubes. “Neutrophils recruited through high endothelial venules of the lymph nodes via PNA $\alpha$  intercept disseminating *Staphylococcus aureus*”. In: *Proceedings of the National Academy of Sciences of the United States of America* 115.10 (2018). ISSN: 10916490. DOI: 10.1073/pnas.1715756115.
- [7] Mettine H A Bos and Rodney M Camire. “Blood coagulation factors V and VIII: Molecular Mechanisms of Procofactor Activation.” In: *Journal of coagulation disorders* 2.2 (2010). ISSN: 2041-7969.
- [8] K. M. Brinkhous and S. A. Walker. “PROTHROMBIN AND FIBRINOGEN IN LYMPH”. In: *American Journal of Physiology-Legacy Content* 132.3 (Mar. 1941), pp. 666–669. ISSN: 0002-9513. DOI: 10.1152/ajplegacy.1941.132.3.666.

- [9] Volker Brinkmann et al. “Neutrophil Extracellular Traps Kill Bacteria”. In: *Science* 303.5663 (2004). ISSN: 00368075. DOI: 10.1126/science.1092385.
- [10] T. Case et al. “Vascular abnormalities in experimental and human lymphatic filariasis”. In: *Lymphology* 24.4 (1991), pp. 174–183. ISSN: 00247766.
- [11] C. E. Castillo and S. Lillioja. “Peripheral lymphatic cannulation for physiological analysis of interstitial fluid compartment in humans”. In: *American Journal of Physiology - Heart and Circulatory Physiology* 261.4 30-4 (1991). ISSN: 00029513. DOI: 10.1152/ajpheart.1991.261.4.h1324.
- [12] Jessica Cedervall, Yanyu Zhang, and Anna Karin Olsson. *Tumor-induced NETosis as a risk factor for metastasis and organ failure*. 2016. DOI: 10.1158/0008-5472.CAN-15-3051.
- [13] Sanjukta Chakraborty et al. “Lipopolysaccharide modulates neutrophil recruitment and macrophage polarization on lymphatic vessels and impairs lymphatic function in rat mesentery”. In: *American Journal of Physiology - Heart and Circulatory Physiology* 309.12 (2015), H2042–H2057. ISSN: 15221539. DOI: 10.1152/ajpheart.00467.2015.
- [14] John C. Chapin and Katherine A. Hajjar. “Fibrinolysis and the control of blood coagulation”. In: *Blood Reviews* 29.1 (2015). ISSN: 15321681. DOI: 10.1016/j.blre.2014.09.003.
- [15] Shu Chien. “Mechanotransduction and endothelial cell homeostasis: The wisdom of the cell”. In: *American Journal of Physiology - Heart and Circulatory Physiology*. Vol. 292. 3. 2007. DOI: 10.1152/ajpheart.01047.2006.
- [16] Jeng Jiann Chiu and Shu Chien. *Effects of disturbed flow on vascular endothelium: Pathophysiological basis and clinical perspectives*. 2011. DOI: 10.1152/physrev.00047.2009.

- [17] L. Chrobák et al. “Coagulation properties of human thoracic duct lymph.” In: *The American journal of the medical sciences* 253.1 (1967). ISSN: 00029629. DOI: 10.1097/00000441-196701000-00013.
- [18] Jonathan Cools-Lartigue et al. “Neutrophil extracellular traps sequester circulating tumor cells and promote metastasis”. In: *Journal of Clinical Investigation* (2013). ISSN: 00219738. DOI: 10.1172/JCI67484.
- [19] Víctor J. Costela-Ruiz et al. *SARS-CoV-2 infection: The role of cytokines in COVID-19 disease*. Aug. 2020. DOI: 10.1016/j.cytogfr.2020.06.001.
- [20] Guohao Dai et al. “Distinct endothelial phenotypes evoked by arterial waveforms derived from atherosclerosis-susceptible and -resistant regions of human vasculature”. In: *Proceedings of the National Academy of Sciences of the United States of America* 101.41 (2004). ISSN: 00278424. DOI: 10.1073/pnas.0406073101.
- [21] Sefer Elezkurtaj et al. “Causes of death and comorbidities in hospitalized patients with COVID-19”. In: *Scientific Reports* 11.1 (Dec. 2021). ISSN: 20452322. DOI: 10.1038/s41598-021-82862-5.
- [22] Alistair Brian James Escott et al. “Sampling Thoracic Duct Lymph after Esophagectomy: A Pilot Study Investigating the "gut-Lymph" Concept”. In: *Lymphatic Research and Biology* 20.3 (2022). ISSN: 15578585. DOI: 10.1089/lrb.2019.0037.
- [23] R. C. Fader and A. Ewert. “Evolution of lymph thrombi in experimental *Brugia malayi* infections: A scanning electron microscopic study”. In: *Lymphology* 19.4 (1986), pp. 146–152. ISSN: 00247766.
- [24] A. Falanga, M. Marchetti, and A. Vignoli. *Coagulation and cancer: Biological and clinical aspects*. 2013. DOI: 10.1111/jth.12075.

- [25] Yun Fang, David Wu, and Konstantin G. Birukov. “Mechanosensing and mechanoregulation of endothelial cell functions”. In: *Comprehensive Physiology* 9.2 (2019). ISSN: 20404603. DOI: 10.1002/cphy.c180020.
- [26] Manuel Fankhauser et al. “Tumor lymphangiogenesis promotes T cell infiltration and potentiates immunotherapy in melanoma”. In: *Science Translational Medicine* (2017). ISSN: 19466242. DOI: 10.1126/scitranslmed.aal4712.
- [27] P. Fantl and J. F. Nelson. “Coagulation in lymph”. In: *The Journal of Physiology* 122.1 (Oct. 1953), pp. 33–37. ISSN: 14697793. DOI: 10.1113/jphysiol.1953.sp004976.
- [28] Eduardo J. Folco et al. “Neutrophil extracellular traps induce endothelial cell activation and tissue factor production through interleukin-1 $\alpha$  and cathepsin G”. In: *Arteriosclerosis, Thrombosis, and Vascular Biology* (2018). ISSN: 15244636. DOI: 10.1161/ATVBAHA.118.311150.
- [29] Gwen Freyd, Stuart K. Kim, and H. Robert Horvitz. “Novel cysteine-rich motif and homeodomain in the product of the *Caenorhabditis elegans* cell lineage gene *lin-II*”. In: *Nature* 344.6269 (1990). ISSN: 00280836. DOI: 10.1038/344876a0.
- [30] Tobias A. Fuchs, Alexander Brill, and Denisa D. Wagner. *Neutrophil extracellular trap (NET) impact on deep vein thrombosis*. Aug. 2012. DOI: 10.1161/ATVBAHA.111.242859.
- [31] Tobias A. Fuchs et al. “Extracellular DNA traps promote thrombosis”. In: *Proceedings of the National Academy of Sciences of the United States of America* 107.36 (Sept. 2010), pp. 15880–15885. ISSN: 00278424. DOI: 10.1073/pnas.1005743107.
- [32] Laure Garnier, Anastasia Olga Gkoutidi, and Stephanie Hugues. *Tumor-associated lymphatic vessel features and immunomodulatory functions*. 2019. DOI: 10.3389/fimmu.2019.00720.



- [33] Juan Esteban Gómez-Mesa et al. *Thrombosis and Coagulopathy in COVID-19*. Mar. 2021. DOI: 10.1016/j.cpcardiol.2020.100742.
- [34] Manuela Gonzalez-Aparicio and Carlos Alfaro. *Influence of interleukin-8 and neutrophil extracellular trap (NET) formation in the tumor microenvironment: Is there a pathogenic role?* 2019. DOI: 10.1155/2019/6252138.
- [35] Carolina V. Gorlino et al. “Neutrophils Exhibit Differential Requirements for Homing Molecules in Their Lymphatic and Blood Trafficking into Draining Lymph Nodes”. In: *The Journal of Immunology* 193.4 (Aug. 2014), pp. 1966–1974. ISSN: 0022-1767. DOI: 10.4049/jimmunol.1301791.
- [36] Jack P. Green et al. “Atheroprone flow activates inflammation via endothelial ATP-dependent P2X7-p38 signalling”. In: *Cardiovascular Research* 114.2 (Feb. 2018), pp. 324–335. ISSN: 17553245. DOI: 10.1093/cvr/cvx213.
- [37] Esra Güç et al. “Long-term intravital immunofluorescence imaging of tissue matrix components with epifluorescence and two-photon microscopy”. In: *Journal of Visualized Experiments* 86 (Apr. 2014). ISSN: 1940087X. DOI: 10.3791/51388.
- [38] Anurag Kumar Gupta et al. “Activated endothelial cells induce neutrophil extracellular traps and are susceptible to NETosis-mediated cell death”. In: *FEBS Letters* 584.14 (July 2010), pp. 3193–3197. ISSN: 00145793. DOI: 10.1016/j.febslet.2010.06.006.
- [39] Cornelia Hahn and Martin A. Schwartz. *Mechanotransduction in vascular physiology and atherogenesis*. 2009. DOI: 10.1038/nrm2596.
- [40] Abdul Hakkim et al. “Impairment of neutrophil extracellular trap degradation is associated with lupus nephritis”. In: *Proceedings of the National Academy of Sciences of the United States of America* (2010). ISSN: 00278424. DOI: 10.1073/pnas.0909927107.

- [41] Henry R. Hampton and Tatyana Chtanova. *The lymph node neutrophil*. Apr. 2016. DOI: 10.1016/j.smim.2016.03.008.
- [42] Hisako Hara et al. “Lymphatic Vessel Thrombosis in a Patient with Secondary Lymphedema”. In: *Plastic and Reconstructive Surgery - Global Open* 7.5 (May 2019), e2268. ISSN: 2169-7574. DOI: 10.1097/gox.0000000000002268.
- [43] Hisako Hara et al. “Lymphoedema caused by idiopathic lymphatic thrombus”. In: *Journal of Plastic, Reconstructive and Aesthetic Surgery* 66.12 (Dec. 2013), pp. 1780–1783. ISSN: 17486815. DOI: 10.1016/j.bjps.2013.04.043.
- [44] Hisako Hara et al. “Pathological Investigation of Acquired Lymphangiectasia Accompanied by Lower Limb Lymphedema: Lymphocyte Infiltration in the Dermis and Epidermis”. In: *Lymphatic Research and Biology* 14.3 (Sept. 2016), pp. 172–180. ISSN: 15578585. DOI: 10.1089/lrb.2016.0016.
- [45] Jasmin D. Haslbauer et al. “Histomorphological patterns of regional lymph nodes in COVID-19 lungs”. In: *Der Pathologe* 42.S1 (2021). ISSN: 0172-8113. DOI: 10.1007/s00292-021-00945-6.
- [46] W. H. Howell. “THE COAGULATION OF LYMPH”. In: *American Journal of Physiology-Legacy Content* 35.4 (Nov. 1914), pp. 483–491. ISSN: 0002-9513. DOI: 10.1152/ajpllegacy.1914.35.4.483.
- [47] Louise A. Johnson and David G. Jackson. “Inflammation-induced secretion of CCL21 in lymphatic endothelium is a key regulator of integrin-mediated dendritic cell transmigration”. In: *International Immunology* 22.10 (2010). ISSN: 09538178. DOI: 10.1093/intimm/dxq435.
- [48] Olena Kamenyeva et al. “Neutrophil Recruitment to Lymph Nodes Limits Local Humoral Response to *Staphylococcus aureus*”. In: *PLoS Pathogens* 11.4 (2015). ISSN: 15537374. DOI: 10.1371/journal.ppat.1004827.

- [49] Naoki Kaneko et al. “Loss of Bcl-6-Expressing T Follicular Helper Cells and Germinal Centers in COVID-19”. In: *Cell* 183.1 (Oct. 2020), pp. 143–157. ISSN: 10974172. DOI: 10.1016/j.cell.2020.08.025.
- [50] Olof Karlsson et al. “Insulin gene enhancer binding protein Isl-1 is a member of a novel class of proteins containing both a homeo- and a Cys-His domain”. In: *Nature* 344.6269 (1990). ISSN: 00280836. DOI: 10.1038/344879a0.
- [51] Wolfgang Kastenmüller et al. “A spatially-organized multicellular innate immune response in lymph nodes limits systemic pathogen spread”. In: *Cell* 150.6 (Sept. 2012), pp. 1235–1248. ISSN: 10974172. DOI: 10.1016/j.cell.2012.07.021.
- [52] Alok A. Khorana. “Cancer and coagulation”. In: *American Journal of Hematology* 87.SUPPL. 1 (2012). ISSN: 03618609. DOI: 10.1002/ajh.23143.
- [53] D. Kirchhofer et al. “Endothelial cells stimulated with tumor necrosis factor- $\alpha$  express varying amounts of tissue factor resulting in inhomogenous fibrin deposition in a native blood flow system. Effects of thrombin inhibitors”. In: *Journal of Clinical Investigation* 93.5 (1994), pp. 2073–2083. ISSN: 00219738. DOI: 10.1172/JCI117202.
- [54] Trudy A. Kohout et al. “Differential desensitization, receptor phosphorylation,  $\beta$ -arrestin recruitment, and ERK1/2 activation by the two endogenous ligands for the CC chemokine receptor 7”. In: *Journal of Biological Chemistry* 279.22 (2004). ISSN: 00219258. DOI: 10.1074/jbc.M402125200.
- [55] Takahisa Kouwaki et al. “Zyxin stabilizes RIG-I and MAVS interactions and promotes type I interferon response”. In: *Scientific Reports* 7.1 (2017). ISSN: 20452322. DOI: 10.1038/s41598-017-12224-7.
- [56] Jan Kranich and Nike Julia Krautler. *How follicular dendritic cells shape the B-cell antigenome*. June 2016. DOI: 10.3389/fimmu.2016.00225.

- [57] Matthew D. Krause et al. “Genetic variant at coronary artery disease and ischemic stroke locus 1p32.2 regulates endothelial responses to hemodynamics”. In: *Proceedings of the National Academy of Sciences of the United States of America* 115.48 (2018). ISSN: 10916490. DOI: 10.1073/pnas.1810568115.
- [58] C. A. Laschinger et al. “Production of plasminogen activator and plasminogen activator inhibitor by bovine lymphatic endothelial cells: Modulation by TNF- $\alpha$ ”. In: *Thrombosis Research* 59.3 (Aug. 1990), pp. 567–579. ISSN: 00493848. DOI: 10.1016/0049-3848(90)90416-A.
- [59] Dzung T. Le et al. “Hemostatic factors in rabbit limb lymph: Relationship to mechanisms regulating extravascular coagulation”. In: *American Journal of Physiology - Heart and Circulatory Physiology* 274.3 43-3 (1998). ISSN: 03636135. DOI: 10.1152/ajpheart.1998.274.3.h769.
- [60] Keum Hwa Lee et al. *Neutrophil extracellular traps (NETs) in autoimmune diseases: A comprehensive review*. Nov. 2017. DOI: 10.1016/j.autrev.2017.09.012.
- [61] WonJae Lee et al. “Neutrophils facilitate ovarian cancer premetastatic niche formation in the omentum”. In: *The Journal of Experimental Medicine* (2019). ISSN: 0022-1007. DOI: 10.1084/jem.20181170.
- [62] Giuseppe Lippi, Emmanuel J. Favalaro, and Gianfranco Cervellin. “Hemostatic properties of the lymph: Relationships with occlusion and thrombosis”. In: *Seminars in Thrombosis and Hemostasis* 38.2 (2012), pp. 213–221. ISSN: 00946176. DOI: 10.1055/s-0032-1301418.
- [63] Jing Liu et al. “Longitudinal characteristics of lymphocyte responses and cytokine profiles in the peripheral blood of SARS-CoV-2 infected patients”. In: *EBioMedicine* 55 (May 2020). ISSN: 23523964. DOI: 10.1016/j.ebiom.2020.102763.

- [64] Jingyuan Liu et al. “Neutrophil-to-lymphocyte ratio predicts critical illness patients with 2019 coronavirus disease in the early stage”. In: *Journal of Translational Medicine* 18.1 (May 2020). ISSN: 14795876. DOI: 10.1186/s12967-020-02374-0.
- [65] Yuchuan Liu, Katrina Pelekanakis, and Marilyn J. Woolkalis. “Thrombin and tumor necrosis factor  $\alpha$  synergistically stimulate tissue factor expression in human endothelial cells: Regulation through c-Fos and c-Jun”. In: *Journal of Biological Chemistry* 279.34 (Aug. 2004), pp. 36142–36147. ISSN: 00219258. DOI: 10.1074/jbc.M405039200.
- [66] Zheng Liu et al. “CCL21/CCR7 Axis Contributes to Trophoblastic Cell Migration and Invasion in Preeclampsia by Affecting the Epithelial Mesenchymal Transition via the ERK1/2 Signaling Pathway”. In: *Biology* 12.2 (2023). ISSN: 20797737. DOI: 10.3390/biology12020150.
- [67] Kenneth J. Livak and Thomas D. Schmittgen. “Analysis of relative gene expression data using real-time quantitative PCR and the  $2^{-\Delta\Delta CT}$  method”. In: *Methods* 25.4 (2001), pp. 402–408. ISSN: 10462023. DOI: 10.1006/meth.2001.1262.
- [68] Laurence S.C. Lok et al. “Phenotypically distinct neutrophils patrol uninfected human and mouse lymph nodes”. In: *Proceedings of the National Academy of Sciences of the United States of America* 116.38 (Sept. 2019), pp. 19083–19089. ISSN: 10916490. DOI: 10.1073/pnas.1905054116.
- [69] Quan Xin Long et al. “Antibody responses to SARS-CoV-2 in patients with COVID-19”. In: *Nature Medicine* 26.6 (June 2020), pp. 845–848. ISSN: 1546170X. DOI: 10.1038/s41591-020-0897-1.
- [70] Carolina Lucas et al. “Longitudinal analyses reveal immunological misfiring in severe COVID-19”. In: *Nature* 584.7821 (Aug. 2020), pp. 463–469. ISSN: 14764687. DOI: 10.1038/s41586-020-2588-y.

- [71] Margo E MacDonald et al. “Lymphatic coagulation and neutrophil extracellular traps in lung-draining lymph nodes of COVID-19 decedents”. In: *Blood Advances* (Aug. 2022). ISSN: 2473-9529. DOI: 10.1182/bloodadvances.2022007798.
- [72] Valy Menkin. “Studies on inflammation”. In: *Journal of Experimental Medicine* 64.3 (Sept. 1936), pp. 485–502. ISSN: 15409538. DOI: 10.1084/jem.64.3.485.
- [73] Elizabeth A Middleton et al. “Neutrophil Extracellular Traps (NETs) Contribute to Immunothrombosis in COVID-19 Acute Respiratory Distress Syndrome.” In: *Blood* (2020). ISSN: 1528-0020. DOI: 10.1182/blood.2020007008.
- [74] George J. Miller et al. “Haemostatic factors in human peripheral afferent lymph”. In: *Thrombosis and Haemostasis* 83.3 (2000). ISSN: 03406245. DOI: 10.1055/s-0037-1613832.
- [75] Dimana O. Miteva et al. “Transmural flow modulates cell and fluid transport functions of lymphatic endothelium”. In: *Circulation Research* 106.5 (2010). ISSN: 00097330. DOI: 10.1161/CIRCRESAHA.109.207274.
- [76] Tobi Nagel et al. “Vascular endothelial cells respond to spatial gradients in fluid shear stress by enhanced activation of transcription factors”. In: *Arteriosclerosis, Thrombosis, and Vascular Biology* 19.8 (1999). ISSN: 10795642. DOI: 10.1161/01.ATV.19.8.1825.
- [77] Naotaka Nakazawa et al. “Matrix mechanics controls FHL2 movement to the nucleus to activate p21 expression”. In: *Proceedings of the National Academy of Sciences of the United States of America* 113.44 (2016). ISSN: 10916490. DOI: 10.1073/pnas.1608210113.
- [78] Peter P. Nawroth and David M. Stern. “Modulation of endothelial cell hemostatic properties by tumor necrosis factor”. In: *Journal of Experimental Medicine* 163.3 (1986). ISSN: 15409538. DOI: 10.1084/jem.163.3.740.

- [79] Katharina Neubauer and Barbara Zieger. *Endothelial cells and coagulation*. 2022. DOI: 10.1007/s00441-021-03471-2.
- [80] Man Nie et al. “Neutrophil Extracellular Traps Induced by IL8 Promote Diffuse Large B-cell Lymphoma Progression via the TLR9 Signaling”. In: *Clinical Cancer Research* 25.6 (2019), pp. 1867–1879. ISSN: 15573265. DOI: 10.1158/1078-0432.CCR-18-1226.
- [81] E L Opie. “Thrombosis and Occlusion of Lymphatics.” In: *The Journal of medical research* 29.1 (1913), pp. 131–13146. ISSN: 0097-3599.
- [82] Eugene L. Opie. “Lymph formation and edema of the liver with experimental nephritis produced by cantharidin”. In: *Journal of Experimental Medicine* 16.6 (Dec. 1912), pp. 831–849. ISSN: 15409538. DOI: 10.1084/jem.16.6.831.
- [83] A. Özcan et al. “CCR7-guided neutrophil redirection to skin-draining lymph nodes regulates cutaneous inflammation and infection”. In: *Science Immunology* 7.68 (2022). ISSN: 24709468. DOI: 10.1126/sciimmunol.abi9126.
- [84] Venizelos Papayannopoulos. *Neutrophil extracellular traps in immunity and disease*. 2018. DOI: 10.1038/nri.2017.105.
- [85] Juwon Park et al. “Cancer cells induce metastasis-supporting neutrophil extracellular DNA traps”. In: *Science Translational Medicine* 8.361 (Oct. 2016). ISSN: 19466242. DOI: 10.1126/scitranslmed.aag1711.
- [86] José Perdomo et al. “Neutrophil activation and NETosis are the major drivers of thrombosis in heparin-induced thrombocytopenia”. In: *Nature Communications* 10.1 (2019). ISSN: 20411723. DOI: 10.1038/s41467-019-09160-7.
- [87] Mercy Halleluyah Periyah, Ahmad Sukari Halim, and Arman Zaharil Mat Saad. *Mechanism action of platelets and crucial blood coagulation pathways in Hemostasis*. 2017.

- [88] Joachim Pircher et al. “Prothrombotic effects of tumor necrosis factor alpha in vivo are amplified by the absence of TNF-alpha receptor subtype 1 and require TNF-alpha receptor subtype 2”. In: *Arthritis Research and Therapy* 14.5 (Oct. 2012). ISSN: 14786354. DOI: 10.1186/ar4064.
- [89] David A. Rigby et al. “Neutrophils rapidly transit inflamed lymphatic vessel endothelium via integrin-dependent proteolysis and lipoxin-induced junctional retraction”. In: *Journal of Leukocyte Biology* 98.6 (Dec. 2015), pp. 897–912. ISSN: 1938-3673. DOI: 10.1189/jlb.1hi0415-149r.
- [90] Davide F. Robbiani et al. “Convergent antibody responses to SARS-CoV-2 in convalescent individuals”. In: *Nature* 584.7821 (Aug. 2020), pp. 437–442. ISSN: 14764687. DOI: 10.1038/s41586-020-2456-9.
- [91] *Role of Neutrophils in Disease Pathogenesis*. 2017. DOI: 10.5772/65581.
- [92] Erica Russo et al. “Intralymphatic CCL21 Promotes Tissue Egress of Dendritic Cells through Afferent Lymphatic Vessels”. In: *Cell Reports* 14.7 (2016). ISSN: 22111247. DOI: 10.1016/j.celrep.2016.01.048.
- [93] Hanny Al-Samkari et al. “COVID-19 and coagulation: Bleeding and thrombotic manifestations of SARS-CoV-2 infection”. In: *Blood* 136.4 (July 2020), pp. 489–500. ISSN: 15280020. DOI: 10.1182/BLOOD.2020006520.
- [94] Laura Santambrogio. *Immunology of the lymphatic system*. 2011. DOI: 10.1007/978-1-4614-3235-7.
- [95] Monica Schenone, Barbara C. Furie, and Bruce Furie. *The blood coagulation cascade*. 2004. DOI: 10.1097/01.moh.0000130308.37353.d4.
- [96] Philipp Schineis, Peter Runge, and Cornelia Halin. *Cellular traffic through afferent lymphatic vessels*. Jan. 2019. DOI: 10.1016/j.vph.2018.08.001.



- [97] R. R. Schleef et al. "Cytokine activation of vascular endothelium. Effects on tissue-type plasminogen activator and type 1 plasminogen activator inhibitor". In: *Journal of Biological Chemistry* 263.12 (1988). ISSN: 00219258. DOI: 10.1016/s0021-9258(18)60636-2.
- [98] Alessandro Sette and Shane Crotty. *Adaptive immunity to SARS-CoV-2 and COVID-19*. Feb. 2021. DOI: 10.1016/j.cell.2021.01.007.
- [99] B. G.P. Shafiroff and Q. Y. Kau. "Cannulation of the human thoracic lymph duct". In: *Surgery* 45.5 (1959). ISSN: 00396060.
- [100] Hideaki Shimada and Lakshman E. Rajagopalan. "Rho-kinase mediates lysophosphatidic acid-induced IL-8 and MCP-1 production via p38 and JNK pathways in human endothelial cells". In: *FEBS Letters* 584.13 (2010). ISSN: 00145793. DOI: 10.1016/j.febslet.2010.04.064.
- [101] Steven A. Stacker et al. *Lymphangiogenesis and cancer metastasis*. 2002. DOI: 10.1038/nrc863.
- [102] Dimitrios A. Stakos et al. "Expression of functional tissue factor by neutrophil extracellular traps in culprit artery of acute myocardial infarction". In: *European Heart Journal* 36.22 (June 2015), pp. 1405–1414. ISSN: 15229645. DOI: 10.1093/eurheartj/ehv007.
- [103] Marisa Stebeegg et al. *Regulation of the germinal center response*. Oct. 2018. DOI: 10.3389/fimmu.2018.02469.
- [104] Matthew Stephens and Shan Liao. *Neutrophil-lymphatic interactions during acute and chronic disease*. Mar. 2018. DOI: 10.1007/s00441-017-2779-5.
- [105] Antonio V. Sterpetti et al. "Shear stress increases the release of interleukin-1 and interleukin-6 by aortic endothelial cells". In: *Surgery* 114.5 (1993). ISSN: 00396060.

- [106] Simon Stritt, Katarzyna Koltowska, and Taija Mäkinen. *Homeostatic maintenance of the lymphatic vasculature*. 2021. DOI: 10.1016/j.molmed.2021.07.003.
- [107] Barbara D. Summers et al. “Lung lymphatic thrombosis and dysfunction caused by cigarette smoke exposure precedes emphysema in mice”. In: *Scientific Reports* 12.1 (2022). ISSN: 20452322. DOI: 10.1038/s41598-022-08617-y.
- [108] Melody A. Swartz. “Immunomodulatory roles of lymphatic vessels in cancer progression”. In: *Cancer Immunology Research* 2.8 (2014). ISSN: 23266074. DOI: 10.1158/2326-6066.CIR-14-0115.
- [109] Akira Takeda et al. “Single-Cell Survey of Human Lymphatics Unveils Marked Endothelial Cell Heterogeneity and Mechanisms of Homing for Neutrophils”. In: *Immunity* 51.3 (Sept. 2019), pp. 561–572. ISSN: 10974180. DOI: 10.1016/j.immuni.2019.06.027.
- [110] Ian A. Tamargo et al. *Flow-induced reprogramming of endothelial cells in atherosclerosis*. Nov. 2023. DOI: 10.1038/s41569-023-00883-1.
- [111] Ning Tang et al. “Abnormal coagulation parameters are associated with poor prognosis in patients with novel coronavirus pneumonia”. In: *Journal of Thrombosis and Haemostasis* 18.4 (Apr. 2020), pp. 844–847. ISSN: 15387836. DOI: 10.1111/jth.14768.
- [112] Alvaro Teixeira et al. “Differential Interleukin-8 thresholds for chemotaxis and netosis in human neutrophils”. In: *European Journal of Immunology* 51.9 (2021). ISSN: 15214141. DOI: 10.1002/eji.202049029.
- [113] Hawa Racine Thiama et al. “NETosis proceeds by cytoskeleton and endomembrane disassembly and PAD4-mediated chromatin decondensation and nuclear envelope rupture”. In: *Proceedings of the National Academy of Sciences of the United States of America* 117.13 (2020). ISSN: 10916490. DOI: 10.1073/pnas.1909546117.

- [114] Victor W.M. Van Hinsbergh. *Endothelium - Role in regulation of coagulation and inflammation*. 2012. DOI: 10.1007/s00281-011-0285-5.
- [115] Imre Varjú and Krasimir Kolev. *Networks that stop the flow: A fresh look at fibrin and neutrophil extracellular traps*. Oct. 2019. DOI: 10.1016/j.thromres.2019.08.003.
- [116] Flavio Protasio Veras et al. “SARS-CoV-2-triggered neutrophil extracellular traps mediate COVID-19 pathology”. In: *Journal of Experimental Medicine* 217.12 (Dec. 2020). ISSN: 15409538. DOI: 10.1084/jem.20201129.
- [117] Cristina Viúdez-Pareja, Ewa Kreft, and Melissa García-Caballero. *Immunomodulatory properties of the lymphatic endothelium in the tumor microenvironment*. 2023. DOI: 10.3389/fimmu.2023.1235812.
- [118] Jeffrey C. Way and Martin Chalfie. “mec-3, a homeobox-containing gene that specifies differentiation of the touch receptor neurons in *C. elegans*”. In: *Cell* 54.1 (1988). ISSN: 00928674. DOI: 10.1016/0092-8674(88)90174-2.
- [119] Jonathan D. Winkelman et al. “Evolutionarily diverse LIM domain-containing proteins bind stressed actin filaments through a conserved mechanism”. In: *Proceedings of the National Academy of Sciences of the United States of America* 117.41 (2020). ISSN: 10916490. DOI: 10.1073/pnas.2004656117.
- [120] Matthew C. Woodruff et al. “Extrafollicular B cell responses correlate with neutralizing antibodies and morbidity in COVID-19”. In: *Nature Immunology* 21.12 (Dec. 2020), pp. 1506–1516. ISSN: 15292916. DOI: 10.1038/s41590-020-00814-z.
- [121] Jingna Xue et al. “Lymph-derived chemokines direct early neutrophil infiltration in the lymph nodes upon *Staphylococcus aureus* skin infection”. In: *Proceedings of the National Academy of Sciences of the United States of America* 119.32 (2022). ISSN: 10916490. DOI: 10.1073/pnas.2111726119.

- [122] Lin Yang et al. “ICAM-1 regulates neutrophil adhesion and transcellular migration of TNF- $\alpha$ -activated vascular endothelium under flow”. In: *Blood* (2005). ISSN: 00064971. DOI: 10.1182/blood-2004-12-4942.
- [123] Luyu Yang et al. “IL-8 mediates a positive loop connecting increased neutrophil extracellular traps (NETs) and colorectal cancer liver metastasis”. In: *Journal of Cancer* 11.15 (2020), pp. 4384–4396. ISSN: 18379664. DOI: 10.7150/jca.44215.
- [124] Jonathan W. Yau, Hwee Teoh, and Subodh Verma. *Endothelial cell control of thrombosis*. 2015. DOI: 10.1186/s12872-015-0124-z.
- [125] Michael Yeh et al. “Increased transcription of IL-8 in endothelial cells is differentially regulated by TNF- $\alpha$  and oxidized phospholipids”. In: *Arteriosclerosis, Thrombosis, and Vascular Biology* 21.10 (2001). ISSN: 10795642. DOI: 10.1161/hq1001.097027.
- [126] David C. Zawieja et al. “Lymphatic Cannulation for Lymph Sampling and Molecular Delivery”. In: *The Journal of Immunology* 203.8 (2019). ISSN: 0022-1767. DOI: 10.4049/jimmunol.1900375.
- [127] Wendi Zhang et al. *Coagulation in Lymphatic System*. 2021. DOI: 10.3389/fcvm.2021.762648.
- [128] Fei Zhou et al. “Clinical course and risk factors for mortality of adult inpatients with COVID-19 in Wuhan, China: a retrospective cohort study”. In: *The Lancet* 395.10229 (Mar. 2020), pp. 1054–1062. ISSN: 1474547X. DOI: 10.1016/S0140-6736(20)30566-3.
- [129] Ping Zhou et al. “Attenuation of TNF- $\alpha$ -induced inflammatory injury in endothelial cells by ginsenoside Rb1 via inhibiting NF- $\kappa$ B, JNK and p38 signaling pathways”. In: *Frontiers in Pharmacology* 8.AUG (2017). ISSN: 16639812. DOI: 10.3389/fphar.2017.00464.

- [130] Yu Zuo et al. “Neutrophil extracellular traps (NETs) as markers of disease severity in COVID-19”. In: *JCI Insight* 5.11 (2020), p. 138999. ISSN: 2379-3708. DOI: 10.1101/2020.04.09.20059626.